The Mechanism of Fibrosis Induced by Biomaterials

The Mechanism of Fibrosis Induced by Biomaterials

By

Albert C. Chang, B. ENG

A Thesis

Submitted to the School of Graduate Studies

In Partial Fulfillment of the Requirements

for the Degree

Master of Applied Science, Chemical Engineering

McMaster University

Master of Applied Science — McMaster Univerisity

(Chemical Engineering) — Hamilton, Ontario

Title: The Mechanism of Fibrosis Induced by Biomaterials

Author: Albert C. Chang, B. ENG

Supervisor: Dr. K. Jones

Number of Pages: vi, 130

Abstract

Biomaterials are used in many different areas. Often, after implantation, severe host reactions occur which cause the malfunction or failure of the device. In our study, we wanted to investigate the mechanism of biomaterial-induced fibrosis. We focused on three areas: i) the relationship between inflammation and fibrosis after implantation, ii) the role that the SMAD3 gene plays, and iii) how MRL mice react to biomaterials.

After implantation, acute inflammation occurs immediately. In pathological fibrosis, it has traditionally been believed that the inflammation is linked to the downstream fibrosis, though this theory has been challenged recently. In our project, we did not observe a direct relationship between intentionally induced inflammation and biomaterial-induced fibrosis. We did observe the dependency of the host reaction on the type of implanted biomaterial. The SMAD3 gene is tightly linked to the pro-fibrotic cytokine TGF-β. The SMAD3 protein mediates the TGF-β pathway intracellularly. It was found in pulmonary fibrosis, SMAD3 knockout (KO) mice had lower production of collagen. In our project, we did not observe a difference in cellular behaviour on the surface of the implanted biomaterial between wild-type (WT) and SMAD3 KO mice. We did observe a difference in the production of TGF-β1. This could be a clue that biomaterial-induced fibrosis has more than one mechanism/pathway that is not dependent on TGF-β. In our last project, we studied MRL mice that showed potential in scarless wound healing. We observed a higher production of MMP-2, MMP-9 and TGF-β1. Histologically, however, we did not see a difference in cellular behaviour between MRL and C57BL/6 mice. Our results open up the possibilities of different mechanisms and

pathways in biomaterial-induced fibrosis. Future studies of cytokines and specific cells could help us further understand the process of encapsulation of the implanted biomaterials.

Acknowledgement

First and foremost, I would like to thank my supervisor Dr. K. Jones for making this all possible. Without her guidance, I would not have been able to complete this task. I would like to thank her for being patient with me, and her advices in, not only research, but also different aspects of my life.

I would also like to thank all my colleagues from the biomaterial/tissue engineering lab, for their support and encouragement inside and outside of the lab. The memories of spending time them, from learning how to use a new equipment/technique to how to play the game of softball, will always be cherished.

I would not be who I am today without the love from my family. The positive work ethic influence from my father, the heart warming advice from my mother, the relaxing laughter from my sister, and finally the love from my recently passed away Ah-ma (grandmother) are all part of my motivation to finish this degree.

Finally, I would like to thank God for his Love.

Title Page.....i
Descriptive Note.....ii
Abstract.....iii
Acknowledgement.....iv

1. Introduction.....1

2. Literature Review.....4

2.1 Wound Healing.....4
2.2 Tissue Engineering.....9
2.3 Implanted Biomaterials and Host Reactions.....12
2.3.1 Protein Adhesion and Complement Activation.....15
2.3.2 Adhesion and Fusion of Macrophages in Fibrous Encapsulati.....16
2.3.3 The NEW Biomaterials.....18
2.4 Inflammation and Fibrosis.....20
2.5 SMAD3.....20
2.6 The Scarless Wonder- MRL Mice.....22

3. Acute Inflammation and Fibrosis Induced by Biomaterials.....36
3.1 Introduction.....36
3.2 Experimental Methods.....37
3.2.1 Experimental Outline.....37
3.2.2 Material Preparation.....38
3.2.3 IL-1β and TGF-β concentrations.....39
3.2.4 H&E Staining and Cell Layer Thickness on Material Surface.....40
3.2.5 Collagen.....40
3.2.6 Flow Cytometry.....41
3.2.7 Animals.....42
3.2.8 Statistical Analysis.....42
3.3 Results.....42
3.3.1 Concentration of IL-1 and TGF-β in different treatments.....43
3.3.2 Material Surface Cellular Behaviour.....45
3.3.3 Cell Type Distribution.....46
3.4 Discussion.....47

4. Fibrosis Induced by Silicone in SMAD3 KO Mice.....71
4.1 Introduction.....71
4.2 Experimental Methods.....72
4.2.1 Experimental Outline.....72
4.2.2 Material Preparation.....73
4.2.3 TGF-β1 concentrations.....73
4.2.4 H&E Staining and Cell Layer Thickness on Material Surface.....74
4.2.5 Flow Cytometry.....75

4.2.6 Animals.....75

4.3 Results.....76
4.4 Discussion.....80

5. Fibrosis Induced by Silicone in MRL Mice.....96
5.1 Introduction.....96
5.2 Experimental Methods.....97
4.2.1 Experimental Outline.....97
4.2.2 Material Preparation.....98
4.2.3 TGF-β1 concentrations.....98
4.2.4 MMP-2 and MMP-9 concentrations.....99
4.2.5 H&E Staining and Cell Layer Thickness on Material Surface.....99
4.2.6 Flow Cytometry.....100
4.2.7 Animals.....101
4.2.8 Statistical Analysis.....101

5.3 Results.....101
5.4 Discussion.....105

6. Conclusion and Future Recommendations.....123

Appendix A: ELISA (IL-1β).....127
Appendix B: ELISA (TGF-β1).....129

1. Introduction

Imagine one day that a kidney failure patient does not need a transplant anymore, and a knee anterior-cruciate-ligament torn athlete can have the ligament replaced without cutting a piece of the tendon off their hamstring. With the idea of tissue engineering, the dreams mentioned above are all possible. Damaged tissues/organs in the body are sometimes irreparable without intervention. With the combination of research and application, scientists and engineers created the idea of tissue engineering: to replace a damaged tissue/organ by using a scaffold to mimic its mechanical and biological properties and induce self repair and regeneration. Polymeric biomaterials are usually used as the scaffold (an artificial extracellular matrix) to deliver the essential cells and biological molecules to induce the growth. Ideally, the growth of the tissue/organ occurs as the biomaterial degrades, as when it is fully repaired the biomaterial is completely degraded. During the implantation, the biomaterial makes the initial contact with the body and usually induces a severe host response. A damaging fibrotic response usually results, in which the biomaterial is treated as a foreign object and induces encapsulation. The deposition of collagen on the surface of the biomaterial blocks the communication between the introduced cells and molecules, and the surrounding environment, which defeats the purpose of tissue replacement for regeneration. Therefore, to achieve the goal of repair and regeneration, we must understand the mechanism of the fibrotic response toward the biomaterials in order to control its severity.

Fibrosis in different tissues and organs (eg. lung, renal) is well studied, though not when it is induced by an implanted biomaterial. We hypothesized that pathological

fibrosis and biomaterial-induced fibrosis share similar pathways, though there are factors to biomaterial-induced fibrosis that are yet to be discovered.

Rather than randomly testing different types of biomaterials and hopefully finding a biocompatible one, we focused our study on understanding the mechanism of biomaterial-induced fibrosis in order to control it. We investigated, with the implanted biomaterial:

i) how is inflammation involved and related to biomaterial-induced fibrosis?

ii) how important is the SMAD3 pathway in biomaterial-induced fibrosis?

iii) does a "scarless-healing" mouse strain have as severe a fibrotic response when it is induced by a implanted biomaterial?

In our first project we focused on the relationship between inflammation and biomaterial-induced fibrosis. We measured the concentrations of pro-fibrotic and pro-inflammatory cytokines and studied how they correlate to the cellular population at the implantation site and the cellular behaviour on the surface of the biomaterial. In our second project, we switched our focus to the potential influence of the SMAD3 gene on biomaterial-induced fibrosis. We studied how SMAD3 knockout (KO) mice behave differently to wild-type (WT) mice in TGF-β1 production, cellular population and the biomaterial surface interaction. In our third project, we studied how a "scarless-healing" mouse strain behaves when the "scar" is induced by a implanted biomaterial, and whether this strain of mice can perform "scarlessly" when responding to an implanted biomaterial. If they did, we wanted to determine the difference in the mechanism between the normally fibrotic and the non-fibrotic responses to implanted biomaterials.

In the Literature Review, we will give an explanation of tissue engineering. We will also talk about in what areas biomaterials are used other than tissue engineering. Finally, we will give background information on each of the projects that we studied and how they are related to each other.

2. Literature Review

2.1 Wound Healing

The understanding of wound healing is the base of understanding how the body reacts to an implanted biomaterial. The process of wound healing is broken down into three phases: inflammation, proliferation, and maturation [1]. In wound healing, the body must first control the bleeding. The process involved is called hemostasis. The blood vessels constrict and the surrounding epithelium and platelets start the coagulation cascade immediately. The clot formed from coagulation is composed of collagen, fibronectin, thrombin, and platelets. Cytokines and growth factors are then released by these factors to induce acute inflammation [2]. The clot also acts as the three dimensional scaffold for the migrated cells like neutrophils, monocytes and fibroblasts, and to cytokines and growth factors [3,4]. Inflammation is characterized by the immediate response by neutrophils. The inflammatory mediators such as IL-1 (interleukin-1) and TNF-α (tumour necrosis factor-alpha) induce the dilation of the vessel and draw the neutrophils to the site of injury [5,6]. The main role of neutrophils in the injury site is to eliminate the invading bacteria and cellular debris by releasing proteolytic enzymes. One would wonder, how does the protease know not to harm the healthy tissue? They are in fact protected by the protease inhibitors [7]. Though if the inflammation is overwhelmingly strong, the protection could be invaded and penetrated. Nearby monocytes also migrate to the area and differentiate into macrophages 48-96 hours after injury. It is crucial that the macrophages are activated to allow the smooth transition from inflammation to proliferation [1]. Macrophages phagocytosize the dead neutrophils

that enter apoptosis, and continue neutrophils' unfinished job. Macrophages kill the pathogens by producing NO (nitric oxide). The presence of IL-1 and TNF-α also helps the production of NO [8]. MMPs (matrix metalloproteinase) which are secreted by fibroblasts, monocytes, and macrophages (with the help of TNF-α) clean up the injured ECM (extracellular matrix). MMPs also help guide the wound cells to migrate through the ECM [9]. Eventually inflammation reaches its checkout points by a series of signals [10,11].

After inflammation, wound healing enters the proliferation stage. Epithelial cells on the skin edge of the injury start to proliferate and build a protective layer to prevent fluid loss from the body and bacterial invasion from the outer environment, and the epithelial cells close to inner venules start to form capillaries. TGF-β and EGF (epithelial growth factor) secreted by macrophages and activated platelets play an important role as chemoattractants in inducing the proliferation of epithelial cells [12,13]. Another type of cell that proliferates rapidly in this stage is the fibroblast. These cells migrate to the injury site, after activation (signaled by PDGF (platelet derived growth factor) and EGF derived from platelets and macrophages), start to produce collagen and continue to proliferate. Autocrine and paracrine signaling also increase the magnitude of PDGF expression by fibroblasts. Fibroblasts continue to produce collagen and prepare for wound contraction by transforming into myofibroblasts, induced by TGF- β. At this point, the proliferation rate has dropped from its elevated level at the beginning of the stage [14-16]. Provisional matrix is also synthesized at this point. Through the interaction with integrins, cells are guided to the matrix and upregulated by TNF-α [17]. The

concentration of TGF-β peaks at the same time as rapid production of collagen I to build the ECM, and decreases with maturation/remodeling/degradation. This multi-functional cytokine also decreases the production of MMP, increases the production of TIMP (tissue inhibitor of metalloproteinase), and increases the production of cell adhesion proteins [8].

After inflammation and proliferation, wound healing enters the stage of maturation and remodeling. The wound matrix built from the first two stages is made of mainly fibrin and fibronectin. The area is thin, which allows cells like neutrophils and macrophages to migrate through. This unorganized matrix is later replaced by collagen produced by fibroblasts, and becomes denser, thicker and therefore stronger. Collagen in healthy skin is 80 to 90 percent type I, and 10 to 20 percent type III. In granulation tissue, type II collagen increases to 30 percent and is back down to 10 percent in a mature scar [15]. There is more than one set of MMPs, each with a different function, that, with the influence of cytokines, induces different types of collagens. As mentioned earlier, the cytokines that affect MMPs' activity are TGF-β, PDGF, IL-1 and EGF. TIMP also inhibits the activation of MMPs in order to upregulate TGF-β and IL-6; the production of IL-6 by fibroblasts is also influenced by TNF-α [18]. It is obvious all these cytokines, growth factors, and cells have very complicated yet elegant and precise relationships in order to complete the process of wound healing.

As mentioned earlier, fibroblasts transform into myofibroblasts with the aid of TGF-β. The transformation is to increase the contractibility of the cells [19]. The production of collagen continues for 4 to 5 weeks. The number of fibroblasts and collagen production per fibroblast increases as well during this period [20,21]. Over time,

the strength of collagen increases, though it will never be as strong as the uninjured skin. Figure 2.1 gives an outline of factor production with time, and Figure 2.2 gives an outline of time-cell population relationship post injury [2].

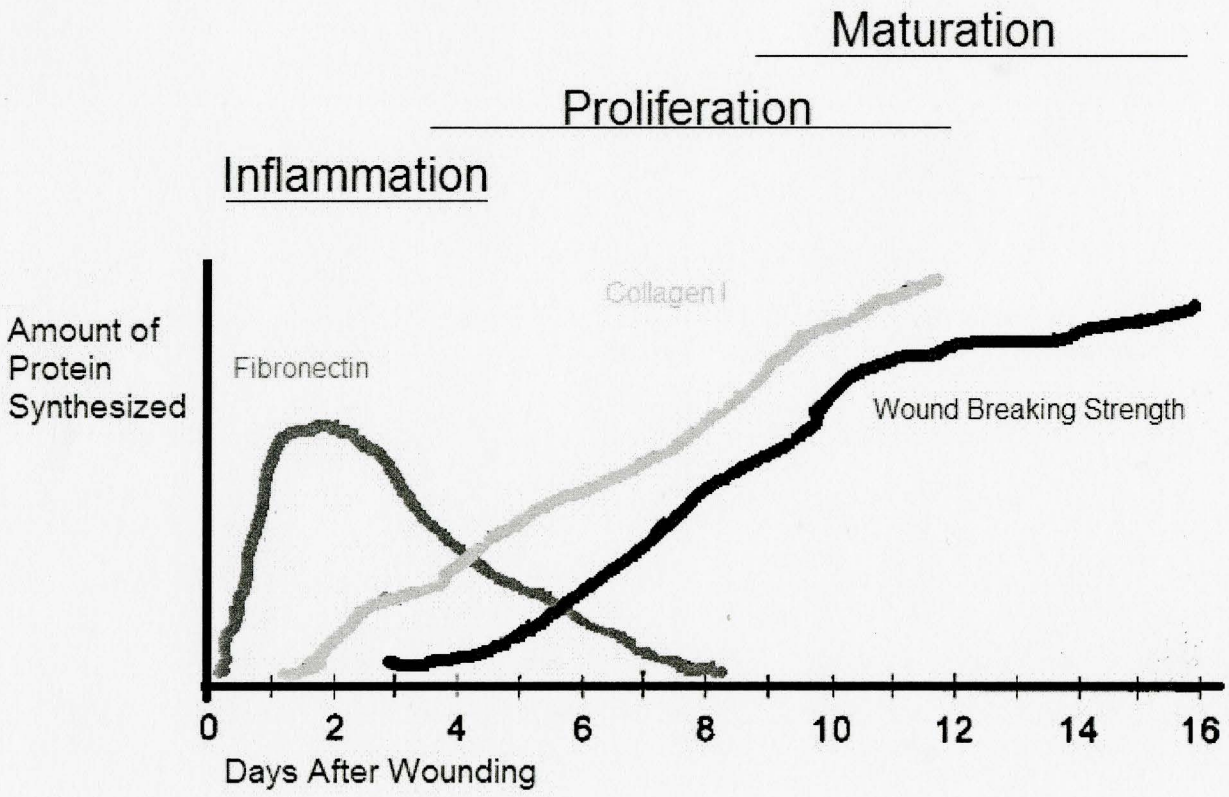

Figure 2.1. The relationship between time and matrix components. Fibronectin is the main component of early matrix structure. As the concentration of collagen I increases, the strength of the scar increases as well [2]. Adapted from Witte, M., and Barbul, A. General principles of wound healing. *Surg. Clin. North Am. 77: 509, 1997*

We will focus on the cells that play important roles in wound healing at the end of this section. Neutrophils are the first cellular defense line of the body. They enter the

injury site minutes after injury and peak within the first 24 hours. Factors that that help the migration of neutrophils to the site include: vascular permeability due to inflammation, and chemoattractants released by platelets like IL-1, TNF-α [2,6]. Neutrophils move to the initial provisional matrix made of fibrin and thrombus, and adhere to the epithelium. These cells then move through the vessel wall and to the wound site. The integrins on the surface of the cells help the adhesion of the cells to ECM [2]. The main role of neutrophils is to destroy the invading organisms and cells by phagocytosing them and releasing proteolytic enzymes. Protease inhibitor protects the matrix. To complete the job, neutrophils also produce free oxygen radicals to bind with chloride to aid the killing of bacteria [7]. Note that neutrophils are not needed for collagen synthesis [22].

Macrophages have a role in both inflammation and proliferation stages of wound healing. These cells have vast involvements in wound healing. Other than phagocytosis, the secretion of NO by macrophages makes sure there is no replication of DNA from viruses within cells. Cytokines and growth factors secreted by macrophages regulate the recruitment of cells like fibroblasts and their proliferation, even the repair cells like epithelial cells [23,24]. Monocytes are the precursor of macrophages, and their differentiation is induced by cytokines like IL-2, TNF-α and PDGF [18].

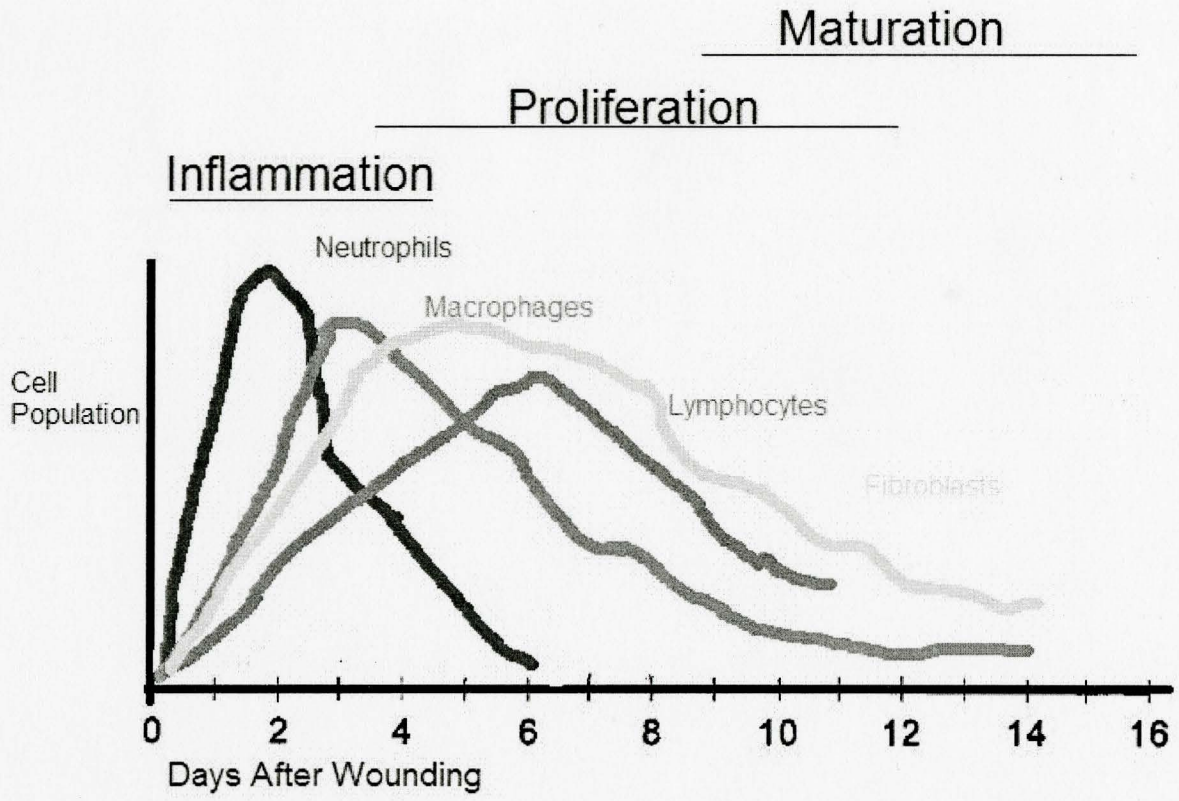

Figure 2.2. The relationship between time and cell populations. Neutrophils peak earliest as they are the first cell line of defense. The population of fibroblasts proliferates to increase the production of collagen I [2]. Adapted from Witte, M., and Barbul, A. General principles of wound healing. *Surg. Clin. North Am. 77: 509, 1997*

2.2 Tissue Engineering

The purpose of tissue engineering is to use biomaterials as a scaffold to carry necessary cells and bioactive molecules to interact with the environment in vivo to induce the regeneration (wound healing) of the damaged tissues/organs without causing excessive host reactions which could eventually cause more harm than good [25,26].

Tissue engineering, by approach, can be categorized in (at least) two: acellular matrices, and matrices with cells. Acellular matrices are tissues with the removal of cells by mechanical or chemical manipulation to produce collagen-rich matrices. After implantation, the matrices are desired to be degraded with the ingrowth of cells from the environment in vivo [25,27]. In cell based tissue engineering, the cells are seeded into a scaffold made of biomaterials. The biomaterials are desired to have similar biological, chemical and mechanical properties of the injured tissue or native ECM (extracellular matrix) in order to serve as a temporary replacement until the tissue is fully regenerated [25]. The scaffolds are usually designed as a three dimensional structure in order to carry the cells and bioactive factors efficiently. In early stages of regeneration, the scaffold should be able to allow the cells to expand within, and interact with the cells and bioactive factors, such as cytokines and growth factors, at the site of implantation [28]. The characteristics of the surface should allow the surrounding proteins and cells to adhere in order to have interactions and desired subsequent influences on wound healing [29].

The biomaterial is desired to: i) mimic the properties of the tissue it replaces; ii) not cause chronic inflammation, and iii) be biodegradable with time. An incompatible biomaterial will eventually lead to rejection and foreign body reactions by the host, and cause necrosis of the surrounding tissue. This process is discussed in the section of Implanted Biomaterials and Host Reactions in detail. The degradability of the biomaterial is also very important. The rate of degradation should be at the level that is tolerable to the host. By tolerable we mean that the degraded particles should be non-

toxic and able to be metabolized by the body [30]. At later stages of regeneration, the biomaterial should not hinder the regeneration and the growing of the cells and tissue [28].

Typically, biomaterials are divided into two classes: naturally derived and synthetic. Naturally derived biomaterials (e.g., alginates, gelatin, collagen) are composed of polypeptides, polysaccharides, proteins and nucleic acids [31-33]. Collagen has been used in the areas of nerve repair [34] and bladder engineering [35]; matrigel has contributed in the repairing of spinal cord [36]. Natural biomaterials have several advantages over synthetic biomaterials, including: adhesion selectivity (recognizable to the host cells), similarity of mechanical properties to tissues, and ability to be degraded without toxic byproducts. The main disadvantages of natural biomaterials include: i) risk of bacterial or viral infection if not sterilized properly; ii) unstable supplying source, iii) change of properties after sterilization, and iv) inability to be manipulated due to the possibility of denaturing the material [26,37,38]. Synthetic biomaterials have much wider ranges in terms of structures, and chemical and mechanical properties, but they often cause strong host reactions. Synthetic biomaterials can also be divided into biodegradable and non-biodegradable classes [39]. Non-biodegradable materials like Teflon has been used in vascular grafts [40], and high density polyethylene for hip implants [41]. For the purpose of tissue engineering, the materials that make the scaffold are typically biodegradable.

2.3 Implanted Biomaterials and Host Reactions

Biomaterials are used in many different ways in our life as shown in Table 2.1 [42]. This area of study consists of many different fields including surface science, bioengineering, biology, medicine, and chemical engineering. Over the past fifty years, this has cost over one hundred billion dollars [42].

Implants have been used for at least 2000 years, though most cases in early stages ended with failure due to host reactions to the biomaterials. Even though the mechanisms of host reactions were not defined, different materials were chosen through trial and error. Implanted biomaterials usually cause initial inflammation, then fibrosis and the encapsulation of the biomaterial. The host reaction toward an implanted biomaterial could be broken down to several steps: surgical injury, blood-material contact, provisional matrix formation, acute and chronic inflammation, development of granulation tissue, foreign body reaction, and finally fibrosis and fibrous encapsulation with thickness ranges from 50-200μm [42-45]. A chronological outline is shown in Figure 2.3 [42].

Table 2.1. Different applications of biomaterials. Adapted from Ratner, B., and Bryant, S., Biomaterials: Where We Have Been and Where We Are Going. *Annu. Rev. Biomed. Eng. 6:41-75, 2004*

Applications of Biomaterials
Artery graft
Breast implant
Cochlear implant
Ear drainage tube
Dental implant
Feeding tube
Glaucoma drainage tube
Hydrocephalous shunt
Intraocular lens
Joints (hip, knee, shoulder)
Keratorprothesis
Left ventricular assit device
Mechanical heart valve
Nerve guidance tube
Ophthalmic drug delivery device
Pacemaker
Renal dialyzer
Stent
Tissue adhesive
Urinary catheter
Heart Valve
Wound dressing
X-ray guide
Zirconium knee joint

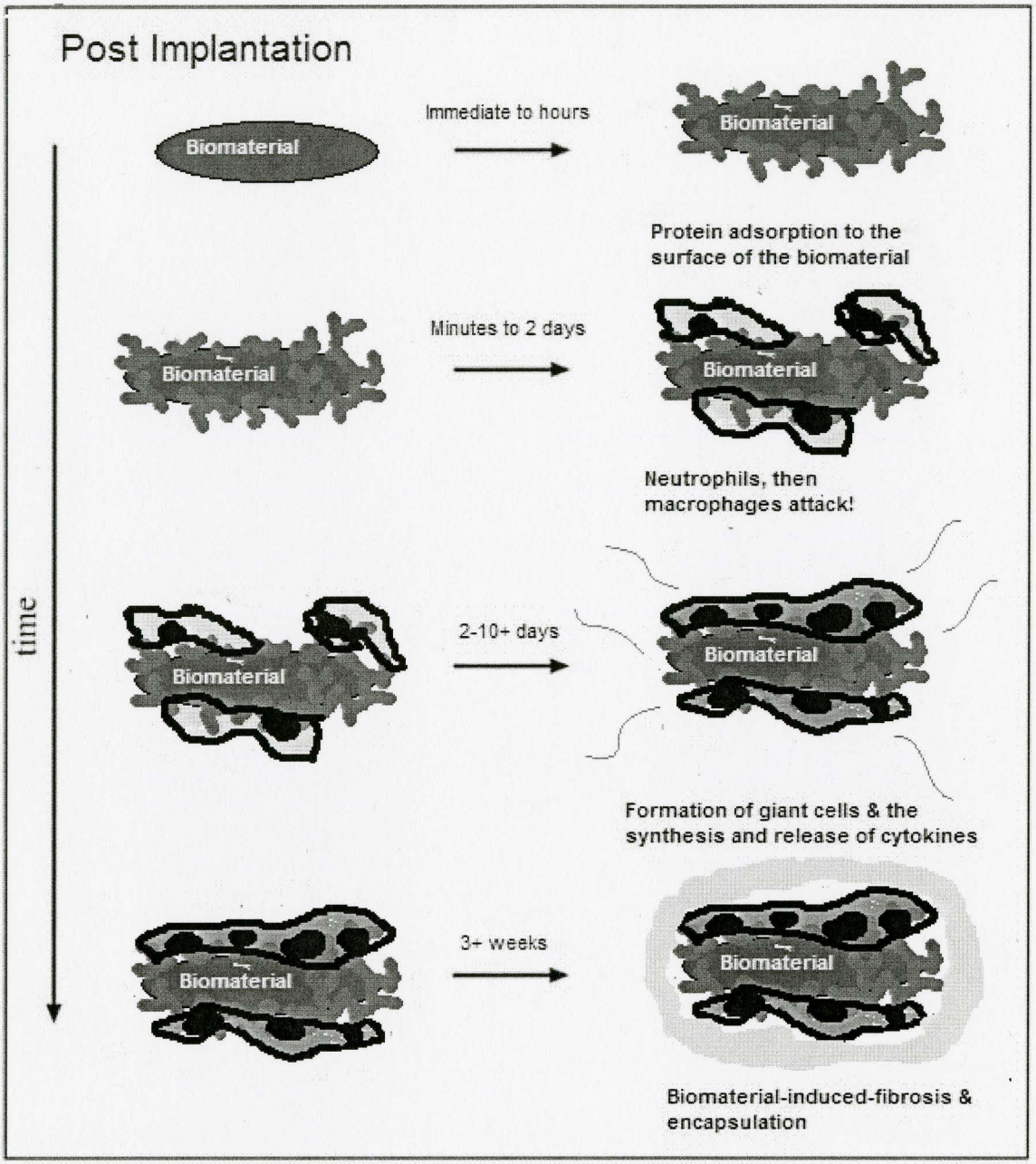

Figure 2.3. An outline of foreign body reaction to an implanted biomaterial. Adapted from Ratner, B., and Bryant, S., Biomaterials: Where We Have Been and Where We Are Going. *Annu. Rev. Biomed. Eng. 6:41-75, 2004*

2.3.1 Protein Adsorption and Complement Activation

After implantation, there is unavoidable immediate blood contact with the implanted biomaterial due to surgery. Proteins are adsorbed to the surface of the biomaterial and a blood-based transient provisional matrix (mostly fibrin) forms around the biomaterial. Acute and chronic inflammation then occurs and the severity of the response is influenced by the type of biomaterial, the location of the implantation and the degree of surgery [46]. We will discuss inflammation induced by biomaterials in more detail in the Inflammation and Fibrosis section.

Protein adsorption is the first interaction that the implanted biomaterial has with the host. A layer of protein is immediately adsorbed to the surface of the biomaterial. The types of protein that are attached to the surface of the biomaterial is influenced by the Vroman Effect [47]. The concentrations, types and conformations of adsorbed and desorbed proteins to the surface of the biomaterial further influence the sequence of reaction from the host toward the implant [48], including the adhesion and activities of cells like monocytes, macrophages and FBGCs (foreign body giant cells). The interaction between the adsorbed proteins like albumin, γ globulin, complement, fibronectin, and fibrinogen, and the receptors on the surface of the inflammatory cells consequently affect the recognition of cells toward the implanted biomaterial [49-51].

The complement system is a major host defense toward infection and foreign substances. Implantation of biomaterials such as catheters, hemodialyzers, oxygenators and stents that have strong blood/material interactions often induce strong complement activation, and cause adverse side-effects such as leukocyte adhesion, clotting and

inflammation [52-54].

2.3.2 Adhesion and Fusion of Macrophages in Fibrous Encapsulation

Monocytes and macrophages are guided to the surface of the biomaterial on the first two to three days of implantation by chemokines and chemoattractants [46,55]. Chemokines are cytokines that are active in cell activation, differentiation and trafficking. They are divided into four major families: CC, CXC, C and CX3C [56]. The platelets and clot on the surface of the biomaterial release chemoattractants such as TGF-β (transforming growth factor beta) to guide macrophages to the implant site [1]. Macrophages themselves also produce more factors, such as PDGF (platelet-derived growth factor) and TNF-α (tumour necrosis factor-alpha), that attract more macrophages to the site [1]. As shown in Figure 2.4 [46], the monocytes first adhere to the biomaterial and differentiate into macrophages and FBGCs. The communication between extracellular matrix and intracellular activities is through integrins. They are receptors on the surface of monocytes/macrophages that mediate the communication between the adsorbed protein matrix on the surface of the biomaterial and the intracellular activities of the cells [57,58]. Through the communication, it allows the cells to interact with the surrounding environment and the cells close by [57]. Integrins are heterodimers and the partnering of the two different subunits α and β gives the receptors variety in function [59]. Macrophage behaviour could be affected by the surface integrin binding to the protein layer on the surface of implanted biomaterial. The intracellular signal conduction could change the cytoskeletal arrangement and structure [60]. The adhesion structure of

the macrophage onto the surface is the podosome. After adhesion, cytoskeletal remodeling occurs and the macrophages spread over the material surface [61]. The properties of the surface of the implanted biomaterial play an important role on what types of protein are absorbed and released over time, and subsequently affect the type of the integrins that bind to the surface [62] and downstream reactions from the host. Integrins not only control the adhesion of the cells to the biomaterial surface, they also play an important role in cell death and cell detachment from the surface of the implant and the remodeling of the regenerated tissue [63].

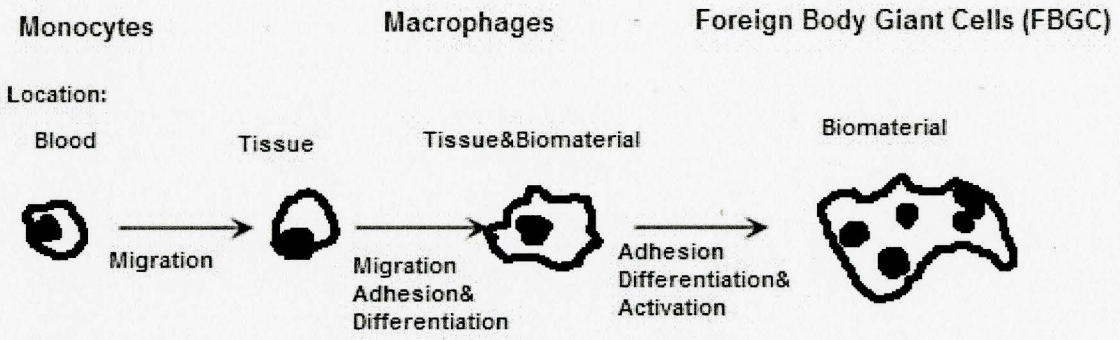

Figure 2.4. The transition and differentiation from monocytes to macrophages, and the fusion of macrophages to FBGCs. Adapted from Ratner, B., and Bryant, S., Biomaterials: Where We Have Been and Where We Are Going. *Annu. Rev. Biomed. Eng. 6:41-75, 2004*

Macrophages adhered on the surface of the biomaterial fuse together and form FBGCs, though the exact mechanism has not been determined. There is evidence that FBGCs have similar antigenic phenotype as monocytes and macrophages [64]. A study

did show that the fusion is material dependent which could be an indication that the adsorbed proteins on the surface of the biomaterial again play an important role in host reaction to the implant [65]. After fusion, macrophages and FBGCs release mediators in an attempt to degrade the implanted biomaterial. The macrophages activated by the implanted biomaterial also affect fibroblast activity by causing over expression of pro-fibrotic ECM (extra cellular matrix) protein fibronectin and by producing pro-fibrotic factors [66,67]. A fibrous capsule is then developed around the surface of the biomaterial and interferes with the function of the implant.

Fibrosis is the end stage of host reaction to the implanted biomaterial. It is also called fibrous encapsulation, a layer of thick, dense, compact collagen. From the aspect of tissue engineering, ideally with the regeneration of the tissue, the biomaterial would be degraded at the same time. Unfortunately, what actually happens is fibrosis induced by the implanted biomaterial. The fibrous layer on the surface of the implanted biomaterial, i) in tissue engineering: blocks the integration and communication between the carried molecules of the scaffold and the surrounding environment; ii) limits the performance of the biomaterial in applications such as biosensors, drug delivery, electrical lead/electrodes, or orthopedic prostheses [54,68-70]. In the current stage of research, we still do not have a full understanding of the mechanism of biomaterial-induced fibrosis.

2.3.3 The NEW Biomaterials

With the understanding of host responses to the implanted biomaterials, scientists/engineers have responded with the design of a new generation of biomaterials.

They could be classified into surface-modified, drug and cell delivery designed, biological inspired, and sophisticated three dimensional biomaterials [42].

Surface-modified biomaterials are designed to overcome the non-specific adsorption of proteins, which as mentioned earlier, could have a downstream influence on host response. The focus has been on modifying the surface of the biomaterial in order to prevent or control the protein interaction and to coat the surface with appropriate signaling molecules. A very commonly studied biomaterial that prevents the adsorption of proteins [71,72] and the adhesion of cells [73,74] is PEG (Poly(ethylene glycol)). An example of surface modification intending to guide and control cell adhesion is the application of arginine-glycine-aspartic acid (RGD) onto the surface of the biomaterial. RGD is a short amino acid chain that is commonly found in proteins like fibronectin, laminin, collagen, and vitronectin [75-78]. A biologically inspired material is designed to mimic the properties and processes that occur in the body. This type of biomaterial can usually be categorized as self-assembled, biomimetic or acellular material [42]. Self-assembled biomaterials are controlled by covalent bonds, hydrogen, ionic or van der Waals bonds. The final three dimensional structure of this type of material is mainly affected by the molecule's length and composition [79]. Biomimetic biomaterials are synthetic biomaterials with biological cues in order to mimic the repairing tissues. As mentioned earlier, both PEG and RGD are used for this purpose. Acellular biomaterials, as mentioned earlier, are biomaterials without cellular components to reduce host immune response.

2.4 Inflammation and Fibrosis

Acute inflammation occurs minutes after the biomaterial is implanted into the body, though it is not clear what the relationship is between biomaterial-induced-inflammation and biomaterial-induced fibrosis. Many studies have been done on pathological fibrosis to understand its mechanism and its relation to inflammation, for example, in pulmonary fibrosis [80].

Traditionally, scientists believed that fibrosis was an end result of repeated repair of the tissue and occurrence of inflammation characterized by flux of cytokines like interleukin-1 (IL-1) and cells like neutrophils [81], but this idea has been challenged recently [82]. TGF-β (transforming growth factor-beta) is a well known pro-fibrotic cytokine, which causes the differentiation of myofibroblasts that play a crucial role in fibrosis [83-85]. IL-1 (interleukin-1) is a pro-inflammatory cytokine and is characteristic of acute inflammation [86-88]. The technique of adenovirus vectors has been used to over-express IL-1 and TGF-β genes in mice. In the mice that had over expression of IL-1, acute inflammation was observed though no significant evidence of fibrosis [88]. In mice over expressing TGF-β, there was fibrosis independent of acute inflammation [89]. In our study, we are interested in how inflammation is related to biomaterial-induced fibrosis.

2.5 SMAD3

SMAD2 and SMAD3 are cytoplasmic signal transducer proteins, and function in mediating the signals from activated TGF-βR(receptor) [90]. Particularly related to

fibrosis, one study has shown that SMAD3 is the key mediator in TGF-β signaling in fibroblasts [91]. The relationships between the SMAD3 gene, TGF-β1 and fibrosis have been widely studied, including in cystic, skin, vascular, renal and pulmonary fibrosis [92-97].

In vascular fibrosis, it was found that mice that stimulated Ang II upregulated TGF-β1 in both human and animal models [98-100]. Even though TGF-β1 receptors are undetectable near fibrotic regions, intracellular SMAD2 and SMAD3 are expressed [101]. Activation of SMAD2 and SMAD3 expression were also found to precede, in vivo, the accumulation of collagen in the thickened intima of human renal arteries obtained from hypertension and atherosclerosis patients. It was further demonstrated that the induction of collagen and CTGF required SMAD3 but not SMAD2 by using vascular SMCs obtained from SMAD2 and SMAD3 knockout mice [102]. In cystic fibrosis, the reduction of SMAD3 protein expression altered TGF-β1-mediated signaling [93]. SMAD3 KO mice did not show a different healing mechanism than WT mice in early time points after skin lesions, but by the 28^{th} day, SMAD3 KO mice had attenuated fibrosis with lower synthesis and accumulation of collagen [94]. Studies have also shown a less severe renal fibrosis induced by unilateral ureteral obstruction in SMAD3 lacking and null mice [92,103]. Pulmonary fibrosis' relationships with SMAD3 gene and TGF-β1 have been studied as well, mostly by Gauldie and colleagues. SMAD3 KO mice are found to be resistant to TGF-β1 mediated fibrosis [104]. Transient gene transfer of TGF-β1 into SMAD3 KO mice did not induce progressive fibrosis, nor did it induce the activation of other fibrogenisis-related genes [105]. Similar results were also found by

another group: SMAD3 deficient mice had attenuated collagen deposition when fibrosis was bleomycin-induced [96].

Studies have shown that SMAD3 KO mice do not develop lung fibrosis induced by bleomycin [106], and the link between fibrosis and TGF-β-SMAD3 signaling pathway has been shown in different tissues [107-114].

2.6 The Scarless Wonder: MRL Mice

The scarless healing ability of MRL mice was first observed by accident as ear punch marks were healed without scarring [115]. These mice are an interbreed of LG mouse, the AKR mouse, the C3H mouse and the C57BL/6 mouse [116]. In several studies, MRL mice showed the potential for scarless repair and regeneration of wounded tissue. This strain of mice has shown scarless regeneration at different sites of the body, including: ears [117,118], myocardial tissue after a cryo-injury [119], and accelerated healing in alkali-burned corneas with reduced inflammation [120], though scarless healing is not always the case. Other studies have also shown that MRL mice did not display the same scarless phenomena, for example, heart injury induced by ischemia-reperfusion [121,122], and dorsal subcutaneous injury [123].

MMPs are involved in many biological pathways and pathological diseases, especially in remodeling responses involving collagen and other extracellular matrix molecules [124-126]. In our study, we focus on MMP-2 and MMP-9. Studies have shown that MRL mice express higher levels of MMP-2 and MMP-9 [127,128], and tissue inhibitors of metalloproteinases (TIMP) levels are lower in MRL mice than in C57BL/6

mice [129]. These two enzymes are secreted by different types of cells in ECM remodeling at injured tissue sites [130,131]. These two MMPs are up-regulated only in migratory, not stationary or adhered, fibroblasts [132]. Other than fibroblasts, neutrophils and macrophages also produce MMPs during the process of wound healing [133]. On a cellular level, both neutrophils and macrophages show positive expression for MMP-2 and MMP-9, though at different time points, and MMPs were found in both pro and active form [134]. The high expression of MMPs gives us a possible explanation of the scarless healing in MRL mice: high concentration MMPs with low concentration of its inhibitor. MMP-9 has also been shown to be involved in fetal scarless healing [135].

Reference List

[1] G. Broughton, J. E. Janis, and C. E. Attinger, The basic science of wound healing, Plast. Reconstr. Surg., 117 (2006) 12S-34S.

[2] M. B. Witte and A. Barbul, General principles of wound healing, Surg. Clin. North Am., 77 (1997) 509-528.

[3] M. Kurkinen, A. Vaheri, P. J. Roberts, and S. Stenman, Sequential appearance of fibronectin and collagen in experimental granulation tissue, Lab Invest, 43 (1980) 47-51.

[4] P. Martin, Wound healing--aiming for perfect skin regeneration, Science, 276 (1997) 75-81.

[5] M. P. Bevilacqua, J. S. Pober, M. E. Wheeler, R. S. Cotran, and M. A. Gimbrone, Jr., Interleukin 1 acts on cultured human vascular endothelium to increase the adhesion of polymorphonuclear leukocytes, monocytes, and related leukocyte cell lines, J. Clin. Invest, 76 (1985) 2003-2011.

[6] T. H. Pohlman, K. A. Stanness, P. G. Beatty, H. D. Ochs, and J. M. Harlan, An endothelial cell surface factor(s) induced in vitro by lipopolysaccharide, interleukin 1, and tumor necrosis factor-alpha increases neutrophil adherence by a CDw18-dependent mechanism, J. Immunol., 136 (1986) 4548-4553.

[7] D. R. Yager and B. C. Nwomeh, The proteolytic environment of chronic wounds, Wound. Repair Regen., 7 (1999) 433-441.

[8] R. Goldman, Growth factors and chronic wound healing: past, present, and future, Adv. Skin Wound. Care, 17 (2004) 24-35.

[9] D. J. Abraham, X. Shiwen, C. M. Black, S. Sa, Y. Xu, and A. Leask, Tumor necrosis factor alpha suppresses the induction of connective tissue growth factor by transforming growth factor-beta in normal and scleroderma fibroblasts, J. Biol. Chem., 275 (2000) 15220-15225.

[10] C. N. Serhan and N. Chiang, Novel endogenous small molecules as the checkpoint controllers in inflammation and resolution: entree for resoleomics, Rheum. Dis. Clin. North Am., 30 (2004) 69-95.

[11] C. Nathan, Points of control in inflammation, Nature, 420 (2002) 846-852.

[12] W. T. Lawrence and R. F. Diegelmann, Growth factors in wound healing, Clin. Dermatol., 12 (1994) 157-169.

[13] G. R. Grotendorst, Y. Soma, K. Takehara, and M. Charette, EGF and TGF-alpha are potent chemoattractants for endothelial cells and EGF-like peptides are present at sites of tissue regeneration, J. Cell Physiol, 139 (1989) 617-623.

[14] M. C. Regan, S. J. Kirk, H. L. Wasserkrug, and A. Barbul, The wound environment as a regulator of fibroblast phenotype, J. Surg. Res., 50 (1991) 442-448.

[15] H. P. Ehrlich and T. M. Krummel, Regulation of wound healing from a connective tissue perspective, Wound. Repair Regen., 4 (1996) 203-210.

[16] A. Desmouliere, A. Geinoz, F. Gabbiani, and G. Gabbiani, Transforming growth factor-beta 1 induces alpha-smooth muscle actin expression in granulation tissue myofibroblasts and in quiescent and growing cultured fibroblasts, J. Cell Biol., 122 (1993) 103-111.

[17] J. Gailit, J. Xu, H. Bueller, and R. A. Clark, Platelet-derived growth factor and inflammatory cytokines have differential effects on the expression of integrins alpha 1 beta 1 and alpha 5 beta 1 by human dermal fibroblasts in vitro, J. Cell Physiol, 169 (1996) 281-289.

[18] G. Henry and W. L. Garner, Inflammatory mediators in wound healing, Surg. Clin. North Am., 83 (2003) 483-507.

[19] F. Grinnell, Fibroblast biology in three-dimensional collagen matrices, Trends Cell Biol., 13 (2003) 264-269.

[20] J. W. Madden and H. C. Smith, The rate of collagen synthesis and deposition in dehisced and resutured wounds, Surg. Gynecol. Obstet., 130 (1970) 487-493.

[21] R. F. Diegelmann, Analysis of collagen synthesis, Methods Mol. Med., 78 (2003) 349-358.

[22] D. M. Simpson and R. Ross, The neutrophilic leukocyte in wound repair a study with antineutrophil serum, J. Clin. Invest, 51 (1972) 2009-2023.

[23] A. Barbul, Immune aspects of wound repair, Clin. Plast. Surg., 17 (1990) 433-442.

[24] J. E. Park and A. Barbul, Understanding the role of immune regulation in wound healing, Am. J. Surg., 187 (2004) 11S-16S.

[25] C. J. Koh and A. Atala, Tissue engineering, stem cells, and cloning: opportunities for regenerative medicine, J. Am. Soc. Nephrol., 15 (2004) 1113-1125.

[26] F. Rosso, G. Marino, A. Giordano, M. Barbarisi, D. Parmeggiani, and A. Barbarisi, Smart materials as scaffolds for tissue engineering, J. Cell Physiol, 203 (2005)

465-470.

[27] F. Chen, J. J. Yoo, and A. Atala, Acellular collagen matrix as a possible "off the shelf" biomaterial for urethral repair, Urology, 54 (1999) 407-410.

[28] B. S. Kim and D. J. Mooney, Development of biocompatible synthetic extracellular matrices for tissue engineering, Trends Biotechnol., 16 (1998) 224-230.

[29] R. O. Hynes, Integrins: versatility, modulation, and signaling in cell adhesion, Cell, 69 (1992) 11-25.

[30] J. E. Bergsma, F. R. Rozema, R. R. Bos, G. Boering, W. C. de Bruijn, and A. J. Pennings, In vivo degradation and biocompatibility study of in vitro pre-degraded as-polymerized polyactide particles, Biomaterials, 16 (1995) 267-274.

[31] T. M. Freyman, I. V. Yannas, R. Yokoo, and L. J. Gibson, Fibroblast contractile force is independent of the stiffness which resists the contraction, Exp. Cell Res., 272 (2002) 153-162.

[32] J. D. Guest, A. Rao, L. Olson, M. B. Bunge, and R. P. Bunge, The ability of human Schwann cell grafts to promote regeneration in the transected nude rat spinal cord, Exp. Neurol., 148 (1997) 502-522.

[33] W. J. Marijnissen, G. J. van Osch, J. Aigner, d. van, V, A. P. Hollander, H. L. Verwoerd-Verhoef, and J. A. Verhaar, Alginate as a chondrocyte-delivery substance in combination with a non-woven scaffold for cartilage tissue engineering, Biomaterials, 23 (2002) 1511-1517.

[34] S. Liu, P. Peulve, O. Jin, N. Boisset, J. Tiollier, G. Said, and M. Tadie, Axonal regrowth through collagen tubes bridging the spinal cord to nerve roots, J. Neurosci. Res., 49 (1997) 425-432.

[35] A. Atala, Tissue engineering for bladder substitution, World J. Urol., 18 (2000) 364-370.

[36] X. M. Xu, S. X. Zhang, H. Li, P. Aebischer, and M. B. Bunge, Regrowth of axons into the distal spinal cord through a Schwann-cell-seeded mini-channel implanted into hemisected adult rat spinal cord, Eur. J. Neurosci., 11 (1999) 1723-1740.

[37] C. H. Lee, A. Singla, and Y. Lee, Biomedical applications of collagen, Int. J. Pharm., 221 (2001) 1-22.

[38] C. E. Schmidt and J. M. Baier, Acellular vascular tissues: natural biomaterials for tissue repair and tissue engineering, Biomaterials, 21 (2000) 2215-2231.

[39] E. Lavik and R. Langer, Tissue engineering: current state and perspectives, Appl. Microbiol. Biotechnol., 65 (2004) 1-8.

[40] R. D. Sayers, S. Raptis, M. Berce, and J. H. Miller, Long-term results of femorotibial bypass with vein or polytetrafluoroethylene, Br. J. Surg., 85 (1998) 934-938.

[41] G. Garellick, H. Malchau, and P. Herberts, The Charnley versus the Spectron hip prosthesis: clinical evaluation of a randomized, prospective study of 2 different hip implants, J. Arthroplasty, 14 (1999) 407-413.

[42] B. D. Ratner and S. J. Bryant, Biomaterials: where we have been and where we are going, Annu. Rev. Biomed. Eng, 6 (2004) 41-75.

[43] J. M. Anderson, Multinucleated giant cells, Curr. Opin. Hematol., 7 (2000) 40-47.

[44] C. Gretzer, L. Emanuelsson, E. Liljensten, and P. Thomsen, The inflammatory cell influx and cytokines changes during transition from acute inflammation to fibrous repair around implanted materials, J. Biomater. Sci. Polym. Ed, 17 (2006) 669-687.

[45] D. T. Luttikhuizen, M. C. Harmsen, and M. J. van Luyn, Cellular and molecular dynamics in the foreign body reaction, Tissue Eng, 12 (2006) 1955-1970.

[46] J. M. Anderson, A. Rodriguez, and D. T. Chang, Foreign body reaction to biomaterials, Semin. Immunol., 20 (2008) 86-100.

[47] L. C. Xu and C. A. Siedlecki, Effects of surface wettability and contact time on protein adhesion to biomaterial surfaces, Biomaterials, 28 (2007) 3273-3283.

[48] C. J. Wilson, R. E. Clegg, D. I. Leavesley, and M. J. Pearcy, Mediation of biomaterial-cell interactions by adsorbed proteins: a review, Tissue Eng, 11 (2005) 1-18.

[49] C. R. Jenney and J. M. Anderson, Adsorbed IgG: a potent adhesive substrate for human macrophages, J. Biomed. Mater. Res., 50 (2000) 281-290.

[50] C. R. Jenney and J. M. Anderson, Adsorbed serum proteins responsible for surface dependent human macrophage behavior, J. Biomed. Mater. Res., 49 (2000) 435-447.

[51] W. J. Hu, J. W. Eaton, T. P. Ugarova, and L. Tang, Molecular basis of biomaterial-mediated foreign body reactions, Blood, 98 (2001) 1231-1238.

[52] K. Kottke-Marchant, J. M. Anderson, K. M. Miller, R. E. Marchant, and H. Lazarus, Vascular graft-associated complement activation and leukocyte adhesion

in an artificial circulation, J. Biomed. Mater. Res., 21 (1987) 379-397.

[53] B. Nilsson, K. N. Ekdahl, T. E. Mollnes, and J. D. Lambris, The role of complement in biomaterial-induced inflammation, Mol. Immunol., 44 (2007) 82-94.

[54] M. B. Gorbet and M. V. Sefton, Biomaterial-associated thrombosis: roles of coagulation factors, complement, platelets and leukocytes, Biomaterials, 25 (2004) 5681-5703.

[55] W. G. Brodbeck, M. Macewan, E. Colton, H. Meyerson, and J. M. Anderson, Lymphocytes and the foreign body response: lymphocyte enhancement of macrophage adhesion and fusion, J. Biomed. Mater. Res. A, 74 (2005) 222-229.

[56] C. Esche, C. Stellato, and L. A. Beck, Chemokines: key players in innate and adaptive immunity, J. Invest Dermatol., 125 (2005) 615-628.

[57] I. Delon and N. H. Brown, Integrins and the actin cytoskeleton, Curr. Opin. Cell Biol., 19 (2007) 43-50.

[58] F. G. Giancotti and E. Ruoslahti, Integrin signaling, Science, 285 (1999) 1028-1032.

[59] G. Berton and C. A. Lowell, Integrin signalling in neutrophils and macrophages, Cell Signal., 11 (1999) 621-635.

[60] D. M. Rose, R. Alon, and M. H. Ginsberg, Integrin modulation and signaling in leukocyte adhesion and migration, Immunol. Rev., 218 (2007) 126-134.

[61] J. Marx, Cell biology. Podosomes and invadopodia help mobile cells step lively, Science, 312 (2006) 1868-1869.

[62] L. T. Allen, M. Tosetto, I. S. Miller, D. P. O'Connor, S. C. Penney, I. Lynch, A. K. Keenan, S. R. Pennington, K. A. Dawson, and W. M. Gallagher, Surface-induced changes in protein adsorption and implications for cellular phenotypic responses to surface interaction, Biomaterials, 27 (2006) 3096-3108.

[63] C. H. Damsky and D. Ilic, Integrin signaling: it's where the action is, Curr. Opin. Cell Biol., 14 (2002) 594-602.

[64] N. A. Athanasou and J. Quinn, Immunophenotypic differences between osteoclasts and macrophage polykaryons: immunohistological distinction and implications for osteoclast ontogeny and function, J. Clin. Pathol., 43 (1990) 997-1003.

[65] J. A. Jones, M. Dadsetan, T. O. Collier, M. Ebert, K. S. Stokes, R. S. Ward, P. A.

Hiltner, and J. M. Anderson, Macrophage behavior on surface-modified polyurethanes, J. Biomater. Sci. Polym. Ed, 15 (2004) 567-584.

[66] A. Gratchev, P. Guillot, N. Hakiy, O. Politz, C. E. Orfanos, K. Schledzewski, and S. Goerdt, Alternatively activated macrophages differentially express fibronectin and its splice variants and the extracellular matrix protein betaIG-H3, Scand. J. Immunol., 53 (2001) 386-392.

[67] E. Song, N. Ouyang, M. Horbelt, B. Antus, M. Wang, and M. S. Exton, Influence of alternatively and classically activated macrophages on fibrogenic activities of human fibroblasts, Cell Immunol., 204 (2000) 19-28.

[68] T. W. Bauer and J. Schils, The pathology of total joint arthroplasty.II. Mechanisms of implant failure, Skeletal Radiol., 28 (1999) 483-497.

[69] V. S. Polikov, P. A. Tresco, and W. M. Reichert, Response of brain tissue to chronically implanted neural electrodes, J. Neurosci. Methods, 148 (2005) 1-18.

[70] P. Wu and D. W. Grainger, Drug/device combinations for local drug therapies and infection prophylaxis, Biomaterials, 27 (2006) 2450-2467.

[71] J. L. Dalsin, B. H. Hu, B. P. Lee, and P. B. Messersmith, Mussel adhesive protein mimetic polymers for the preparation of nonfouling surfaces, J. Am. Chem. Soc., 125 (2003) 4253-4258.

[72] G. P. Lopez, B. D. Ratner, C. D. Tidwell, C. L. Haycox, R. J. Rapoza, and T. A. Horbett, Glow discharge plasma deposition of tetraethylene glycol dimethyl ether for fouling-resistant biomaterial surfaces, J. Biomed. Mater. Res., 26 (1992) 415-439.

[73] W. B. Tsai, J. M. Grunkemeier, C. D. McFarland, and T. A. Horbett, Platelet adhesion to polystyrene-based surfaces preadsorbed with plasmas selectively depleted in fibrinogen, fibronectin, vitronectin, or von Willebrand's factor, J. Biomed. Mater. Res., 60 (2002) 348-359.

[74] M. Shen, I. Garcia, R. V. Maier, and T. A. Horbett, Effects of adsorbed proteins and surface chemistry on foreign body giant cell formation, tumor necrosis factor alpha release and procoagulant activity of monocytes, J. Biomed. Mater. Res. A, 70 (2004) 533-541.

[75] W. D. Staatz, K. F. Fok, M. M. Zutter, S. P. Adams, B. A. Rodriguez, and S. A. Santoro, Identification of a tetrapeptide recognition sequence for the alpha 2 beta 1 integrin in collagen, J. Biol. Chem., 266 (1991) 7363-7367.

[76] J. W. Smith and D. A. Cheresh, The Arg-Gly-Asp binding domain of the

vitronectin receptor. Photoaffinity cross-linking implicates amino acid residues 61-203 of the beta subunit, J. Biol. Chem., 263 (1988) 18726-18731.

[77] M. Aumailley, M. Gerl, A. Sonnenberg, R. Deutzmann, and R. Timpl, Identification of the Arg-Gly-Asp sequence in laminin A chain as a latent cell-binding site being exposed in fragment P1, FEBS Lett., 262 (1990) 82-86.

[78] M. D. Pierschbacher and E. Ruoslahti, Cell attachment activity of fibronectin can be duplicated by small synthetic fragments of the molecule, Nature, 309 (1984) 30-33.

[79] M. R. Caplan, E. M. Schwartzfarb, S. Zhang, R. D. Kamm, and D. A. Lauffenburger, Control of self-assembling oligopeptide matrix formation through systematic variation of amino acid sequence, Biomaterials, 23 (2002) 219-227.

[80] P. A. Ward and G. W. Hunninghake, Lung inflammation and fibrosis, Am. J. Respir. Crit Care Med., 157 (1998) S123-S129.

[81] J. Gauldie, M. Kolb, and P. J. Sime, A new direction in the pathogenesis of idiopathic pulmonary fibrosis?, Respir. Res., 3 (2002) 1.

[82] M. Selman, T. E. King, and A. Pardo, Idiopathic pulmonary fibrosis: prevailing and evolving hypotheses about its pathogenesis and implications for therapy, Ann. Intern. Med., 134 (2001) 136-151.

[83] A. Desmouliere, A. Geinoz, F. Gabbiani, and G. Gabbiani, Transforming growth factor-beta 1 induces alpha-smooth muscle actin expression in granulation tissue myofibroblasts and in quiescent and growing cultured fibroblasts, J. Cell Biol., 122 (1993) 103-111.

[84] J. Gauldie, P. J. Sime, Z. Xing, B. Marr, and G. M. Tremblay, Transforming growth factor-beta gene transfer to the lung induces myofibroblast presence and pulmonary fibrosis, Curr. Top. Pathol., 93 (1999) 35-45.

[85] J. A. Lasky and A. R. Brody, Interstitial fibrosis and growth factors, Environ. Health Perspect., 108 Suppl 4 (2000) 751-762.

[86] L. H. Pan, H. Ohtani, K. Yamauchi, and H. Nagura, Co-expression of TNF alpha and IL-1 beta in human acute pulmonary fibrotic diseases: an immunohistochemical analysis, Pathol. Int., 46 (1996) 91-99.

[87] S. H. Phan and S. L. Kunkel, Lung cytokine production in bleomycin-induced pulmonary fibrosis, Exp. Lung Res., 18 (1992) 29-43.

[88] M. Kolb, P. J. Margetts, D. C. Anthony, F. Pitossi, and J. Gauldie, Transient

expression of IL-1beta induces acute lung injury and chronic repair leading to pulmonary fibrosis, J. Clin. Invest, 107 (2001) 1529-1536.

[89] P. J. Sime, Z. Xing, F. L. Graham, K. G. Csaky, and J. Gauldie, Adenovector-mediated gene transfer of active transforming growth factor-beta1 induces prolonged severe fibrosis in rat lung, J. Clin. Invest, 100 (1997) 768-776.

[90] A. B. Roberts, The ever-increasing complexity of TGF-beta signaling, Cytokine Growth Factor Rev., 13 (2002) 3-5.

[91] Y. C. Yang, E. Piek, J. Zavadil, D. Liang, D. Xie, J. Heyer, P. Pavlidis, R. Kucherlapati, A. B. Roberts, and E. P. Bottinger, Hierarchical model of gene regulation by transforming growth factor beta, Proc. Natl. Acad. Sci. U. S. A, 100 (2003) 10269-10274.

[92] K. Inazaki, Y. Kanamaru, Y. Kojima, N. Sueyoshi, K. Okumura, K. Kaneko, Y. Yamashiro, H. Ogawa, and A. Nakao, Smad3 deficiency attenuates renal fibrosis, inflammation,and apoptosis after unilateral ureteral obstruction, Kidney Int., 66 (2004) 597-604.

[93] T. J. Kelley, H. L. Elmer, and D. A. Corey, Reduced Smad3 protein expression and altered transforming growth factor-beta1-mediated signaling in cystic fibrosis epithelial cells, Am. J. Respir. Cell Mol. Biol., 25 (2001) 732-738.

[94] G. Lakos, S. Takagawa, S. J. Chen, A. M. Ferreira, G. Han, K. Masuda, X. J. Wang, L. A. DiPietro, and J. Varga, Targeted disruption of TGF-beta/Smad3 signaling modulates skin fibrosis in a mouse model of scleroderma, Am. J. Pathol., 165 (2004) 203-217.

[95] D. Sorescu, Smad3 mediates angiotensin II- and TGF-beta1-induced vascular fibrosis: Smad3 thickens the plot, Circ. Res., 98 (2006) 988-989.

[96] J. Zhao, W. Shi, Y. L. Wang, H. Chen, P. Bringas, Jr., M. B. Datto, J. P. Frederick, X. F. Wang, and D. Warburton, Smad3 deficiency attenuates bleomycin-induced pulmonary fibrosis in mice, Am. J. Physiol Lung Cell Mol. Physiol, 282 (2002) L585-L593.

[97] Y. Zhao and D. A. Geverd, Regulation of Smad3 expression in bleomycin-induced pulmonary fibrosis: a negative feedback loop of TGF-beta signaling, Biochem. Biophys. Res. Commun., 294 (2002) 319-323.

[98] S. Rosenkranz, TGF-beta1 and angiotensin networking in cardiac remodeling, Cardiovasc. Res., 63 (2004) 423-432.

[99] C. Kupfahl, D. Pink, K. Friedrich, H. R. Zurbrugg, M. Neuss, C. Warnecke, J.

Fielitz, K. Graf, E. Fleck, and V. Regitz-Zagrosek, Angiotensin II directly increases transforming growth factor beta1 and osteopontin and indirectly affects collagen mRNA expression in the human heart, Cardiovasc. Res., 46 (2000) 463-475.

[100] S. Kim, K. Ohta, A. Hamaguchi, T. Omura, T. Yukimura, K. Miura, Y. Inada, Y. Ishimura, F. Chatani, and H. Iwao, Angiotensin II type I receptor antagonist inhibits the gene expression of transforming growth factor-beta 1 and extracellular matrix in cardiac and vascular tissues of hypertensive rats, J. Pharmacol. Exp. Ther., 273 (1995) 509-515.

[101] N. Kalinina, A. Agrotis, Y. Antropova, O. Ilyinskaya, V. Smirnov, E. Tararak, and A. Bobik, Smad expression in human atherosclerotic lesions: evidence for impaired TGF-beta/Smad signaling in smooth muscle cells of fibrofatty lesions, Arterioscler. Thromb. Vasc. Biol., 24 (2004) 1391-1396.

[102] W. Wang, X. R. Huang, E. Canlas, K. Oka, L. D. Truong, C. Deng, N. A. Bhowmick, W. Ju, E. P. Bottinger, and H. Y. Lan, Essential role of Smad3 in angiotensin II-induced vascular fibrosis, Circ. Res., 98 (2006) 1032-1039.

[103] M. Sato, Y. Muragaki, S. Saika, A. B. Roberts, and A. Ooshima, Targeted disruption of TGF-beta1/Smad3 signaling protects against renal tubulointerstitial fibrosis induced by unilateral ureteral obstruction, J. Clin. Invest, 112 (2003) 1486-1494.

[104] J. Gauldie, M. Kolb, K. Ask, G. Martin, P. Bonniaud, and D. Warburton, Smad3 signaling involved in pulmonary fibrosis and emphysema, Proc. Am. Thorac. Soc., 3 (2006) 696-702.

[105] J. Gauldie, P. Bonniaud, P. Sime, K. Ask, and M. Kolb, TGF-beta, Smad3 and the process of progressive fibrosis, Biochem. Soc. Trans., 35 (2007) 661-664.

[106] J. Zhao, W. Shi, Y. L. Wang, H. Chen, P. Bringas, Jr., M. B. Datto, J. P. Frederick, X. F. Wang, and D. Warburton, Smad3 deficiency attenuates bleomycin-induced pulmonary fibrosis in mice, Am. J. Physiol Lung Cell Mol. Physiol, 282 (2002) L585-L593.

[107] P. Reisdorf, D. A. Lawrence, V. Sivan, E. Klising, and M. T. Martin, Alteration of transforming growth factor-beta1 response involves down-regulation of Smad3 signaling in myofibroblasts from skin fibrosis, Am. J. Pathol., 159 (2001) 263-272.

[108] T. J. Kelley, H. L. Elmer, and D. A. Corey, Reduced Smad3 protein expression and altered transforming growth factor-beta1-mediated signaling in cystic fibrosis epithelial cells, Am. J. Respir. Cell Mol. Biol., 25 (2001) 732-738.

[109] J. Zhao, W. Shi, Y. L. Wang, H. Chen, P. Bringas, Jr., M. B. Datto, J. P. Frederick, X. F. Wang, and D. Warburton, Smad3 deficiency attenuates bleomycin-induced pulmonary fibrosis in mice, Am. J. Physiol Lung Cell Mol. Physiol, 282 (2002) L585-L593.

[110] P. Bonniaud, M. Kolb, T. Galt, J. Robertson, C. Robbins, M. Stampfli, C. Lavery, P. J. Margetts, A. B. Roberts, and J. Gauldie, Smad3 null mice develop airspace enlargement and are resistant to TGF-beta-mediated pulmonary fibrosis, J. Immunol., 173 (2004) 2099-2108.

[111] M. Sato, Y. Muragaki, S. Saika, A. B. Roberts, and A. Ooshima, Targeted disruption of TGF-beta1/Smad3 signaling protects against renal tubulointerstitial fibrosis induced by unilateral ureteral obstruction, J. Clin. Invest, 112 (2003) 1486-1494.

[112] G. Lakos, S. Takagawa, S. J. Chen, A. M. Ferreira, G. Han, K. Masuda, X. J. Wang, L. A. DiPietro, and J. Varga, Targeted disruption of TGF-beta/Smad3 signaling modulates skin fibrosis in a mouse model of scleroderma, Am. J. Pathol., 165 (2004) 203-217.

[113] K. Kobayashi, K. Yokote, M. Fujimoto, K. Yamashita, A. Sakamoto, M. Kitahara, H. Kawamura, Y. Maezawa, S. Asaumi, T. Tokuhisa, S. Mori, and Y. Saito, Targeted disruption of TGF-beta-Smad3 signaling leads to enhanced neointimal hyperplasia with diminished matrix deposition in response to vascular injury, Circ. Res., 96 (2005) 904-912.

[114] A. B. Roberts, The ever-increasing complexity of TGF-beta signaling, Cytokine Growth Factor Rev., 13 (2002) 3-5.

[115] L. D. Clark, R. K. Clark, and E. Heber-Katz, A new murine model for mammalian wound repair and regeneration, Clin. Immunol. Immunopathol., 88 (1998) 35-45.

[116] E. Heber-Katz, J. Leferovich, K. Bedelbaeva, D. Gourevitch, and L. Clark, The scarless heart and the MRL mouse, Philos. Trans. R. Soc. Lond B Biol. Sci., 359 (2004) 785-793.

[117] C. Rajnoch, S. Ferguson, A. D. Metcalfe, S. E. Herrick, H. S. Willis, and M. W. Ferguson, Regeneration of the ear after wounding in different mouse strains is dependent on the severity of wound trauma, Dev. Dyn., 226 (2003) 388-397.

[118] A. S. Colwell, T. M. Krummel, W. Kong, M. T. Longaker, and H. P. Lorenz, Skin wounds in the MRL/MPJ mouse heal with scar, Wound. Repair Regen., 14 (2006) 81-90.

[119] J. M. Leferovich, K. Bedelbaeva, S. Samulewicz, X. M. Zhang, D. Zwas, E. B.

Lankford, and E. Heber-Katz, Heart regeneration in adult MRL mice, Proc. Natl. Acad. Sci. U. S. A, 98 (2001) 9830-9835.

[120] M. Ueno, B. L. Lyons, L. M. Burzenski, B. Gott, D. J. Shaffer, D. C. Roopenian, and L. D. Shultz, Accelerated wound healing of alkali-burned corneas in MRL mice is associated with a reduced inflammatory signature, Invest Ophthalmol. Vis. Sci., 46 (2005) 4097-4106.

[121] Y. S. Oh, L. E. J. Thomson, M. C. Fishbein, D. S. Berman, B. Sharifi, and P. S. Chen, Scar formation after ischemic myocardial injury in MRL mice, Cardiovascular Pathology, 13 (2004) 203-206.

[122] I. Abdullah, J. J. Lepore, J. A. Epstein, M. S. Parmacek, and P. J. Gruber, MRL mice fail to heal the heart in response to ischemia-reperfusion injury, Wound. Repair Regen., 13 (2005) 205-208.

[123] A. H. Beare, A. D. Metcalfe, and M. W. Ferguson, Location of injury influences the mechanisms of both regeneration and repair within the MRL/MpJ mouse, J. Anat., 209 (2006) 547-559.

[124] H. C. Grillo, C. M. Lapiere, M. H. Dresden, and J. Gross, Collagenolytic activity in regenerating forelimbs of the adult newt (Triturus viridescens), Dev. Biol., 17 (1968) 571-583.

[125] E. V. Yang and S. V. Bryant, Developmental regulation of a matrix metalloproteinase during regeneration of axolotl appendages, Dev. Biol., 166 (1994) 696-703.

[126] E. A. Chernoff, C. M. O'Hara, D. Bauerle, and M. Bowling, Matrix metalloproteinase production in regenerating axolotl spinal cord, Wound. Repair Regen., 8 (2000) 282-291.

[127] E. Heber-Katz, J. Leferovich, K. Bedelbaeva, D. Gourevitch, and L. Clark, The scarless heart and the MRL mouse, Philos. Trans. R. Soc. Lond B Biol. Sci., 359 (2004) 785-793.

[128] D. Gourevitch, L. Clark, P. Chen, A. Seitz, S. J. Samulewicz, and E. Heber-Katz, Matrix metalloproteinase activity correlates with blastema formation in the regenerating MRL mouse ear hole model, Dev. Dyn., 226 (2003) 377-387.

[129] D. Gourevitch, L. Clark, P. Chen, A. Seitz, S. J. Samulewicz, and E. Heber-Katz, Matrix metalloproteinase activity correlates with blastema formation in the regenerating MRL mouse ear hole model, Dev. Dyn., 226 (2003) 377-387.

[130] W. C. Parks, Matrix metalloproteinases in repair, Wound. Repair Regen., 7 (1999)

423-432.

[131] B. Steffensen, L. Hakkinen, and H. Larjava, Proteolytic events of wound-healing--coordinated interactions among matrix metalloproteinases (MMPs), integrins, and extracellular matrix molecules, Crit Rev. Oral Biol. Med., 12 (2001) 373-398.

[132] L. Hakkinen, V. J. Uitto, and H. Larjava, Cell biology of gingival wound healing, Periodontol. 2000., 24 (2000) 127-152.

[133] V. W. Yong, C. A. Krekoski, P. A. Forsyth, R. Bell, and D. R. Edwards, Matrix metalloproteinases and diseases of the CNS, Trends Neurosci., 21 (1998) 75-80.

[134] E. Heber-Katz, J. Leferovich, K. Bedelbaeva, D. Gourevitch, and L. Clark, The scarless heart and the MRL mouse, Philos. Trans. R. Soc. Lond B Biol. Sci., 359 (2004) 785-793.

[135] Z. M. Peled, E. D. Phelps, D. L. Updike, J. Chang, T. M. Krummel, E. W. Howard, and M. T. Longaker, Matrix metalloproteinases and the ontogeny of scarless repair: the other side of the wound healing balance, Plast. Reconstr. Surg., 110 (2002) 801-811.

3. Acute Inflammation and Fibrosis Induced by Biomaterials

3.1 Introduction

Inflammation was traditionally thought to have a direct relationship to the severity to fibrosis, though recently studies have challenged such a theory. A lack of definitive evidence was found between inflammation and idiopathic pulmonary fibrosis [1]. Recent findings have shown that acute inflammation and disease fibrosis share the initial pathway, though the severity of acute inflammation does not correlate to the severity of fibrosis [2]. TGF-β (transforming growth factor-beta) is a well known pro-fibrotic cytokine [3,4] and was found to link inflammation to chronic fibrogenesis [5]. The roles that this cytokine plays includes promoting the transformation of fibroblasts to myofibroblasts, inducing matrix protein synthesis, and inhibiting the degradation of deposited collagen [2,5]. IL-1 (interleukin-1) is an inflammatory cytokine which has been found in tissues undergoing chronic inflammation and fibrogenesis in some animal models [2,6-8]. Inhibition of IL-1β at the early stage of fibrosis in animal models was also found to cause attenuation [2,9] which gives the potentially important role of IL-1β in the conversion of inflammation to fibrosis [2]. Though many studies have been done on pathological fibrosis, there has not been much work done toward studying the relationship between inflammation and fibrosis induced by an implanted biomaterial.

In this study, we wanted to investigate the relationship between early stage inflammation and biomaterial-induced fibrosis in vivo. The two materials used were silicone and poly(lactic-co-glycolic acid) (PLGA 85:15). LPS (Lipopolysaccharide) was

applied to intentionally induce acute inflammation. We observed that silicone induced much more severe inflammation and fibrosis than PLGA did. The application of LPS increased the production of IL-1β, though not TGF-β1.

3.2 Experimental Methods

3.2.1 Experimental Outline

We were interested in how the host animal responded to the implanted biomaterial, in particular the fibrotic response. We first implanted a small piece of biomaterial into the peritoneal cavity. After 3 days of implantation, we explanted the material and studied the host response at the cellular and molecular level.

Prior to the explantation of the biomaterial, we injected 2ml of phosphate-buffered- saline (PBS) solution into the peritoneal cavity of the animal. This method was designed to collect the migrated/proliferated cells and secreted cytokines due to the responses toward the implanted biomaterial. The extracted PBS was centrifuged at 900RPM for 6 minutes to separate the supernatant from the cells. The supernatant was analyzed using ELISA (Enzyme-Linked ImmunoSorbent Assay) to find the concentration of cytokines Interleukin-1β (IL-1) and Transforming-Growth-Factor-Beta1 (TGF-β1). After explanting, the retrieved biomaterial was first fixed in 10% formalin for 72 hours then stored in 70% ethanol before being treated with H&E (haematoxylin and eosin) and Mason Trichrome stains.

We used ELISA to find the types of cytokines that were present in the peritoneal cavity where the biomaterial was implanted. We used the histology pictures of tubes cut

in cross-section to observe what cells were attracted to the surface of the biomaterials, and Flow Cytometry to investigate the types of cells that were in the peritoneal cavity of the animal.

3.2.2 Material Preparation

We implanted two different types of biomaterial into the peritoneal cavity of the mice to investigate the mechanism of the fibrotic responses toward the biomaterials. There were four different treatments: 1) a silicone tube, 2) a silicone tube incubated with endotoxin (1mg/ml at 37°C) for two hours prior to the implantation, sterilized silicone tube coated with poly(lactic-co-glycolic acid) (PLGA 85:15), and finally PLGA coated silicone tubes incubated with endotoxin for two hours prior to the surgery. The silicone tubes were purchased from VWR International Co. (Brishane Cal.) and were 5mm in diameter and 5mm long; PLGA 85:15 was purchased from Aldrich (Cat: 430471-5G) The coating of PLGA onto the silicone tube was performed in the biocabinet to ensure the sterility. Also all instruments used in the coating process were sterilized prior to preparation. We first dissolved solid PLGA in 100% acetone with the concentration 1g PLGA/ml acetone. The silicone tube was then dipped into the solution and immediately taken out with tweezers and placed on a sterile glass coverslip to be air dried within the biosafety cabinet. The tube was then removed from the glass coverslip using a blade and stored in a sterilized 1.5ml tube. The selected endotoxin was LPS (Lipopolysaccharides from E. coli, serotype 055:B5; Sigma Chemicals, Oakville ON.) which has been widely used and proven as an effective endotoxin to induce acute inflammatory response [10,11].

We expected to see indications of both acute inflammation and fibrosis induced by the endotoxin and biomaterial at the 3 day time point.

3.2.3 IL-1β & TGF-β concentrations

For our study, we were interested in what types of cytokines and cells were involved in the responses of acute inflammation and fibrosis induced by the endotoxin and biomaterial. In order to do so, we used enzyme-linked immunosorbent assays (ELISAs) to measure the concentrations of certain types of cytokines in the lavage sample from the peritoneal cavity, in particular IL-1β and TGF-β1. IL-1β is a pro-inflammatory cytokine, and the concentration was used as an indication as the severity of acute inflammation. The mouse IL-1β ELISA kit was purchased from BD (Mouse ELISA IL-1β kit, Cat: 550605). The assay was performed according to manufacturer instructions.

We applied the method of ELISA to determine the concentration of TGF-β1 as well. Other studies showed that this cytokine is associated with fibrosis, thus we used the concentration as an indication of the severity of the fibrotic response. The capture, enzyme substrate and detection antibodies were purchased separately from BD Biosciences (Cat. 555052, 555053, 554058). The optimal ratio between the antibodies was determined by titration as described in Techniques for Immune Function Analysis found from BD Biosciences. We applied different ratios of primary and secondary antibodies to measure the concentrations of standard protein. We chose the ratio that gave us the most linear concentration profile of the standard protein as our optimal ratio.

The detail protocol of the procedure is attached in the appendices. We used Anova-Two-Factor-With-Duplication for statistical analysis.

3.2.4 H&E staining and cell layer thickness on material surface

The implanted silicone tubes were retrieved from the peritoneal cavity of the animal 3 days after implantation. Each tube was immediately fixed in 10% formalin for 48hrs then transferred to 70% ethanol until being stained in the histology laboratory. The tube was then embedded in paraffin, cut in cross-section, and stained with H&E in order to observe the types of cells on the material surface under microscopy. We took pictures of each tube and measured the thickness of the cell layers on the surface of the biomaterial. The average cell layer thickness on the surface of the tube was then calculated for each mouse. We then calculated the average cell layer thickness for each treatment (n=5-7).

3.2.5 Collagen

Mason Trichrome staining is a common method to show the magnitude of deposition of collagen near the surface of an implanted biomaterial. We had observed the cross-sectional slides after H&E staining. From the slides of each treatment, only 2-3 samples which gave the most common and clear image of the host response toward the material were selected for Mason's Trichrome staining. Collagen deposition could be observed as the green/blue colour staining, and the intensity of deposition was measured using qualitative score system.

3.2.6 Flow Cytometry

Flow cytometry was used to identify the population distribution of different types of cells contained in the PBS extracted from the peritoneal cavity of the mice. We wanted to study whether the implanted biomaterial caused any shifting of the population distribution. As mentioned earlier, we injected 2ml of PBS into the peritoneal cavity of the mouse to collect the cytokines and cells. The extract was centrifuged in order to separate the supernatant and cells. After removing the supernatant, we resuspended the cells in PBS. We used a hemacytometer to calculate the concentration of the cells, then centrifuged the cells again, and adjusted the volume of PBS in order to bring the concentration of the cells to approximately 1million cells /ml PBS. After adjusting the cell concentration, we then used Flow Cytometry to determine the percentage of different cells in the sample. Using the dot plot with Forward-Scatter (measures the cell size) and Side-Scatter (measures the cell granularity) as the axes, we were able to observe four distinct populations separated from each other. They were assigned as debris/RBC (red blood cells), lymphocytes, monocytes and neutrophils according to the size and granularity. The software FlowJo was used to determine the total cell count. We then eliminated the population of debris/RBC from the cell count to obtain the total cell count of lymphocytes, monocytes and neutrophils. The population percentages of the three types of cells were then calculated.

3.2.7 Animals

The strain of mice used was C57BL/6. We chose to use this strain of mice because from our preliminary study, we did not observe a difference between C57BL/6 and BALB/c mice when C57BL/6 was expected to be the fibrotic-prone strain. All animal work was approved by the Animal Research Ethics Board at McMaster University. Female C57BL/6 mice were purchased from Charles River Breeding Laboratories (Wilmington, MA). The surgeries and implantation were performed when the mice were 4-7 weeks old.

3.2.8 Statistical Analysis

Statistical tests were conducted using Microsoft Excel Data Analysis. Data is presented in mean ± standard error of the mean (sem).

3.3 Results

In our study, we investigated the mechanisms of fibrosis induced by biomaterials. We first implanted two different types of biomaterials (silicone and PLGA) into the peritoneal cavity of the mice. We studied the fibrotic response of the body toward the implanted biomaterial by: i) using ELISA to measure the concentrations of cytokines from the lavage sample; ii) using Flow Cytometry to determine the shifting of cell population distribution in the peritoneal lavage with or without implant; iii) staining the cross-sectionally cut biomaterial to observe the cellular behaviour on the surface of the implanted biomaterials.

3.3.1 Concentration of IL-1 and TGF-β in different treatments

We first wanted to determine whether the application of endotoxin (LPS) to our biomaterials affects the severity of induced acute inflammation. We hypothesized that the application of LPS would induce more severe acute inflammation. Figure 3.1a, shows that the application of endotoxin increased the concentration of IL-1β in the peritoneal cavity for both silicone and PLGA treated mice. IL-1β is known as a pro-inflammatory cytokine. This result confirmed that when LPS was applied, the acute inflammation was more severe. We then compared the concentrations of IL-1β between the two types of biomaterials to determine which type of material caused more severe acute inflammation. We observed that silicone induced higher IL-1β production than PLGA coated silicone. We then compared the two types of biomaterials, both with the application of LPS. Again, silicone with LPS induced higher IL-1β production than PLGA coated silicone with LPS. This result indicated that silicone induced more severe acute inflammation than PLGA in both cases of the material alone or with intentional LPS contamination. The concentration of IL-1β in sham-treated animals was significantly lower than in animals treated with silicone implants, though the same effect was not as significant in the cases when silicone tubes were coated with PLGA. We concluded that the production of IL-1β was more dependent on the type of biomaterial implanted than the application of endotoxin.

We also measured the concentration of TGF-β1 in the supernatant extracted from the peritoneal cavity of the mouse to study the relationship between TGF-β1 production and

the severity of acute inflammation and fibrotic response toward the implanted biomaterial. We hypothesized that the production of TGF-β1 does not have a direct relationship with the production of IL-1β. By comparing the TGF-β1 concentrations in the extracted supernatant from mice that were implanted with a silicone tube to mice that received a PLGA-coated silicone tube, we were able to determine which biomaterial had a stronger effect on TGF-β production. The concentration of TGF-β after implantation with a silicone tube was significantly higher than after implantation with a PLGA-coated silicone tube. The relationship was similar when the two materials were incubated in LPS prior to implantation; a silicone tube incubated with LPS induced higher TGF-β1 production than a PLGA-coated silicone tube incubated in LPS. This helped us to conclude that silicone induced a higher TGF-β1 concentration than PLGA did, despite the additional inflammatory stimulus. This trend was similar to the IL-1β concentration data described earlier. Interestingly, when we compared the TGF-β1 concentrations between the standard and LPS incubated silicone tubes, the silicone tube that had been incubated with LPS induced lower TGF-β production than the standard silicone tube. The relationship was similar when the biomaterial was a silicone tube coated with PLGA. This trend was opposite to that observed with IL-1β, in which LPS induced higher production. By comparing the two different trends observed: i) the concentration of IL-1β increased with the application of endotoxin, and ii) the concentration of TGF-β1 decreased with the application of endotoxin; we concluded that the production of IL-1β decreased with or had no direct relationship to the production of TGF-β1 3 days after implantation of the biomaterial.

3.3.2 Material Surface Cellular Behaviour

We cut the sample in cross-section and treated with H&E stain in order to observe the cell layer thickness on the surface of implanted biomaterials. The severity of acute inflammation and fibrosis induced could be determined by the densities of different cell types attached to the surface of the biomaterial. The cell layer thickness on the solely silicone tubes was observed to be slightly thicker than on silicone tubes incubated in LPS, though not significantly. For both treatments using silicone as the implanted biomaterial, there were severe necrosis and the recruitment of neutrophils and monocytes and macrophages on the surface of the implant. The differences between the cells were observed by comparing the granularity and size of the cells under microscopy. The types of the cells determined with the advice of a histologist and image comparison to a histology text book. Neutrophils were attracted before macrophages as expected (closer to the surface of the biomaterial). The cells were packed very tightly on top of each other (Figure 3.2-a, 2-b), especially in the area occupied with mostly neutrophils. The thickness of cells on the tubes from PLGA-coated silicone (with or without LPS treatment) was much thinner than from silicone or silicone/LPS treatments. Again, there was no significant difference in cell layer thickness between the two treatments (with or without LPS) when using silicone coated with PLGA. The cells were not packed onto the surface of the biomaterial as tightly when compared with the two silicone treatments. The cells observed from the H&E stain were mostly neutrophils with severe necrosis.

Figure 3.3 shows the average thickness of the cell layers due to all four treatments.

As mentioned earlier, the two treatments with the silicone induced much thicker layers of cells than the two treatments with silicone coated with PLGA. Incubation with LPS did not have a significant effect for treatments of the same material. We concluded that the application of LPS did not affect the cell layer thicknesses in either type of material. The cell layer thickness was dependent on the type of material rather than the application of endotoxin.

We used Mason's Trichrome stain to detect whether there was any deposition of collagen after 3 days of implantation. For all four treatments, we did not observe any significant deposition of collagen on the surface of biomaterial. We can conclude that there was no significant amount of collagen deposited after 3 days of implantation.

3.3.3 Cell Type Distribution

We used a flow cytometer to determine the distribution of cell types within the peritoneal cavity. Different cells play different roles in host response toward the implanted biomaterial. We expected to see an early increase in neutrophils due to acute inflammation caused by implanted biomaterial. Neutrophils are the first line of cellular defense when a foreign material is detected in the body. An increase of monocytes due to fibrotic response caused by the implanted biomaterial is expected to be observed in a later time point after implantation. As shown in Figure 5a, we saw silicone/LPS treated mice had the highest percentage of neutrophils in their peritoneal cavity. This observation indicated there was most severe acute inflammation when the mice were treated with silicone/LPS. When the mice were treated with solely silicone or PLGA, the two

treatments induced similar neutrophil productions in the peritoneal cavity of the mice. The mice treated with PLGA/LPS had similar neutrophil percentages to the mice treated with sham surgery which were the two lowest neutrophils population observed.

Macrophages play a significant role in pathological fibrosis. We wanted to investigate if they also have a significant role when the fibrosis is induced by biomaterials. The relative population percentages of monocytes in the four treatments of implantations were similar 3 days after implantation. All four treatments had higher population percentages than sham-operated treated mice, though not significantly. We conclude that the treatment did not affect, or the effect had not been amplified to be observable, the attraction of macrophages to the peritoneal cavity of the mice 3 days after implantation.

Lymphocytes were observed most in sham surgery mice. The results we obtained showed the opposite trend to that observed with neutrophils. Silicone coated with PLGA incubated in LPS had the highest percentage of lymphocytes when there were materials implanted, though not by a significant amount.

Discussion

In our study, we were particularly interested in the fibrotic response from the host toward the implanted biomaterials. Polymeric biomaterials are often used as scaffolds to support cells, and to deliver bioactive molecules in regenerative medicine. These biomaterials are typically designed to provide temporarily mechanical support during the replacement of the damaged tissue. Cells in the construct will interact with the

surrounding environment, and repair the damaged tissues as the biomaterials degrade gradually without toxic effects to the body. Unfortunately, when implanted, biomaterials are treated as foreign objects by the body, and cause various host responses. Often after implantation, collagen is deposited on the surface of implanted biomaterials, known as encapsulation. The collagen layer would then block the communication between the delivered cells and the surrounding environment. The purpose of "regeneration" is defeated when severe fibrosis occurs. Fibrosis is not only relevant in regenerative medicine, it could also cause trouble in tissue/organ replacement, for example, heart valves. In addition, fibrotic capsule formation around medical devices, probes and drug delivery vehicles is likely to interfere with function. Other than fibrosis, acute and chronic inflammation could also occur when the body recognizes the implanted biomaterial as a foreign object [12,13]. Inflammation could further damage the healthy tissues/organs in proximity to the implanted biomaterial [13,14].

The relationship between acute inflammation and pathological fibrosis has been widely studied, though the effect of biomaterials in this context has not been deeply investigated. It is not clear to researchers how the two responses correlate to each other when both are caused by implanted biomaterial. It is generally believed that acute inflammation and pathological fibrosis share the initial common pathway, but the prolonged severity of fibrosis is not determined or related to the severity of acute inflammation. Based on work done in understanding pathological fibrosis, we hypothesized that acute inflammation does not correlate with fibrosis induced by the biomaterials *in vivo*.

In our study, we wanted to investigate how the severity of acute inflammation correlates to the severity of fibrosis induced by implanted biomaterials. We studied how the severity of host responses differs due to different types of implanted biomaterials: PLGA (poly(lactic-co-glycolic acid), 85:15) and silicone. There were four different treatments: 1) a silicone tube, 2) a silicone tube incubated with endotoxin (1mg/ml at 37°C) for two hours prior to the implantation, 3) a sterilized silicone tube coated with PLGA, and finally, 4) a PLGA coated silicone tube incubated with endotoxin for two hours prior to the surgery. We were also interested in how fibrosis would be influenced by intentionally inducing acute inflammation by incubating the biomaterial in endotoxin. The endotoxin we used, LPS (Lipopolysaccharides), has been shown to effectively induce acute inflammations in other studies [10,11]. The biomaterials we used have been well studied in various studies for different purposes. For example, PLGA have been tested as the carrier in drug delivery [15-17] and silicone in breast implants [18,19]. In our experiment, we observed that silicone induced more severe responses than PLGA did, in both acute inflammation and fibrosis, after 3 days of implantation. This conclusion was made by analyzing the cell behaviour on the surface of the implanted biomaterials. We then focused on the relationship between the production of IL-1β (Interleukin-1) and TGF-β1 (Transforming-Growth-Factor-Beta1). We did not observe a correlated relationship between the concentrations of the two cytokines. Finally, we studied the population distribution of three types of cells, neutrophils, monocytes and lymphocytes, in extracted intraperitoneal lavage samples from mice. The population of neutrophil was the highest in silicone/LPS treated mice compared to other treatments after 3 days of

implantation. The populations of monocytes were found to be at higher percentages in all four biomaterial-treated mice than sham-treated mice. .

TGF-β1 is a pro-fibrotic cytokine. It induces the transformation of fibroblasts into myofibroblasts [5,18,20]. Many studies have been done on TGF-β1 in interstitial lung disease. It has been shown that over-expression of TGF-β1 by adenoviral gene transfer leads to progressive fibrosis [21,22]. IL-1β is a pro-inflammatory cytokine [2]. It is found that in pathological fibrosis, IL-1β is necessary to initiate fibrosis but the concentration of IL-1β does not correlate to the occurrence fibrosis; acute inflammation would most likely lead to fibrosis, but it is not required [2]. The concentrations of TGF-β1 and IL-1β in the peritoneal cavity were measured after the implantation to determine the effect of the biomaterial on both cytokines. For the mice that were treated with LPS, biomaterials were incubated in LPS prior to the implantation to induce acute inflammation. From our ELISA results (Figure 3.1a), we have shown that the type of material was a greater factor on affecting the concentration of IL-1β than the endotoxin was. Silicone based treatments had much higher concentrations in both IL-1β and when compared with sham treatments. When comparing the concentrations of IL-1β from the mice that were treated by the "clean" and LPS-treated biomaterials, the treatment with LPS induced a higher concentration than the treatment with "clean" biomaterials. From our TGF-β1 ELISA (enzyme-linked immunosorbent assay) result (Figure 3.1b), when comparing the "clean" biomaterials and LPS applied treatments, it was observed that the LPS applied treatments had much lower TGF-β1 concentration that sterilized. We speculate that the addition of LPS delayed the response of fibrosis because strong acute

inflammation was still in progress. When the TGF-β1 concentrations were compared between the two types of biomaterials, silicone induced higher production than PLGA. This was a similar trend as observed from our IL-1β ELISA results.

The concentrations of IL-1β and TGF-β1 gave us the information on the molecular side of the story, but we also wanted to study the cellular side of the host responses. When an injury occurs, neutrophils are the first group of cells arrive the injured tissue, a sign of the beginning of acute inflammation, followed by monocytes which are the precursors of macrophages. Both play important roles in acute inflammation and immune responses by the host [23]. When injury occurs or when foreign materials enter the body, these defensive cells travel from the peripheral circulation to site of injury and initiate the process of foreign body response and wound healing [23]. We wanted to study the types of cells that were attracted to the surface of the implanted biomaterials. With the help of microscopic images, we were able to calculate the average cell layer thicknesses on the surface of the implanted biomaterial, and to observe what types of cells arrived at the surface of the biomaterial chronologically (by the distance of the cell to the surface of biomaterial) after implantation. The cell layer thicknesses on the surface of silicone tube implants were much thicker than silicone tubes coated with PLGA, and the application of LPS on the surface of biomaterial yielded very little difference in thickness comparing to the "clean" implants. Histology also gave us some information on how the cells behaved on the biomaterial surface. There was denser population of neutrophils, monocytes, macrophages and signs of fibroblasts on the surface of silicone implant. Silicone induced

much more severe acute inflammation and fibrosis compared with PLGA. For the PLGA coated silicone tubes, it seemed that the host response to implanted biomaterial was still at the acute inflammation stage, though not very severe, three days after implantation. The magnitude of acute inflammation, observed from histology, in each treatment agreed with the trend observed in the ELISA results of IL-1β: silicone induced more severe acute inflammation and therefore produced higher IL-1β concentration than PLGA which induced weaker acute inflammation and lower concentration of IL-1β.

We were able to find the percentages of different types of cells collected from the peritoneum of the animals by using flow cytometry. In all of the animal samples, the percentages of neutrophils were well bellow peripheral values. The percentage of neutrophils in sham treated animals was the lowest indicating that the inflammation due to surgery was minimal. Silicone/LPS implanted animals had the highest neutrophil percentage followed by PLGA-coated-silicone- tube-treatment and silicone-treatment.

The percentage of monocytes increased significantly relative to peripheral blood levels. The only factor that all five treatments had in common was the trauma due to surgery, which indicates that the process of fibrosis due to the trauma is still present 3 days post implantation. The percentages of the four treatments with implanted materials are slightly larger than then animals undergoing sham surgery. This result could potentially indicate that the wound healing process of the trauma is dominating over the foreign body response due to the implanted biomaterial.

The percentages of lymphocytes decreased in all samples except for sham treated animals. This suggests that there is no viral infection at the surgical site and a specific

immune response has not been developed in response to the implanted biomaterial.

One concern while designing the experiments was the stability of PLGA coating on the silicone tube. Prior to implantation, the material was incubated in water at 37°C for several days to make sure the coating still wraps around the silicone tube. The PLGA coating was still intact after the implants were retrieved from the animals.

With a better understanding of what cytokines and cells are involved and what role each of them plays, we can better develop a strategy to decrease the severity of fibrotic response due to the implanted material. For our study, in summary, silicone based treatments caused much more severe inflammation and material-induced fibrosis. There were much thicker cell layers on the surface of silicone based implants when compared with PLGA implants. The collagen depositions were also more severe around the surface with the silicone based materials. Finally, wound healing due to surgical trauma seemed to be the dominant response over foreign body response after three days. The host response observed seemed to be at the transition stage between acute inflammation and fibrosis induced by the material. In conclusion, the application of LPS (to induce more sever acute inflammation) did not cause a stronger fibrotic response after 3 days of implantation, and the severity of host responses observed were biomaterial dependent.

List of Figures

Figure 3.1a) Concentrations of IL-1β (pg/ml) in the peritoneal lavage of the mice (n=5-7). Biomaterial implanted mice had higher concentrations than the sham surgery treated mice, though not significant (SE=4.67). Silicone induced higher IL-1β production than PLGA did. And biomaterial with LPS induced higher IL-1β production than sterilized biomaterial implantation.

Figure 3.1b) Concentrations of TGF-β1 (pg/ml) in the peritoneal lavage of the mice (n=5-7). Biomaterial treated mice had higher concentrations of the cytokine than sham surgery treated, though not significant (SE=9.74). The addition of LPS decreased the production of the cytokine when compared to the sterilized biomaterial.

Figure 3.2 The cellular activity on the surface of the biomaterial. **a)** Silicone. **b)** Silicone+LPS. Both treatments were observed with severe necrosis and inflammation. There were severe gathering of neutrophils, macrophages and fibroblasts. The cell layer averages between the two treatments were similar between the two treatments, and the addition of LPS did not make a difference. **c)** PLGA. d) PLGA+LPS. The cell layers were not as thick as the ones on silicone surface, though there was still severe necrosis and inflammatory reactions. Like silicone, the addition of LPS did not make a difference to the cell layer thickness and cellular activities.

Figure 3.3 The cell layer thickness of the four treatments with biomaterials (n=5-7). The cellular layer surfaces were much thicker on silicone than PLGA. The addition of LPS did not make a difference in both biomaterials.

Figure 3.4 The cellular activity on the surface of the implanted biomaterials stained with Mason's Trichrome. **a**) Silicone. **b**) Silicone+LPS. **c**) PLGA. **d**) PLGA+LPS. We did not observe significant deposition of collagen on the treatments.

Figure 3.5 The cell population distributions (n=5-7) of: **a**) Neutrophils. All biomaterial, silicone, silicone+LPS and PLGA+LPS, treatments induced similar neutrophil production, except PLGA+LPS which had similar neutrophil production of sham surgery treated mice. **b**) Monocytes. All biomaterial treated mice had slight higher population than sham surgery treated mice. **c**) Lymphocytes. Sham surgery treated animal had the higher lymphocyte production than all four biomaterial treated mice.

Figure 3.1a)

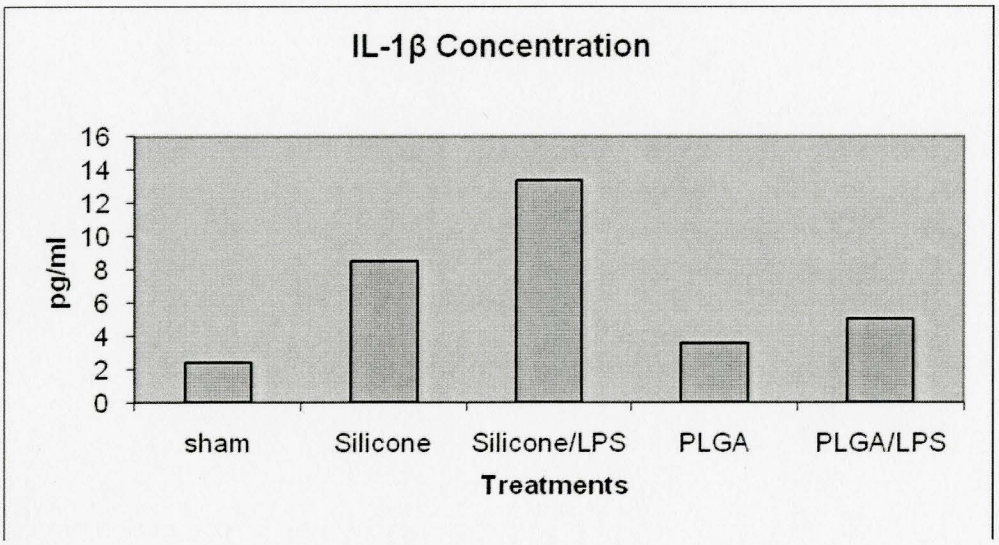

Figure 3.1b)

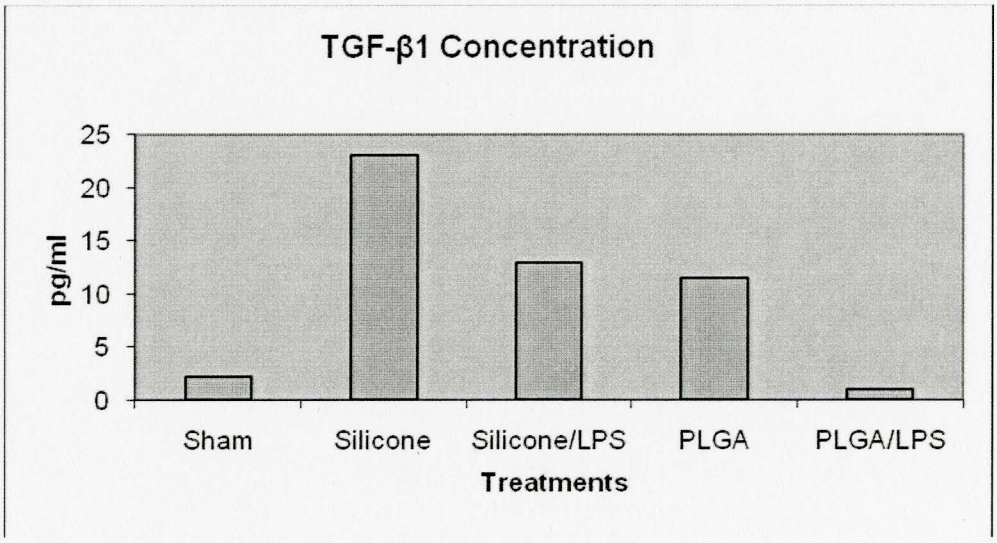

Figure 3.2a)

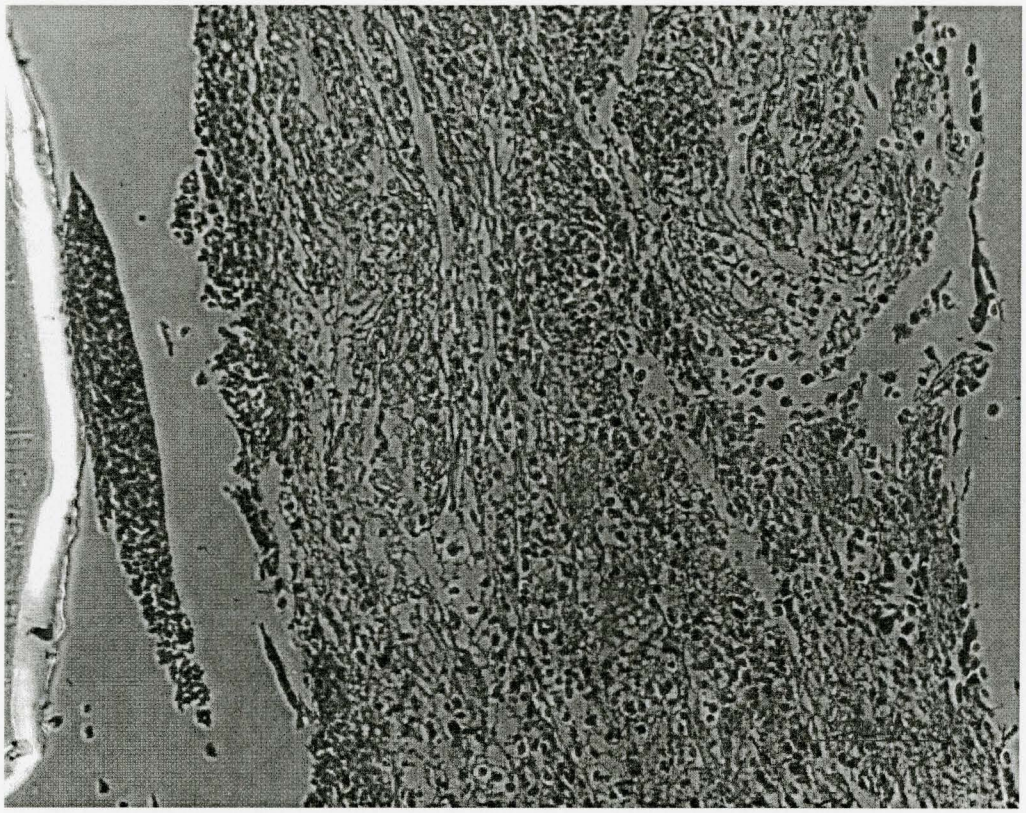

Figure 3.2b)

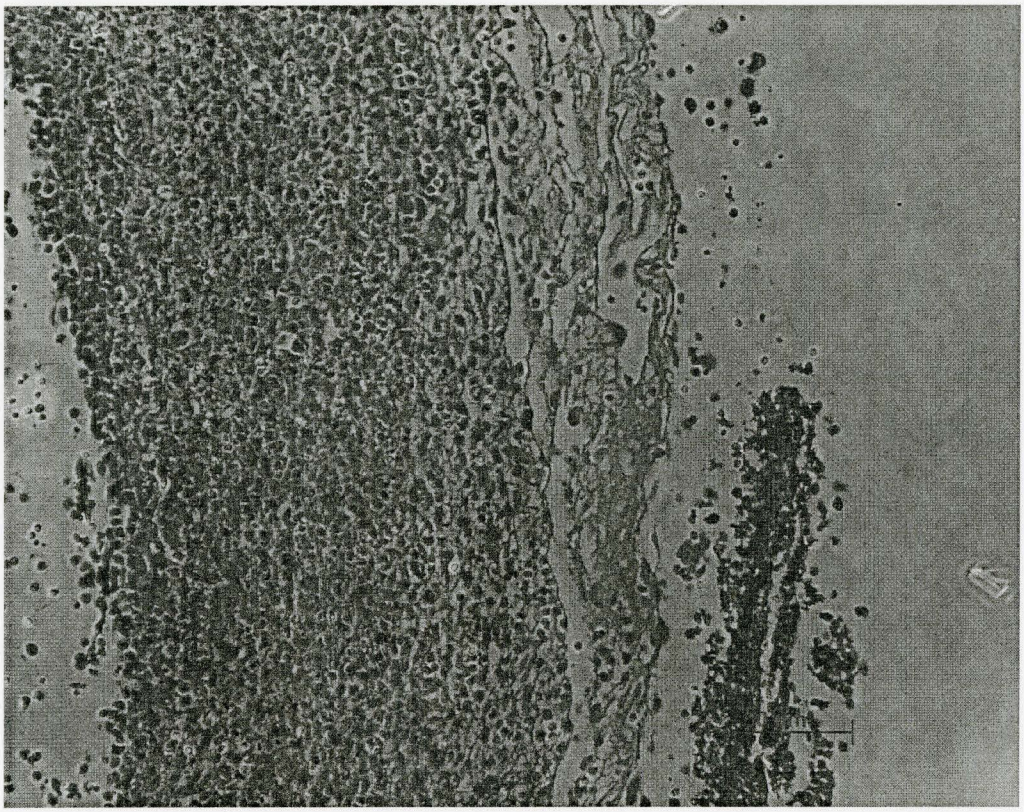

Figure 3.2c)

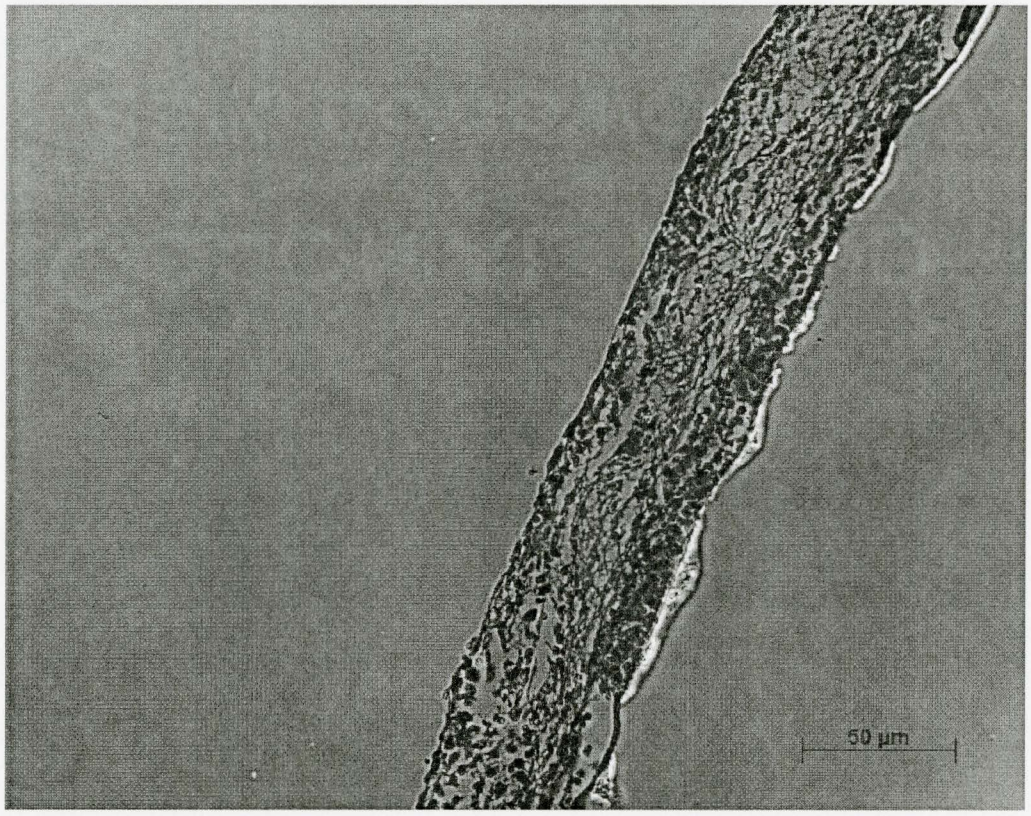

Figure 3.2d)

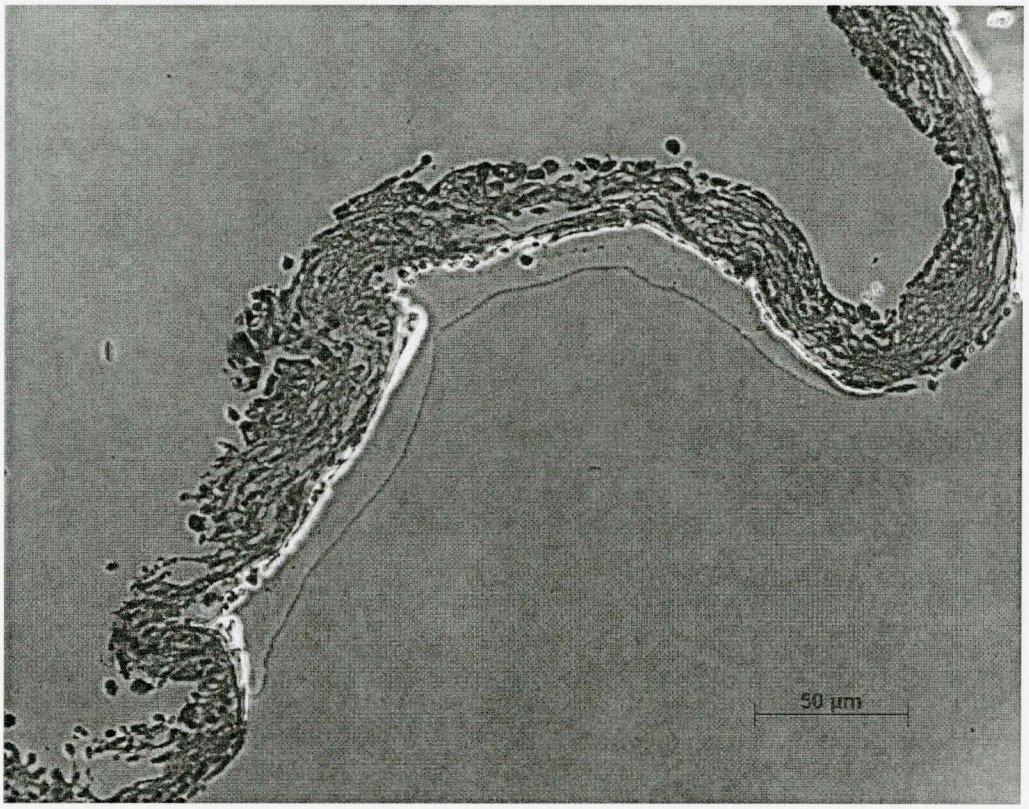

Figure 3.3

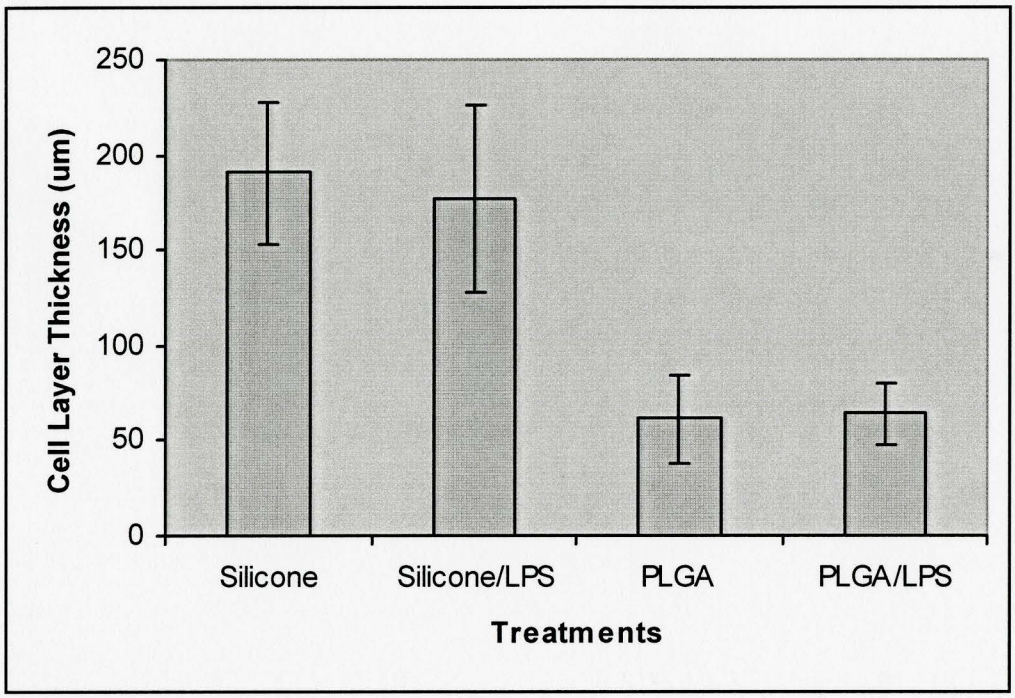
250
200
150
100
50
0
Cell Layer Thickness (um)
Silicone
Silicone/LPS
PLGA
PLGA/LPS
Treatments

Figure 3.4a)

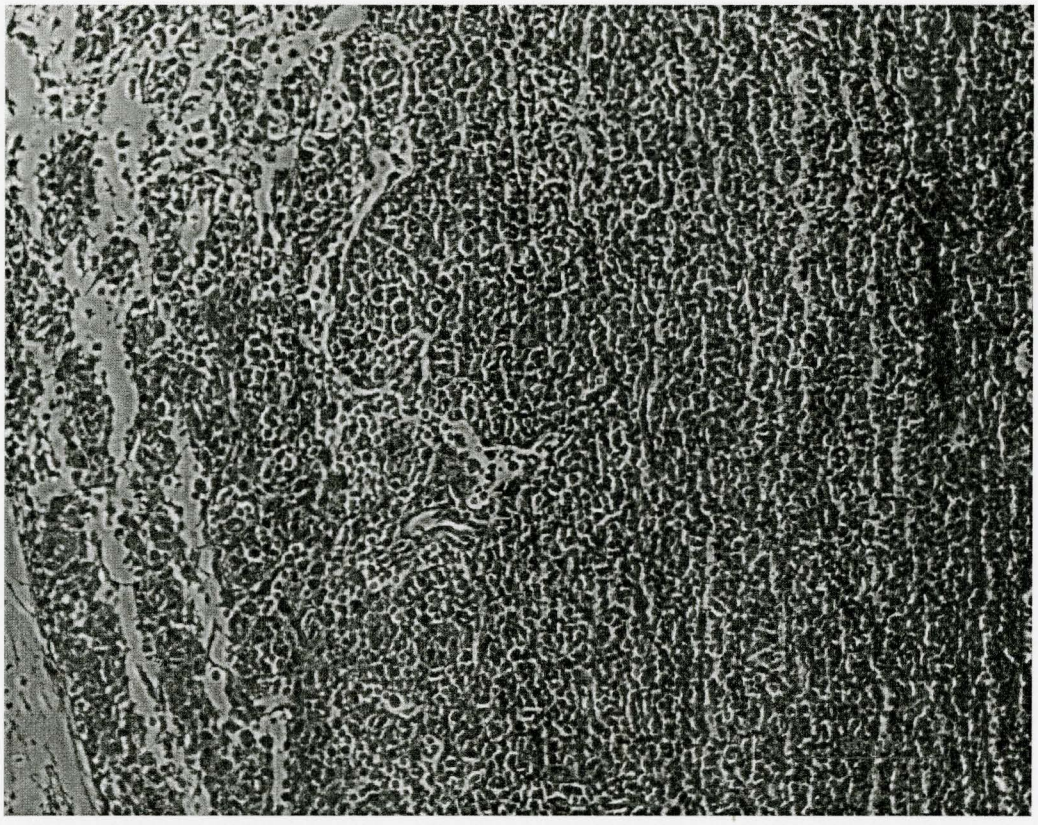

Figure 3.4b)

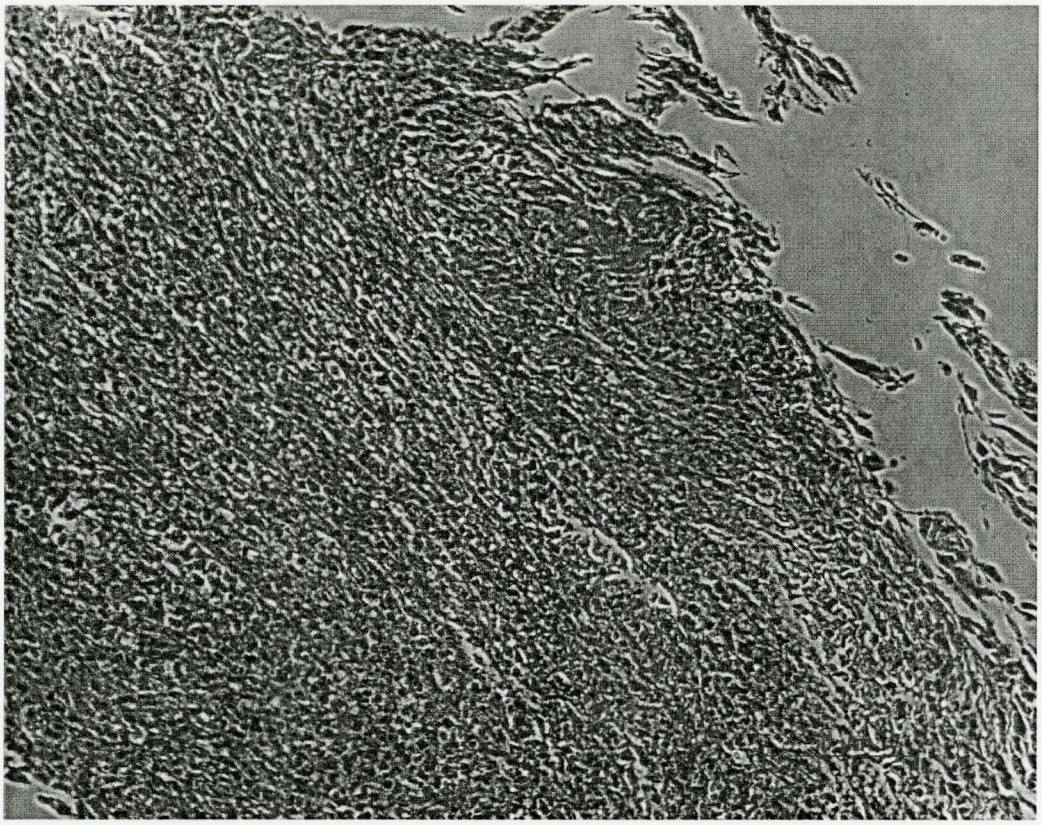

Figure 3.4c)

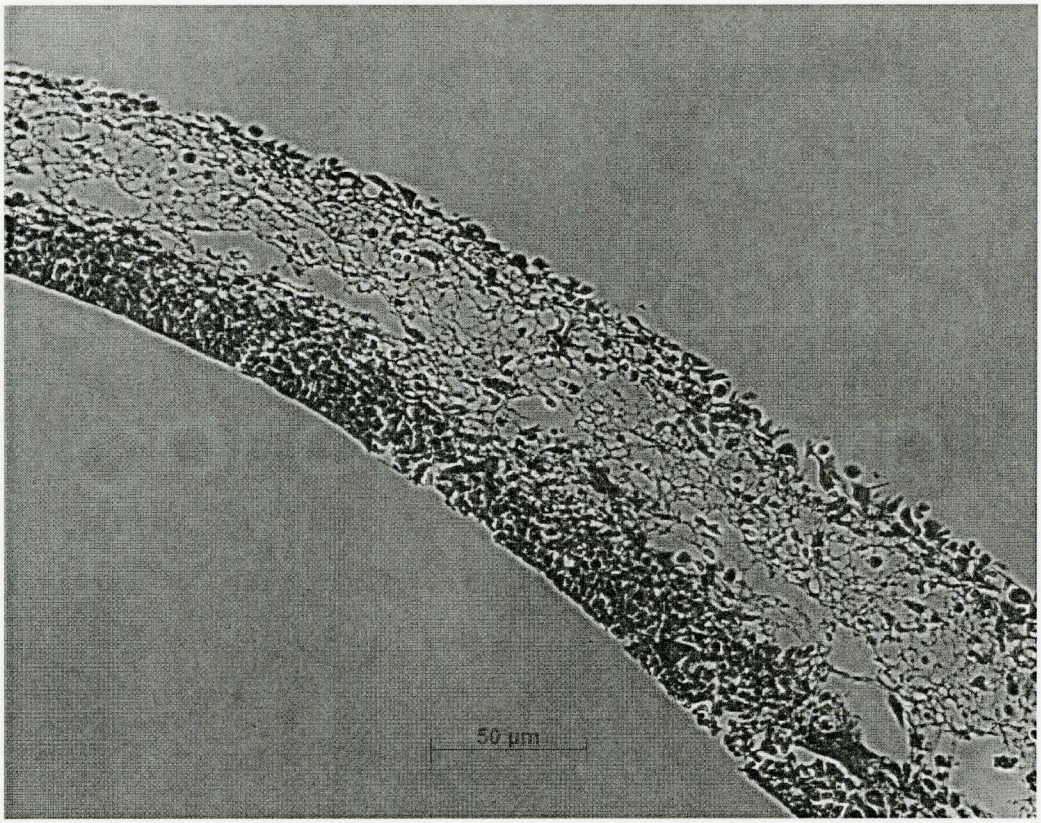

Figure 3.4d)

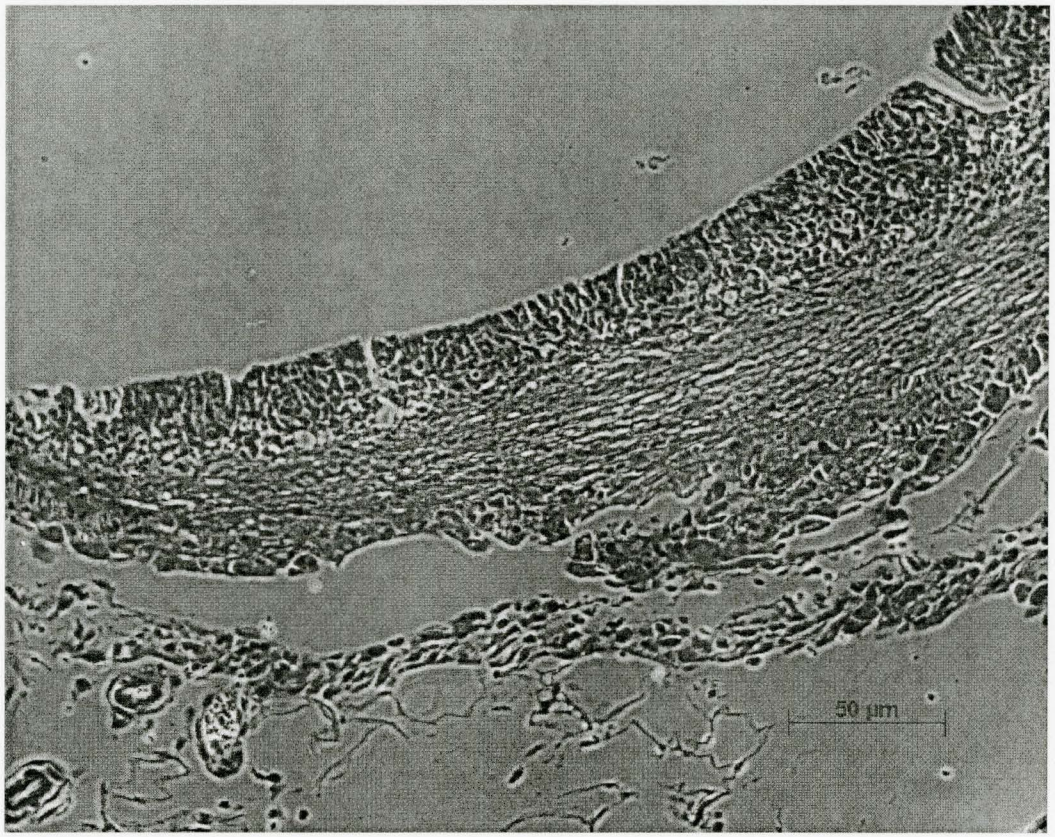

Figure 3.5a)

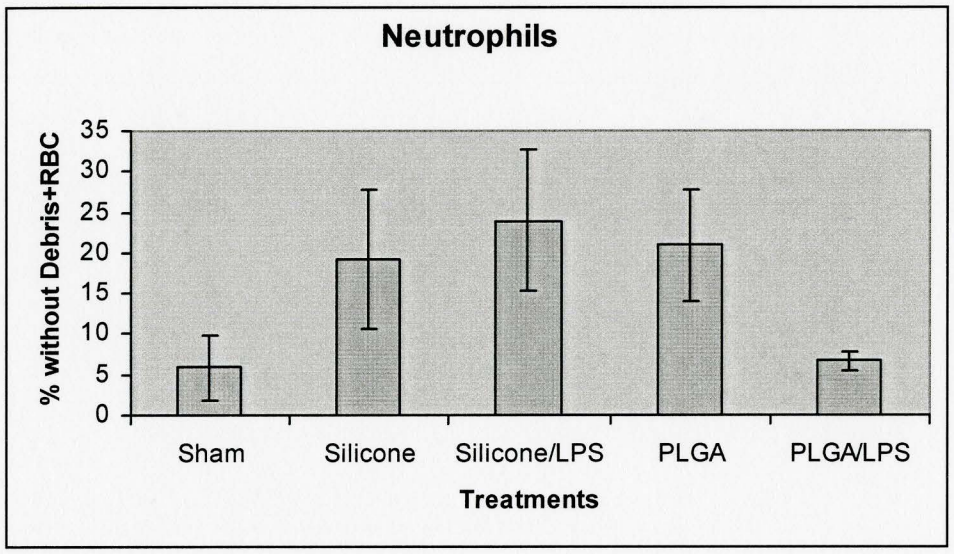

Figure 3.5b)

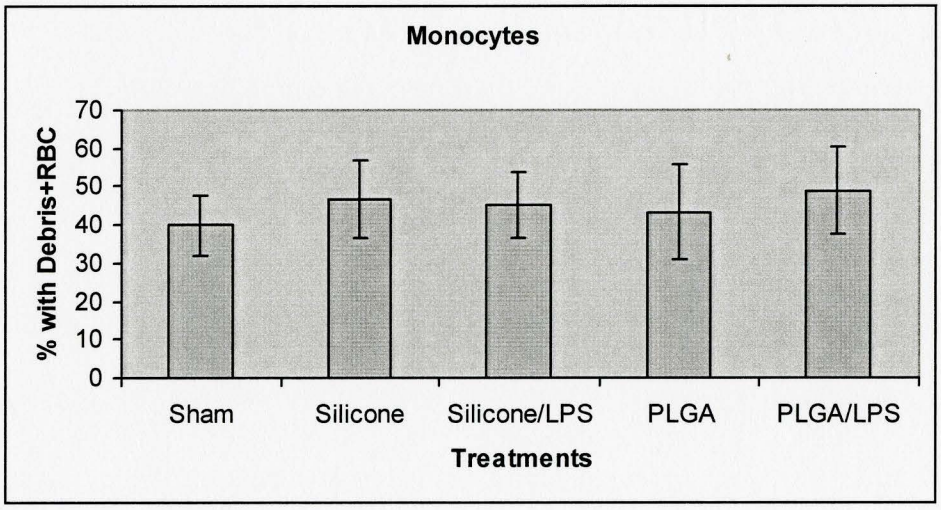

Figure 3.5c)

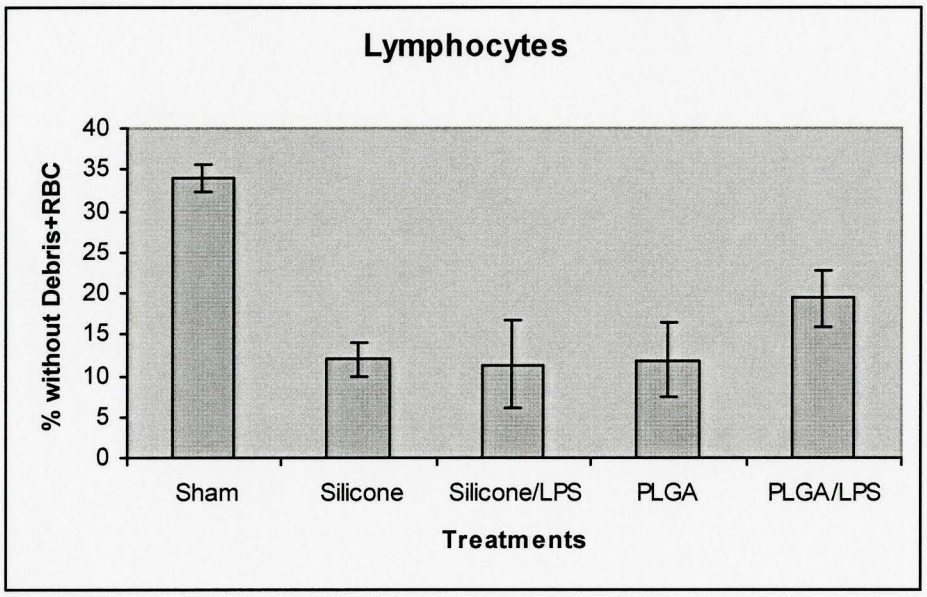
Lymphocytes
% without Debris+RBC
40
35
30
25
20
15
10
5
0
Sham
Silicone
Silicone/LPS
PLGA
PLGA/LPS
Treatments

Reference List

[1] M. Selman, T. E. King, and A. Pardo, Idiopathic pulmonary fibrosis: prevailing and evolving hypotheses about its pathogenesis and implications for therapy, Ann. Intern. Med., 134 (2001) 136-151.

[2] M. Kolb, P. J. Margetts, D. C. Anthony, F. Pitossi, and J. Gauldie, Transient expression of IL-1beta induces acute lung injury and chronic repair leading to pulmonary fibrosis, J. Clin. Invest, 107 (2001) 1529-1536.

[3] J. Gauldie, P. J. Sime, Z. Xing, B. Marr, and G. M. Tremblay, Transforming growth factor-beta gene transfer to the lung induces myofibroblast presence and pulmonary fibrosis, Curr. Top. Pathol., 93 (1999) 35-45.

[4] J. A. Lasky and A. R. Brody, Interstitial fibrosis and growth factors, Environ. Health Perspect., 108 Suppl 4 (2000) 751-762.

[5] P. Bonniaud, P. J. Margetts, K. Ask, K. Flanders, J. Gauldie, and M. Kolb, TGF-beta and Smad3 signaling link inflammation to chronic fibrogenesis, J. Immunol., 175 (2005) 5390-5395.

[6] S. H. Phan and S. L. Kunkel, Lung cytokine production in bleomycin-induced pulmonary fibrosis, Exp. Lung Res., 18 (1992) 29-43.

[7] L. H. Pan, H. Ohtani, K. Yamauchi, and H. Nagura, Co-expression of TNF alpha and IL-1 beta in human acute pulmonary fibrotic diseases: an immunohistochemical analysis, Pathol. Int., 46 (1996) 91-99.

[8] C. J. Johnston, B. Piedboeuf, P. Rubin, J. P. Williams, R. Baggs, and J. N. Finkelstein, Early and persistent alterations in the expression of interleukin-1 alpha, interleukin-1 beta and tumor necrosis factor alpha mRNA levels in fibrosis-resistant and sensitive mice after thoracic irradiation, Radiat. Res., 145 (1996) 762-767.

[9] P. F. Piguet, C. Vesin, G. E. Grau, and R. C. Thompson, Interleukin 1 receptor antagonist (IL-1ra) prevents or cures pulmonary fibrosis elicited in mice by bleomycin or silica, Cytokine, 5 (1993) 57-61.

[10] H. Eutamene, V. Theodorou, F. Schmidlin, V. Tondereau, R. Garcia-Villar, C. Salvador-Cartier, M. Chovet, C. Bertrand, and L. Bueno, LPS-induced lung inflammation is linked to increased epithelial permeability: role of MLCK, Eur. Respir. J., 25 (2005) 789-796.

[11] F. Antonicelli, D. Brown, M. Parmentier, E. M. Drost, N. Hirani, I. Rahman, K. Donaldson, and W. MacNee, Regulation of LPS-mediated inflammation in vivo

and in vitro by the thiol antioxidant Nacystelyn, Am. J. Physiol Lung Cell Mol. Physiol, 286 (2004) L1319-L1327.

[12] J. M. Anderson, A. Rodriguez, and D. T. Chang, Foreign body reaction to biomaterials, Semin. Immunol., 20 (2008) 86-100.

[13] U. M. Gross, Biocompatibility--the interaction of biomaterials and host response, J. Dent. Educ., 52 (1988) 798-803.

[14] J. M. Anderson, A. Rodriguez, and D. T. Chang, Foreign body reaction to biomaterials, Semin. Immunol., 20 (2008) 86-100.

[15] A. Jaklenec, A. Hinckfuss, B. Bilgen, D. M. Ciombor, R. Aaron, and E. Mathiowitz, Sequential release of bioactive IGF-I and TGF-beta 1 from PLGA microsphere-based scaffolds, Biomaterials, 29 (2008) 1518-1525.

[16] B. Liu, S. X. Cai, K. W. Ma, Z. L. Xu, X. Z. Dai, L. Yang, C. Lin, X. B. Fu, K. L. Sung, and X. K. Li, Fabrication of a PLGA-collagen peripheral nerve scaffold and investigation of its sustained release property in vitro, J. Mater. Sci. Mater. Med., 19 (2008) 1127-1132.

[17] S. J. Yoon, K. S. Park, M. S. Kim, J. M. Rhee, G. Khang, and H. B. Lee, Repair of diaphyseal bone defects with calcitriol-loaded PLGA scaffolds and marrow stromal cells, Tissue Eng, 13 (2007) 1125-1133.

[18] V. Molina and Y. Shoenfeld, Infection, vaccines and other environmental triggers of autoimmunity, Autoimmunity, 38 (2005) 235-245.

[19] M. R. McDermott, M. A. Brook, and V. Bartzoka, Adjuvancy effect of different types of silicone gel, J. Biomed. Mater. Res., 46 (1999) 132-134.

[20] J. Gauldie, P. Bonniaud, P. Sime, K. Ask, and M. Kolb, TGF-beta, Smad3 and the process of progressive fibrosis, Biochem. Soc. Trans., 35 (2007) 661-664.

[21] M. Kolb, P. Bonniaud, T. Galt, P. J. Sime, M. M. Kelly, P. J. Margetts, and J. Gauldie, Differences in the fibrogenic response after transfer of active transforming growth factor-beta1 gene to lungs of "fibrosis-prone" and "fibrosis-resistant" mouse strains, Am. J. Respir. Cell Mol. Biol., 27 (2002) 141-150.

[22] P. Bonniaud, P. J. Margetts, M. Kolb, J. A. Schroeder, A. M. Kapoun, D. Damm, A. Murphy, S. Chakravarty, S. Dugar, L. Higgins, A. A. Protter, and J. Gauldie, Progressive transforming growth factor beta1-induced lung fibrosis is blocked by an orally active ALK5 kinase inhibitor, Am. J. Respir. Crit Care Med., 171 (2005) 889-898.

[23] F. Rieder, J. Brenmoehl, S. Leeb, J. Scholmerich, and G. Rogler, Wound healing and fibrosis in intestinal disease, Gut, 56 (2007) 130-139.

4. Fibrosis Induced by Silicone in SMAD3 KO Mice

4.1 Introduction

The relationships between the SMAD3 gene, TGF-β1 and fibrosis have been widely studied, including cystic, skin, vascular, renal and pulmonary fibrosis [1-6]. In vascular fibrosis, it was found in mice that stimulated Ang II upregulate TGF-β1 in both human and animal model [7-9]. Though TGF-β1 receptors are undetectable near fibrotic regions, the intracellular Smad2 and SMAD3 are expressed [10]. Activations of Smad2 and SMAD3 expression were also found to precede, in vivo, the accumulation of collagen in the thickened intima of human renal arteries obtained from hypertension and atherosclerosis patients. It was further demonstrated that the induction of collagen and CTGF required SMAD3 but not SMAD2 by using vascular SMCs obtained from SMAD2 and SMAD3 knockout mice [11]. In cystic fibrosis, the reduction of SMAD3 protein expression altered TGF-β1-mediated signaling [2]. SMAD3 KO mice did not show a different healing mechanism than WT mice in early time points after skin lesions, but by the 28^{th} day, SMAD3 KO mice had attenuated fibrosis with lower synthesis and accumulation of collagen [3]. Studies have also shown a less severe renal fibrosis induced by unilateral ureteral obstruction in SMAD3 lacking and null mice [1,12]. Pulmonary fibrosis' relationships with SMAD3 gene and TGF-β1 have been studied as well, mostly by Gauldie and colleagues. SMAD3 KO mice are found to be resistant to TGF-β1 mediated fibrosis [13]. Transient gene transfer of TGF-β1 into SMAD3 KO mice did not induce progressive fibrosis, nor did it induce the activation of other

fibrogensis-related genes [14]. Similar results were also found by another group: SMAD3 deficient mice had attenuated collagen deposition when fibrosis was bleomycin-induced [5].

In our study, we wanted to investigate the fibrotic behaviour of SMAD3 KO mice when there was a silicone implant in the peritoneal cavity. The results of both SMAD3 KO and WT mice were compared to sham surgery. We observed very little change in the concentration of TGF-β1 in SMAD3 KO after the implantation compared to sham surgery. The cellular behaviour on the surface of the implant was similar between the KO and WT mice. The monocyte populations in the peritoneal lavage from both KO and WT mice showed similar trends as the concentrations of TGF-β1.

4.2 Experimental Methods

4.2.1 Experimental Outline

We were interested in how the host animal responded to the implanted biomaterial, in particular in the fibrotic response, focusing on the role that TGF-β1 plays. We first implanted a small piece of biomaterial into the peritoneal cavity. After 1 and 7 days of implantation, we explanted the material and studied the host response at the cellular and molecular level.

Immediately prior to the explantation of the biomaterial, we injected 2ml of phosphate-buffered- saline (PBS) solution into the peritoneal cavity of the animal for a peritoneal lavage. This method was designed to collect the migrated/proliferated cells and secreted cytokines due to the responses toward the implanted biomaterial. The

extracted PBS was centrifuged at 900RPM for 6 minutes to separate the supernatant from the cells. The supernatant was analyzed using an ELISA (Enzyme-Linked ImmunoSorbent Assay) to find the concentration of Transforming-Growth-Factor-Beta1 (TGF-β1). The cells were analyzed using flow cytometry. After explanting, the retrieved biomaterial was first fixed in 10% formalin for 72 hours then stored in 70% ethanol before being treated with H&E (haematoxylin and eosin) and Mason Trichrome stains.

We used an ELISA method to find the concentration of TGF-β1 in the peritoneal cavity where the biomaterial was implanted. We used the histology pictures of tubes cut in cross-section to observe what cells were attracted to the surface of the biomaterials, and Flow Cytometry to investigate the types of cells that were in the peritoneal cavity of the animal.

4.2.2 Material Preparation

We implanted silicone into the peritoneal cavity of the mice to investigate the mechanism of the fibrotic responses toward the biomaterials. There were two time points (1 and 7 days) to help us observe a more distinct difference between the initial inflammatory host response and fibrosis. The silicone tubes were purchased from VWR International Co. (Brishane Cal.) and were 5mm in diameter and 5mm long. All instruments used in the coating process were sterilized prior to preparation.

4.2.3 TGF-β1 concentration

For our study, we were interested how the concentration of TGF-β1 correlates to

fibrosis induced by polymeric biomaterials. In order to do so, we used enzyme-linked immunosorbent assays (ELISAs) to measure the concentration of the cytokine in the lavage sample from the peritoneal cavity

We applied an ELISA method to determine the concentration of TGF-β1. Other studies showed that this cytokine is associated with pathological fibrosis. The capture antibodies, enzyme substrate and detection antibodies were purchased separately from BD Biosciences (Cat. 555052, 555053, 554058). The optimal ratio between the antibodies was determined by titration as described in Techniques for Immune Function Analysis found from BD Biosciences. We applied different ratios of primary and secondary antibodies to measure the concentrations of standard protein. We chose the ratio that gave us the most linear concentration profile of the standard protein as our optimal ratio. The concentration was determined as in Chapter 2.

4.2.4 H&E staining and cell layer thickness on material surface

The implanted silicone tubes were retrieved from the peritoneal cavity of the animal 1 and 7 days after implantation. Each tube was immediately fixed in 10% formalin for 48hrs then transferred to 70% ethanol until being stained in the histology laboratory. The tube was then embedded in paraffin, cut in cross-section, and stained with H&E in order to observe the types of cells on the material surface under microscopy. We took pictures of each tube to observe the cellular activities on the surface of the implanted biomaterials.

4.2.5 Flow Cytometry

Flow cytometry was used to identify the population distribution of different types of cells contained in the PBS extracted from the peritoneal cavity of the mice. We wanted to study whether the implanted biomaterial caused any shifting of the population distribution. As mentioned earlier, we injected 2ml of PBS into the peritoneal cavity of the mouse to collect the cytokines and cells. The extract was centrifuged in order to separate the supernatant and cells. After removing the supernatant, we resuspended the cells in PBS. We used a hemacytometer to calculate the concentration of the cells, then centrifuged the cells again, and adjusted the volume of PBS in order to bring the concentration of the cells to approximately 1million cells /ml in PBS. After adjusting the cell concentration, we then used Flow Cytometry to determine the percentage of different cells in the sample. Using the dot plot with Forward-Scatter (measures the cell size) and Side-Scatter (measures the cell granularity) as the axes, we were able to observe four distinct populations separated from each other. They were assigned as debris/RBC (red blood cells), lymphocytes, monocytes and neutrophils according to the size and granularity. The software FlowJo was used to determine the total cell count. We then eliminated the population of debris/RBC from the cell count to obtain the total cell count of lymphocytes, monocytes and neutrophils. The population percentages of the three types of cells were then calculated.

Animals

We used SMAD3 KO and WT mice generously provided by Dr. J. Gauldie (ref).

SMAD3 KO mice have shown to have much lower TGF-β1 production and less collagen deposition than WT mice. All animal work was approved by the Animal Research Ethics Board at McMaster University. Female C57BL/6 mice were purchased from Charles River Breeding Laboratories (Wilmington, MA). The surgeries and implantation were performed when the mice were 4-7 weeks old.

4.3 Results

In our study, we investigated the mechanisms of fibrosis induced by biomaterials in SMAD3 KO and WT mice by implanting a biomaterial (silicone) into the peritoneal cavity of the mice. We had eight different treatments: i)1 day implantation in KO; ii) 1 day sham surgery in KO; iii) 7 day implantation in KO; iv) 7 day sham surgery in KO; v) 1 day implantation in WT; vi) 1 day sham surgery in WT; vii) 7 day implantation in WT; viii) 7 day sham surgery in WT. The methods we used to observe and analyze the fibrotic response toward the implanted biomaterial were: i) we used ELISAs to measure the concentration of TGF-β1 from the lavage sample; ii) with the help of Flow Cytometry, we could determine the shifting of cell population distribution in the peritoneal lavage with or without implant; iii) we stained the cross-sectionally cut biomaterial to observe the cellular behaviour on the surface of the implanted biomaterials. We wanted to investigate whether the presence of SMAD3 affect the fibrotic response toward the implanted biomaterial.

The concentration of TGF-β1 did not differ between 1 Day and 7 Day after implantation in KO mice

We wanted to determine if the SMAD3 KO mice respond to the biomaterial differently than WT mice, particularly the concentration of the pro-fibrotic cytokine TGF-β1. We hypothesized that the implantation of a biomaterial (silicone) would not change the TGF-β1 concentration in SMAD3 KO mice compared to sham surgery. From the results as shown in Figure 4.1, we did not observe significant difference on the concentration of TGF-β1 in all four treatments (1 and 7 day, silicone tube implanted and sham surgery) in KO mice. This result could be interpreted that neither the surgery nor the implantation affected the concentration of TGF-β1 in the peritoneal cavity within the time period studied. In WT mice, the concentration of TGF-β1 increased by 3 fold from 1day to 7day when there was an implanted biomaterial. This was expected as a fibrotic response was induced due to the biomaterial.

The cellular behaviour on the surface of silicone were similar in both KO and WT mice

We cut the sample in cross-section and treated it with H&E stain in order to observe the cell layer thickness and cellular behaviour on the surface of implanted biomaterials. The severity of acute inflammation and fibrosis was determined by the densities of different cell types attached to the surface of the biomaterial. On both the 1 day and 7 day time points, there was no significant difference in thickness of the cell layer on the surface of the biomaterial between KO and WT mice as shown in Figure 4.2, though there were some morphological differences observed 7 days after implantation.

After 1 day of implantation, there was about 1 layer of cells on the surface of the biomaterials in both mice, and there was no clear difference in the type of cells recruited. After 7 days of the implantation, some similarities were observed between KO and WT mice. There was severe necrosis and the recruitment of neutrophils, monocytes, macrophages, and multinucleated giant cells scattered on the surface debris of the biomaterial. Edematous of diffuse fibroplasias was also present. In WT mice, we observed slightly more fibrotic deposition on the surface of implanted biomaterial than KO mice. Within the deposition of WT mice, the overall cell density was lower and the cells were more spotted (clusters) compared to KO mice.

The differences between the cells were observed by comparing the granularity and size of the cells under microscopy. The types of the cells were determined with the advice of Dr. Jacek M. Kwiecien. Neutrophils migrated to the surface of the biomaterial before macrophages did as we expected in both WT and KO mice (located closer to the surface of the biomaterial as shown in Figure 4.2). The cells were packed very tightly on top of each other, especially in the area occupied with mostly neutrophils. The cells observed from the H&E stain were mostly neutrophils with severe necrosis. Monocytes and macrophages were also present in the cell layer on the surface of the biomaterial. They were mostly closer to the outer ring of the layer which indicated the later arrival to the site. Randomly located multinucleated giant cells were observed in WT mice, and rarely seen in KO mice.

Cell Type Distribution

We used a flow cytometer to determine the distribution of cell types within the peritoneal cavity. Different cells play different roles in host response toward the implanted biomaterial. We expected to see an early increase in neutrophils due to acute inflammation caused by implanted biomaterial in both KO and WT mice. Neutrophils are the first line of cellular defense when a foreign material is detected in the body. An increase of monocytes caused by the implanted biomaterial is expected to be observed in a later time point after implantation. From Figure 4.3b, we can see the population of neutrophils is much higher in the mice treated with silicone tube, both KO and WT, at both time points of explantation. We conclude that silicone induced severe inflammation, in both KO and WT mice.

Macrophages play a significant role in pathological fibrosis. We wanted to investigate if they also have a significant role when the fibrosis is induced by biomaterials. As shown in Figure 4.3a, we observed a similar trend between the concentrations of TGF-β1 and the population percentages of monocyte, in both WT and KO mice. This could indicate the production of TGF-β1 is related to monocytes or macrophages. The percentages of monocyte population in all the SMAD3 KO mice are around 25-40%. At both time points (1 and 7 days), the Control KO mice had higher monocyte populations than KO mice with silicone implants, though not significant. In WT mice, after 1 day of implantation, control mice had slightly higher monocyte populations than silicone implanted mice; after 7 days of implantation, silicone implanted mice had much higher monocyte population percentage than the control mice. Overall, we did not observe a dramatic change in monocyte population percentages in KO mice

(with or without implant), though the monocyte population percentages were affected by two factors, i) day(s) after surgery, and ii) the implantation of silicone tube.

4.4 Discussion

In our study, we were particularly interested in the fibrotic response from the host toward the implanted biomaterials. Polymeric biomaterials are often used as scaffolds to support cells, and to deliver bioactive molecules in regenerative medicine. These biomaterials are typically designed to provide temporarily mechanical support during the replacement of the damaged tissue. Cells in the construct will interact with the surrounding environment, and repair the damaged tissues as the biomaterials degrade gradually without toxic effects to the body. Unfortunately, when implanted, biomaterials are treated as foreign objects by the body, and cause various host responses. Often after implantation, collagen is deposited on the surface of implanted biomaterials, known as encapsulation. The collagen layer would then block the communication between the delivered cells and the surrounding environment. The purpose of "regeneration" is defeated when severe fibrosis occurs. Fibrosis is not only relevant in regenerative medicine; it could also cause trouble in tissue/organ replacement, for example, heart valves. In addition, fibrotic capsule formation around medical devices, probes and drug delivery vehicles is likely to interfere with function. Other than fibrosis, acute and chronic inflammation could also occur when the body recognizes the implanted biomaterial as a foreign object. Inflammation could further damage the healthy tissues/organs in proximity to the implanted biomaterial (Ratner, et. al).

TGF-β1 is a well known pro-fibrotic cytokine which plays a key role in the process of fibrogenesis [15]; this has been demonstrated in many different organ systems [16]. TGF-β1 causes myofibroblasts to differentiate and induces the expression of connective tissue growth factor (CTGF), therefore increases the production of collagen and fibronectin [17]. Studies have been done to show that transient adenoviral vector-mediated gene transfer of active TGF-β1 leads to progressive and severe fibrosis in different animal models [18-20]. SMAD2 and SMAD3 are cytoplasmic signal transducer proteins, and function in mediating the signals from activated TGF-βR(receptor) [21]; particularly related to fibrosis, one study has shown that SMAD3 is the key mediator in TGF-β signaling in fibroblasts [22]. Studies have shown that SMAD3 KO mice do not develop lung fibrosis induced by bleomycin [23], and the link between fibrosis and TGF-β-SMAD3 signaling pathway has been shown in different tissues [24-31]. We were particularly interested in the relationship between SMAD3, TGF-β1 and fibrosis induced by an implanted biomaterial. We hypothesized that fibrotic response induced by an implanted biomaterial is mediated through the TGF-β and SMAD3 pathway, and there would be a more severe fibrotic response in WT mice than KO.

In our experiments, we used SMAD3 KO and WT mice to observe the difference that the presence of SMAD3 protein made. We implanted a silicone tube into the peritoneal cavity of the mice to observe the responses caused by a foreign object. The time points that we explanted were 1 and 7 days after initial surgery. There were total of 8 treatments. From our results, we found that: i) the silicone implant did not affect the concentration of TGF-β1 in KO mice; ii) the cell layer thickness on the surface of the

implanted silicone tube did not differ between KO and WT mice at either time point, though there was slightly more collagen deposition in WT mice; iii) the population of monocyte/macrophages showed a similar trend as the concentration of TGF-β1 in both KO and WT mice at both time points.

Having a strong understanding of the mechanism of biomaterial-induced fibrosis would help us design a scaffold that could effectively support the cells, and deliver the bioactive molecules to the injured/damaged tissues. After surgery, a fibrous capsule occurs when implanted biomaterials are treated as foreign objects to the body, which defeats the purpose of implantation. TGF-β (isomers: TGF-β1, TGF-β2 and TGF-β3) family proteins function in many different ways in physiology [32]. We were interested in TGF-β1 and the role it plays in fibrosis induced by implanted biomaterials. Studies have been done in pathological fibrosis (ex. idiopathic pulmonary fibrosis, cystic fibrosis); we focused on the investigation of fibrosis induced by implanted biomaterial. In our study, we found that the concentration of TGF-β1 in SMAD3 KO mice changed only slightly between the silicone implanted and sham surgery treated mice. The TGF-β1 concentrations after 1 day of implantation were slightly higher than after 7 days of implantation. In contrast, WT mice, 1 day after surgery, sham surgery treated mice had higher TGF-β1 concentration than silicone tube implanted mice; 7 days after surgery, silicone tube implanted mice had a TGF-β1 concentration much higher than sham surgery mice by more than 2 fold. We observed a similar trend in monocyte population percentages. This observation agreed with the relationship between TGF-β1 and monocytes/macrophages: TGF-β cytokines are chemo-attractants which direct monocytes

(then transformed to macrophages) to the site [33]; and the macrophage itself secretes many different types of cytokines as well, including TGF-β [34]. Also, studies have shown that SMAD3 KO mice lack expressions of fibrosis related genes; TGF-β1 mRNA expression did not increase after rTGF-β1 exposure [35]. This could be an explanation of why in WT mice, the concentrations of TGF-β1 and the cell population percentages of macrophage show a similar trend in different treatments. We could conclude that biomaterial-induced fibrosis shares a similar relationship between macrophages and TGF-β1 with pathological fibrosis. There are also: i) other chemokines and cytokines that macrophages secrete and release [36,37]; ii) cells other than macrophages that TGF-β1 attract and direct to the site [38,39], which would add more complex mechanisms to the process that results in biomaterial-induced fibrosis.

From our histological images, we observed similarities and differences on the implanted biomaterial surface between KO and WT mice. After 1 day of implantation, we observed approximately one layer of cells on the surface of the biomaterial in both mice. We were expecting more layers and varieties of cells; generally acute inflammation occurs minutes to hours after implantation. We suspect that it was due to the location of the implantation. Most implants are blood-contacting, e.g. pacemaker and artificial heart valves. In our study, the implanted silicone is located in the peritoneal cavity of the animal. During surgery, the blood contact was minimal. The lack of blood contact could cause a lower concentration in protein absorption and cells around the site of implantation, therefore the duration it takes for cells such as neutrophils and macrophages to travel to the injury site (location of implant) could be elongated. The similarity of cell type

(neutrophil) on the surface of the implanted biomaterial gave us an indication that acute inflammation occurred in both KO and WT after 1 day of implantation. The absent of SMAD3 gene did not make a difference.

Another similarity we observed was the debris thickness on the surface of the implanted biomaterial between WT and KO mice 7 days after implantation. In both cases, there were neutrophils, monocytes/macrophages, and diffuse fibroplasias, though there was slight more deposition of collagen on the surface of the biomaterial in WT mice. From our ELISA results, we observed the presence of TGF-β1 in all mice, though WT mice treated with 7 day silicone tube implantation had the highest concentration. This gave us indication the development of fibrous capsule does not require a great concentration of TGF-β1. It is possible that when the biomaterial is implanted, it takes WT mice a shorter time to develop the capsule, and the process is decelerated in KO mice due the lack of TGF-β1, though still progressing.

Another difference we observed was that there were random foreign body giant cells (FBGC) scattered in the debris in WT mice, but not KO mice. This indicated that the macrophages on the surface of the biomaterial in KO mice did not fuse. Cell-cell fusion is a complicated event and studies have shown that both Interleukin(IL)-4 and Interleukin(IL)-13 play important roles in macrophage fusion [40,41]. SMAD3 signaling might have an effect in the production of the two cytokines. A further investigation in the production of the two cytokines would give a more clear and conclusive answer.

Acute inflammation usually occurs minutes to hours after injury happens, in our case, due to the implanted biomaterial. At both time points (1 and 7 days), mice treated

with a silicone implant had a much higher neutrophil population percentage than sham surgery treated mice. This observation gave us additional evidence that silicone induced a strong inflammatory response. In both KO and WT mice, the population percentage of neutrophils was slightly higher at 1 day than 7 days after implantation. This could be an indication that after 7 days of implantation, the host response had switched from acute inflammation. In comparing of the population percentages between KO and WT mice that were treated with silicone implants, at both time points, WT mice had a slightly higher level than KO mice.

In conclusion, the relationship between TGF-β and macrophages was confirmed and agreed with current literature: i) TGF-β1 acted as a chemo-attractant that guided macrophages to the implanted site; ii) macrophages secrete and release TGF-β. The fibrotic response toward the implanted biomaterials occurred in both KO and WT mice. There was a slight difference in the severity of collagen deposition, though not as great as expected. The difference in the presence of FBGCs was not expected. Further investigations including in the concentrations of different types of cytokines and chemokines would give us a more clear answer.

List of Figures

Figure 4.1 Concentration of TGF-β1 in different treatments. The concentration of this cytokine did not change with the implanted biomaterial while it was not the case with WT mice. The concentration of TGF-β1 of 1 day implantation of silicone tube was less than 1 day with sham surgery. The trend was opposite when the two strains of mice were treated with implantation for 7 days. The silicone tube implanted mice had much higher concentration of TGF-β1 than sham surgery treated mice.

Figure 4.2 The cellular behaviour on the surface of the biomaterial. **A)** 1 day of implantation in SMAD3 KO mice. **B)** 1 day of implantation in WT mice. There was not difference in cellular behaviour and cell layer thickness between the two strains. **C)** 7 days of implantation in SMAD3 KO mice. **D)** 7 days of implantation in WT mice. There was severe necrosis and the recruitment of neutrophils, monocytes, macrophages, and multinucleated giant cells scattered on the surface debris of the implanted biomaterial in both mouse strain, we did not observe severe difference. In WT mice, we observed slightly more fibrotic deposition than KO mice. Within the collagen deposition of WT mice, the overall cell density was lower and the cells were more spotted compared to KO mice.

Figure 4.3 Population distribution of **A**) Monocytes. The control SMAD3 KO mice had higher monocyte populations than silicone implant treated KO mice at both time points (1 and 7 days). In WT mice, after 1 day of implantation, control mice had slightly higher monocyte populations than silicone implanted mice; after 7 days of implantation, silicone implanted mice had much higher monocyte population percentage than the control mice. We observed a similar trend between the concentrations of TGF-β1 and the population percentages of monocyte, in both WT and KO mice. B) Neutrophils. Silicone implant treated mice (both SMAD3 KO and WT) had higher neutrophil populations that sham surgery treated mice which indicated that silicone induced inflammation.

Figure 4.1

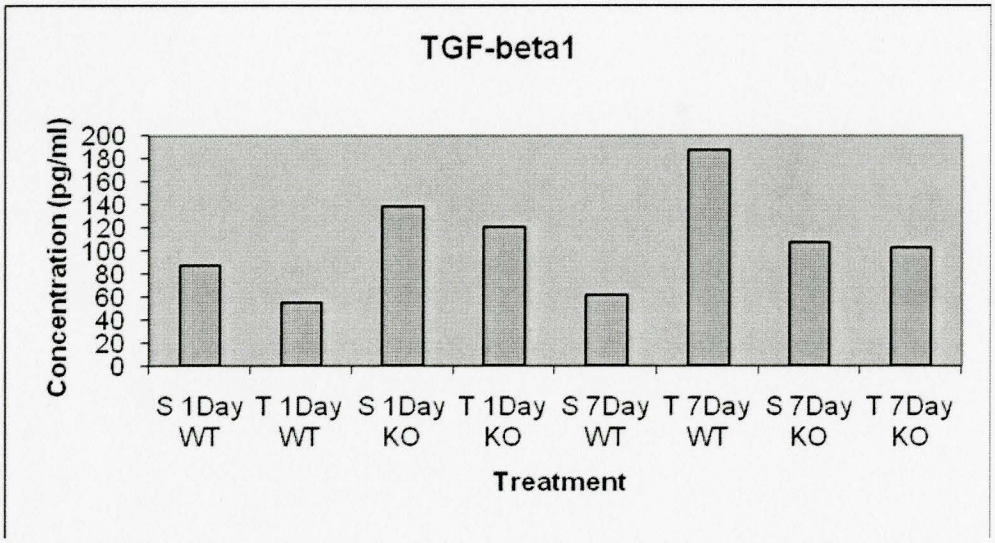
TGF-beta1
Concentration (pg/ml)
200
180
160
140
120
100
80
60
40
20
0
S 1Day WT
T 1Day WT
S 1Day KO
T 1Day KO
S 7Day WT
T 7Day WT
S 7Day KO
T 7Day KO
Treatment

Figure 4.2A)

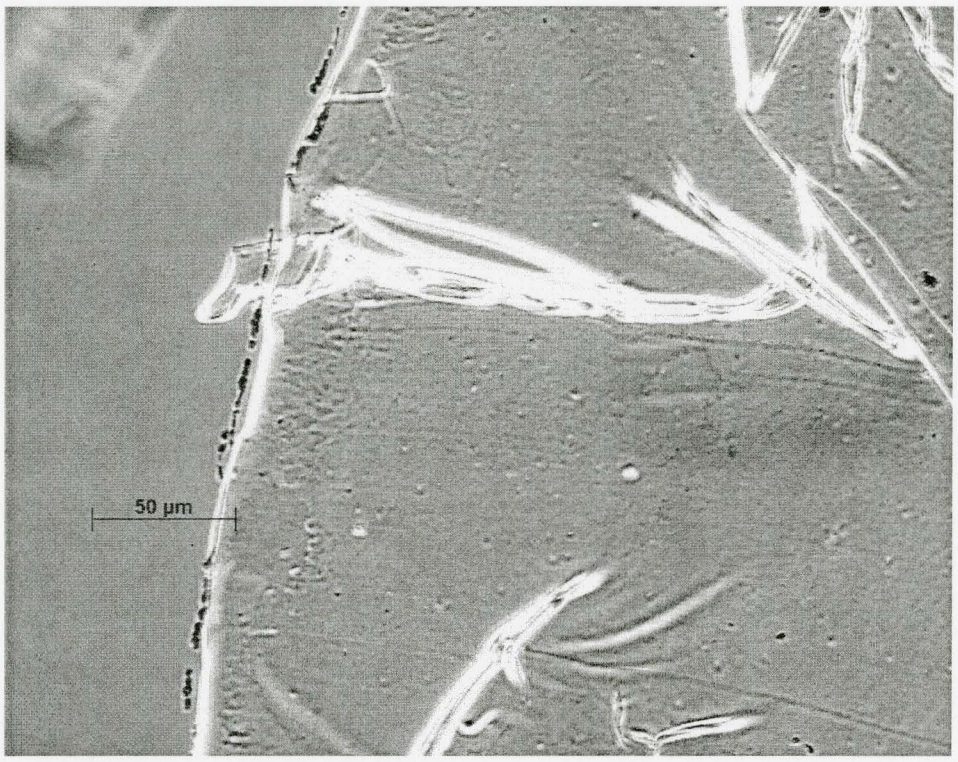

Figure 4.2B)

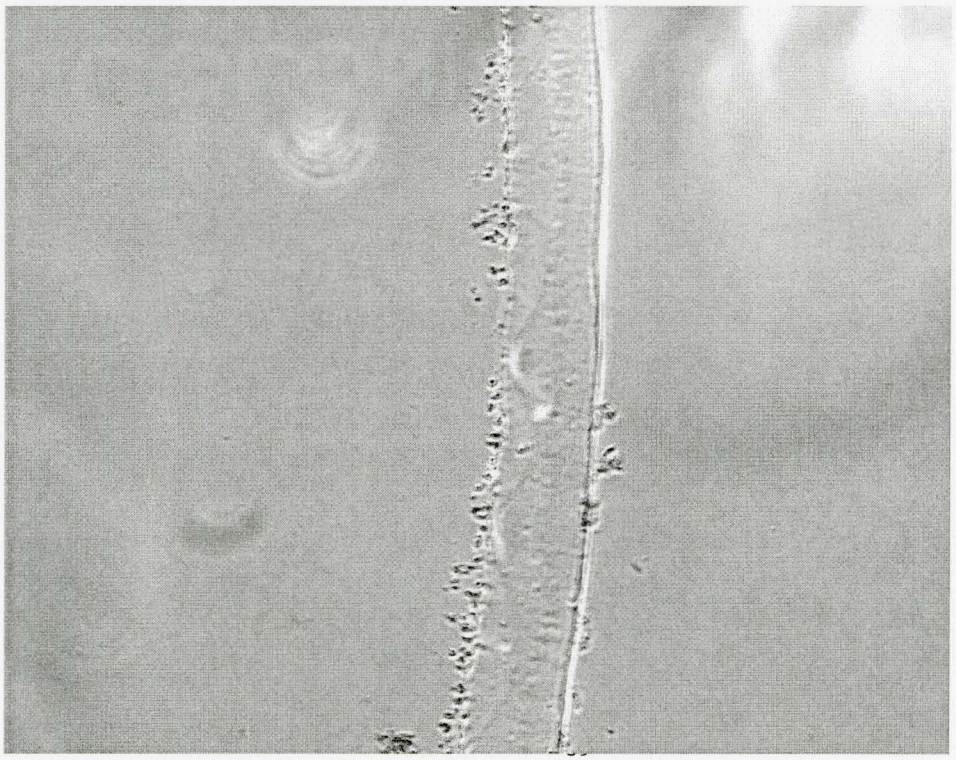

Figure 4.2C)

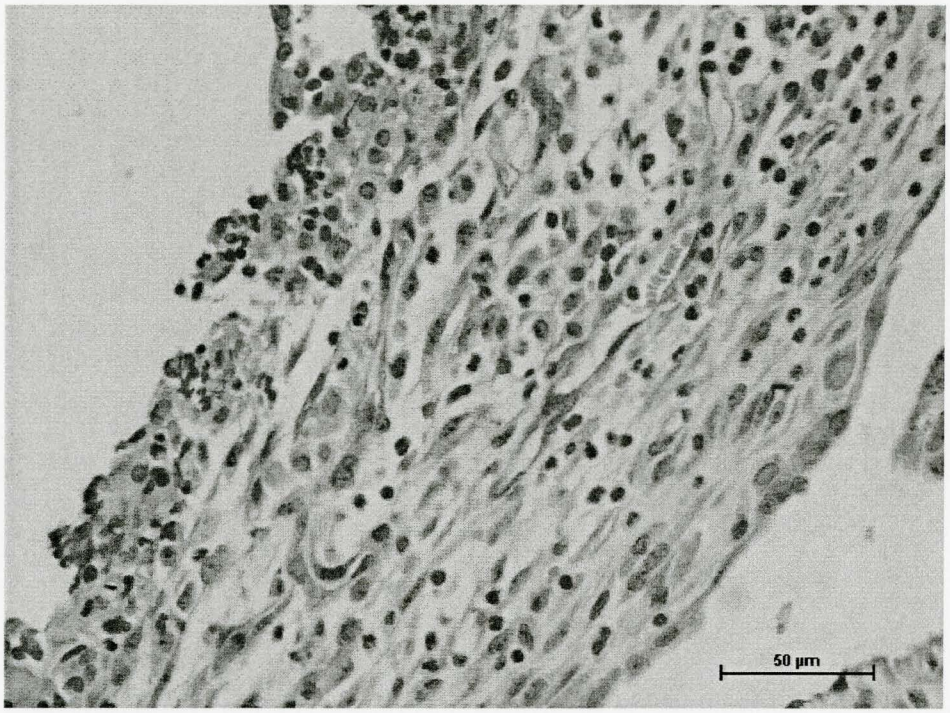

Figure 4.2D)

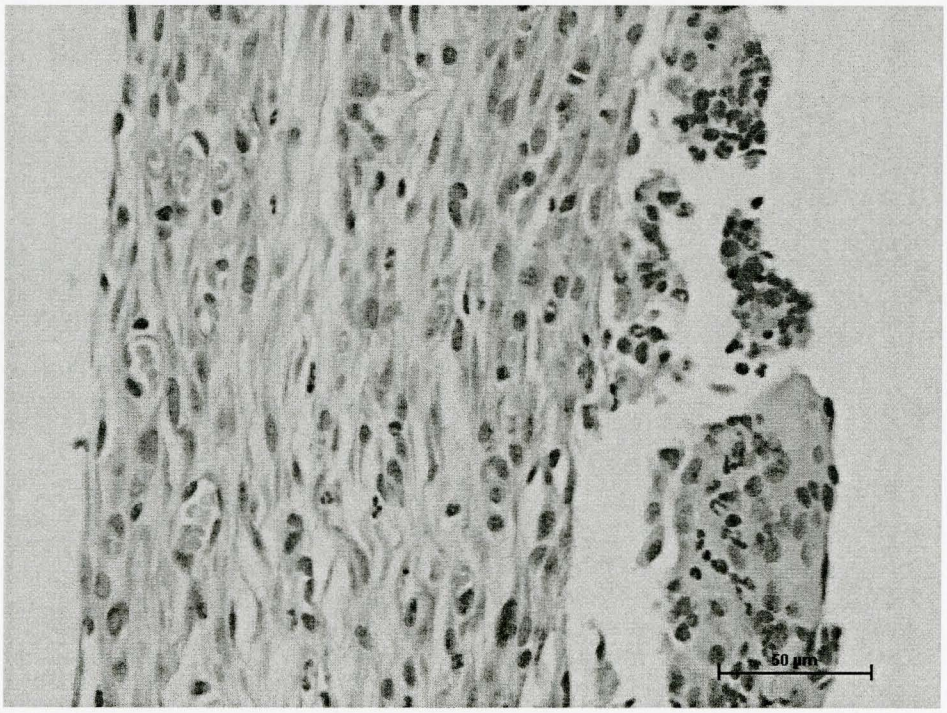

Figure 4.3A)

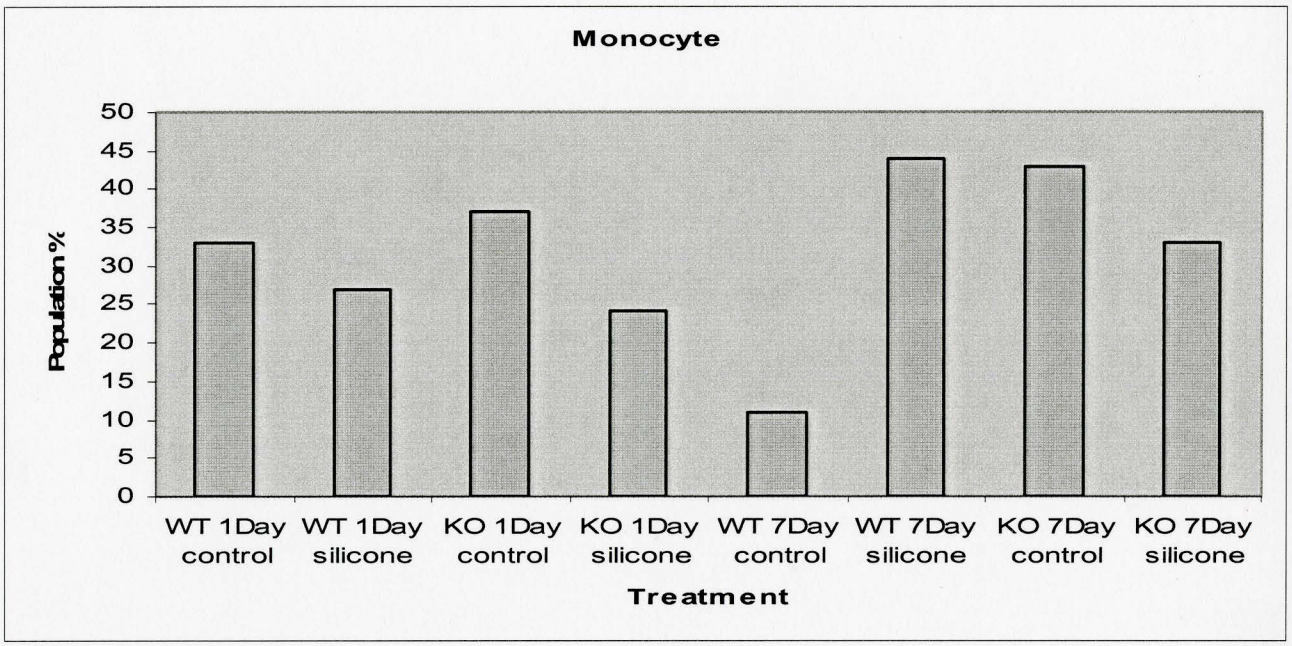

Figure 4.3B)

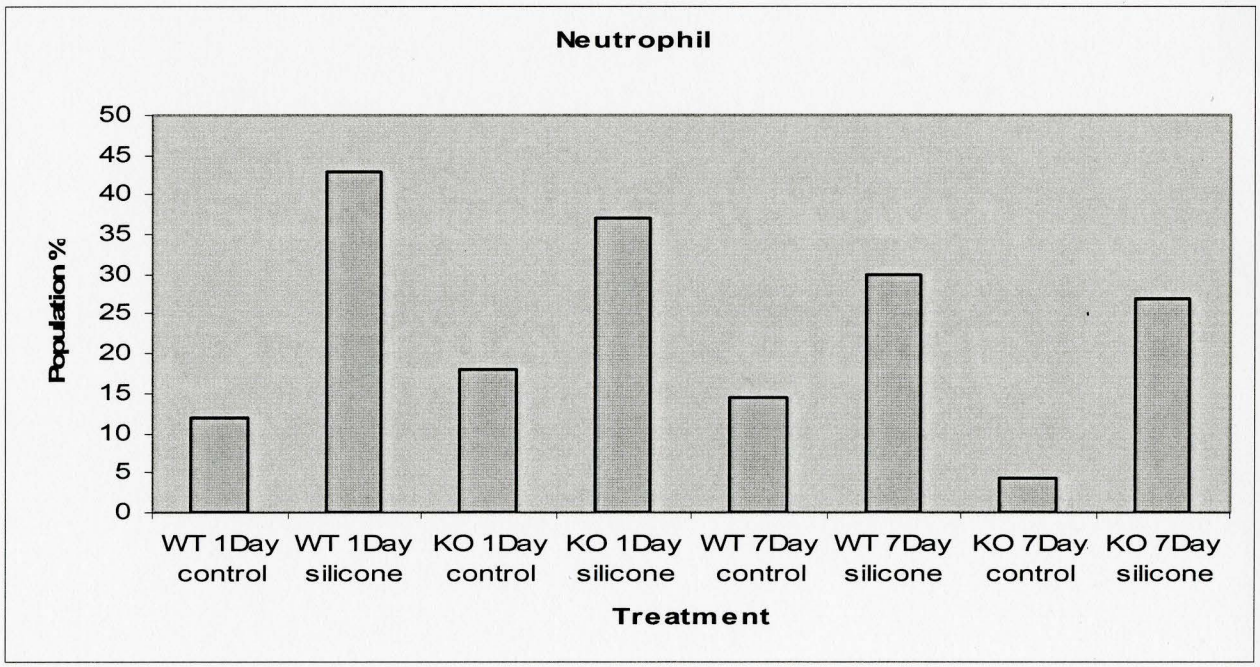

Reference List

[1] K. Inazaki, Y. Kanamaru, Y. Kojima, N. Sueyoshi, K. Okumura, K. Kaneko, Y. Yamashiro, H. Ogawa, and A. Nakao, Smad3 deficiency attenuates renal fibrosis, inflammation,and apoptosis after unilateral ureteral obstruction, Kidney Int., 66 (2004) 597-604.

[2] T. J. Kelley, H. L. Elmer, and D. A. Corey, Reduced Smad3 protein expression and altered transforming growth factor-beta1-mediated signaling in cystic fibrosis epithelial cells, Am. J. Respir. Cell Mol. Biol., 25 (2001) 732-738.

[3] G. Lakos, S. Takagawa, S. J. Chen, A. M. Ferreira, G. Han, K. Masuda, X. J. Wang, L. A. DiPietro, and J. Varga, Targeted disruption of TGF-beta/Smad3 signaling modulates skin fibrosis in a mouse model of scleroderma, Am. J. Pathol., 165 (2004) 203-217.

[4] D. Sorescu, Smad3 mediates angiotensin II- and TGF-beta1-induced vascular fibrosis: Smad3 thickens the plot, Circ. Res., 98 (2006) 988-989.

[5] J. Zhao, W. Shi, Y. L. Wang, H. Chen, P. Bringas, Jr., M. B. Datto, J. P. Frederick, X. F. Wang, and D. Warburton, Smad3 deficiency attenuates bleomycin-induced pulmonary fibrosis in mice, Am. J. Physiol Lung Cell Mol. Physiol, 282 (2002) L585-L593.

[6] Y. Zhao and D. A. Geverd, Regulation of Smad3 expression in bleomycin-induced pulmonary fibrosis: a negative feedback loop of TGF-beta signaling, Biochem. Biophys. Res. Commun., 294 (2002) 319-323.

[7] S. Rosenkranz, TGF-beta1 and angiotensin networking in cardiac remodeling, Cardiovasc. Res., 63 (2004) 423-432.

[8] C. Kupfahl, D. Pink, K. Friedrich, H. R. Zurbrugg, M. Neuss, C. Warnecke, J. Fielitz, K. Graf, E. Fleck, and V. Regitz-Zagrosek, Angiotensin II directly increases transforming growth factor beta1 and osteopontin and indirectly affects collagen mRNA expression in the human heart, Cardiovasc. Res., 46 (2000) 463-475.

[9] S. Kim, K. Ohta, A. Hamaguchi, T. Omura, T. Yukimura, K. Miura, Y. Inada, Y. Ishimura, F. Chatani, and H. Iwao, Angiotensin II type I receptor antagonist inhibits the gene expression of transforming growth factor-beta 1 and extracellular matrix in cardiac and vascular tissues of hypertensive rats, J. Pharmacol. Exp. Ther., 273 (1995) 509-515.

[10] N. Kalinina, A. Agrotis, Y. Antropova, O. Ilyinskaya, V. Smirnov, E. Tararak, and A. Bobik, Smad expression in human atherosclerotic lesions: evidence for

impaired TGF-beta/Smad signaling in smooth muscle cells of fibrofatty lesions, Arterioscler. Thromb. Vasc. Biol., 24 (2004) 1391-1396.

[11] W. Wang, X. R. Huang, E. Canlas, K. Oka, L. D. Truong, C. Deng, N. A. Bhowmick, W. Ju, E. P. Bottinger, and H. Y. Lan, Essential role of Smad3 in angiotensin II-induced vascular fibrosis, Circ. Res., 98 (2006) 1032-1039.

[12] M. Sato, Y. Muragaki, S. Saika, A. B. Roberts, and A. Ooshima, Targeted disruption of TGF-beta1/Smad3 signaling protects against renal tubulointerstitial fibrosis induced by unilateral ureteral obstruction, J. Clin. Invest, 112 (2003) 1486-1494.

[13] J. Gauldie, M. Kolb, K. Ask, G. Martin, P. Bonniaud, and D. Warburton, Smad3 signaling involved in pulmonary fibrosis and emphysema, Proc. Am. Thorac. Soc., 3 (2006) 696-702.

[14] J. Gauldie, P. Bonniaud, P. Sime, K. Ask, and M. Kolb, TGF-beta, Smad3 and the process of progressive fibrosis, Biochem. Soc. Trans., 35 (2007) 661-664.

[15] J. Gauldie, M. Kolb, and P. J. Sime, A new direction in the pathogenesis of idiopathic pulmonary fibrosis?, Respir. Res., 3 (2002) 1.

[16] R. G. Wells, Fibrogenesis. V. TGF-beta signaling pathways, Am. J. Physiol Gastrointest. Liver Physiol, 279 (2000) G845-G850.

[17] J. A. Lasky and A. R. Brody, Interstitial fibrosis and growth factors, Environ. Health Perspect., 108 Suppl 4 (2000) 751-762.

[18] P. J. Sime, Z. Xing, F. L. Graham, K. G. Csaky, and J. Gauldie, Adenovector-mediated gene transfer of active transforming growth factor-beta1 induces prolonged severe fibrosis in rat lung, J. Clin. Invest, 100 (1997) 768-776.

[19] P. J. Sime, Z. Xing, F. L. Graham, K. G. Csaky, and J. Gauldie, Adenovector-mediated gene transfer of active transforming growth factor-beta1 induces prolonged severe fibrosis in rat lung, J. Clin. Invest, 100 (1997) 768-776.

[20] M. Kolb, P. J. Margetts, P. J. Sime, and J. Gauldie, Proteoglycans decorin and biglycan differentially modulate TGF-beta-mediated fibrotic responses in the lung, Am. J. Physiol Lung Cell Mol. Physiol, 280 (2001) L1327-L1334.

[21] A. B. Roberts, The ever-increasing complexity of TGF-beta signaling, Cytokine Growth Factor Rev., 13 (2002) 3-5.

[22] Y. C. Yang, E. Piek, J. Zavadil, D. Liang, D. Xie, J. Heyer, P. Pavlidis, R. Kucherlapati, A. B. Roberts, and E. P. Bottinger, Hierarchical model of gene

regulation by transforming growth factor beta, Proc. Natl. Acad. Sci. U. S. A, 100 (2003) 10269-10274.

[23] J. Zhao, W. Shi, Y. L. Wang, H. Chen, P. Bringas, Jr., M. B. Datto, J. P. Frederick, X. F. Wang, and D. Warburton, Smad3 deficiency attenuates bleomycin-induced pulmonary fibrosis in mice, Am. J. Physiol Lung Cell Mol. Physiol, 282 (2002) L585-L593.

[24] P. Reisdorf, D. A. Lawrence, V. Sivan, E. Klising, and M. T. Martin, Alteration of transforming growth factor-beta1 response involves down-regulation of Smad3 signaling in myofibroblasts from skin fibrosis, Am. J. Pathol., 159 (2001) 263-272.

[25] T. J. Kelley, H. L. Elmer, and D. A. Corey, Reduced Smad3 protein expression and altered transforming growth factor-beta1-mediated signaling in cystic fibrosis epithelial cells, Am. J. Respir. Cell Mol. Biol., 25 (2001) 732-738.

[26] J. Zhao, W. Shi, Y. L. Wang, H. Chen, P. Bringas, Jr., M. B. Datto, J. P. Frederick, X. F. Wang, and D. Warburton, Smad3 deficiency attenuates bleomycin-induced pulmonary fibrosis in mice, Am. J. Physiol Lung Cell Mol. Physiol, 282 (2002) L585-L593.

[27] P. Bonniaud, M. Kolb, T. Galt, J. Robertson, C. Robbins, M. Stampfli, C. Lavery, P. J. Margetts, A. B. Roberts, and J. Gauldie, Smad3 null mice develop airspace enlargement and are resistant to TGF-beta-mediated pulmonary fibrosis, J. Immunol., 173 (2004) 2099-2108.

[28] M. Sato, Y. Muragaki, S. Saika, A. B. Roberts, and A. Ooshima, Targeted disruption of TGF-beta1/Smad3 signaling protects against renal tubulointerstitial fibrosis induced by unilateral ureteral obstruction, J. Clin. Invest, 112 (2003) 1486-1494.

[29] G. Lakos, S. Takagawa, S. J. Chen, A. M. Ferreira, G. Han, K. Masuda, X. J. Wang, L. A. DiPietro, and J. Varga, Targeted disruption of TGF-beta/Smad3 signaling modulates skin fibrosis in a mouse model of scleroderma, Am. J. Pathol., 165 (2004) 203-217.

[30] K. Kobayashi, K. Yokote, M. Fujimoto, K. Yamashita, A. Sakamoto, M. Kitahara, H. Kawamura, Y. Maezawa, S. Asaumi, T. Tokuhisa, S. Mori, and Y. Saito, Targeted disruption of TGF-beta-Smad3 signaling leads to enhanced neointimal hyperplasia with diminished matrix deposition in response to vascular injury, Circ. Res., 96 (2005) 904-912.

[31] A. B. Roberts, The ever-increasing complexity of TGF-beta signaling, Cytokine Growth Factor Rev., 13 (2002) 3-5.

[32] Y. Shi and J. Massague, Mechanisms of TGF-beta signaling from cell membrane to the nucleus, Cell, 113 (2003) 685-700.

[33] G. Broughton, J. E. Janis, and C. E. Attinger, The basic science of wound healing, Plast. Reconstr. Surg., 117 (2006) 12S-34S.

[34] J. M. Anderson, A. Rodriguez, and D. T. Chang, Foreign body reaction to biomaterials, Semin. Immunol., 20 (2008) 86-100.

[35] P. Bonniaud, M. Kolb, T. Galt, J. Robertson, C. Robbins, M. Stampfli, C. Lavery, P. J. Margetts, A. B. Roberts, and J. Gauldie, Smad3 null mice develop airspace enlargement and are resistant to TGF-beta-mediated pulmonary fibrosis, J. Immunol., 173 (2004) 2099-2108.

[36] N. Fujiwara and K. Kobayashi, Macrophages in inflammation, Curr. Drug Targets. Inflamm. Allergy, 4 (2005) 281-286.

[37] P. Martin and S. J. Leibovich, Inflammatory cells during wound repair: the good, the bad and the ugly, Trends Cell Biol., 15 (2005) 599-607.

[38] P. Martin and S. J. Leibovich, Inflammatory cells during wound repair: the good, the bad and the ugly, Trends Cell Biol., 15 (2005) 599-607.

[39] G. Broughton, J. E. Janis, and C. E. Attinger, The basic science of wound healing, Plast. Reconstr. Surg., 117 (2006) 12S-34S.

[40] A. K. McNally, K. M. DeFife, and J. M. Anderson, Interleukin-4-induced macrophage fusion is prevented by inhibitors of mannose receptor activity, Am. J. Pathol., 149 (1996) 975-985.

[41] A. K. McNally and J. M. Anderson, Interleukin-4 induces foreign body giant cells from human monocytes/macrophages. Differential lymphokine regulation of macrophage fusion leads to morphological variants of multinucleated giant cells, Am. J. Pathol., 147 (1995) 1487-1499.

5. Fibrosis Induced by Silicone in MRL Mice

5.1 Introduction

MRL mice have shown the ability to repair damaged tissue without scar deposition, depending on the site and severity of the injuries. It was first noticed when ear punch wounding used to mark the mice was regenerated completely without scar formation, a 2mm punch wound was regenerated [1]. Further studies were pursued by the same group and found that myocardial tissue was regenerated scarlessly with restoration of function after a heart was injured using a cryogenical technique [2-4]. Other than the heart and the ear, MRL mice have also shown a faster regeneration in alkali-burned corneal tissues [5]. There are also studies that showed MRL mice regenerate in the same fashion as other strains of mice. When the central nervous system was injured, MRL mice responded with gliosis, which is the scarring response that blocks the regeneration of axons [6]. Cutaneous wounds in MRL mice also healed with scar tissue[7]. Myocardial injuries induced by ischemia-reperfusion in MRL mice failed to repair and regenerate properly [8]. Molecularly, the expressions of MMP-2 and MMP-9 are elevated in MRL mice when injury occurs [6,9]. Interestingly, one of the studies showed that the pro-fibrotic cytokine TGF-beta had an elevated concentration in MRL mice as well [10].

In this study, we investigated the scarring response toward the implanted biomaterial in MRL mice. We wanted to study whether MRL mice respond to implanted biomaterials differently than fibrosis-prone mice do in molecular and cellular levels; if so, how the two strains of mice respond differently. We did not observe a difference in responses between MRL and C57BL/6 mice. There were severe inflammation and diffuse fibroplasias on

the surface of the biomaterial. We observed elevated levels of MMP-2, Pro-MMP-9, and TGF-β in both strains of mice. Interestingly, the acute inflammation related neutrophils in the peritoneal lavage of MRL mice peaked on the 28th day of implantation, in contrast with C57BL/6 mice which had much higher neutrophil populations in naïve and 7 days after implantation mice.

5.2 Experimental Methods

5.2.1 Experimental Outline

We were interested in how the host animal responded to the implanted biomaterial, particularly in the fibrotic response, focusing on the role of matrix metalloproteinase(MMP)-2 and MMP-9 in MRL mice. We first implanted a small piece of biomaterial into the peritoneal cavity. After 7 and 28 days of implantation, we explanted the material and studied the host response at the cellular and molecular level.

Immediately prior to the explantation of the biomaterial, we injected 2ml of phosphate-buffered- saline (PBS) solution into the peritoneal cavity of the animal for a peritoneal lavage. This method was designed to collect the migrated/proliferated cells and secreted cytokines due to the responses toward the implanted biomaterial. The extracted PBS was centrifuged at 900RPM for 6 minutes to separate the supernatant from the cells. The supernatant was analyzed using an ELISA (Enzyme-Linked ImmunoSorbent Assay) to find the concentrations of TGF-β1, MMP-2 and Pro-MMP-9. The cells were analyzed using flow cytometry. After explanting, the retrieved biomaterial was first fixed in 10% formalin for 72 hours then stored in 70% ethanol before being

treated with H&E (haematoxylin and eosin) stain.

We used an ELISA method to find the concentrations of TGF-β1, MMP-2 and MMP-9 in the peritoneal cavity where the biomaterial was implanted. We used the histology pictures of tubes cut in cross-section to observe what cells were attracted to the surface of the biomaterials, and Flow Cytometry to investigate the types of cells that were in the peritoneal cavity of the animal.

5.2.2 Material Preparation

We implanted silicone into the peritoneal cavity of the mice to investigate the mechanism of the fibrotic responses toward the biomaterials. There were two time points (7 and 28 days) to help us observe the initial and later stages of fibrosis. The silicone tubes were purchased from VWR International Co. (Brishane Cal.) and were 5mm in diameter and 5mm long. All instruments used in the coating process were sterilized prior to preparation.

5.2.3 TGF-β1 concentration

For our study, we were interested how the concentration of TGF-β1 correlates to fibrosis induced by polymeric biomaterials. In order to do so, we used enzyme-linked immunosorbent assays (ELISAs) to measure the concentration of the cytokine in the lavage sample from the peritoneal cavity. We applied an ELISA method to determine the concentration of TGF-β1. Other studies showed that this cytokine is associated with pathological fibrosis. The capture antibodies, enzyme substrate and detection antibodies

were purchased separately from BD Biosciences (Cat. No.:555052, 555053, 554058). The optimal ratio between the antibodies was determined by titration as described in Techniques for Immune Function Analysis found from BD Biosciences. We applied different ratios of primary and secondary antibodies to measure the concentrations of standard protein. We chose the ratio that gave us the most linear concentration profile of the standard protein as our optimal ratio.

5.2.4 MMP-2 and Pro-MMP-9 concentrations

For our study, we were interested how the concentrations of MMP-2 and MMP-9 correlate to fibrosis induced by polymeric biomaterials. In order to do so, we used enzyme-linked immunosorbent assays (ELISAs) to measure the concentration of the two proteases in the lavage sample from the peritoneal cavity. We applied an ELISA method to determine the concentration of MMP-2 and Pro-MMP-9. The ELISA kits were purchased from R&D Systems (Cat. No.: DMP200, MMP900).

5.2.5 H&E staining and cell layer thickness on material surface

The implanted silicone tubes were retrieved from the peritoneal cavity of the animal 7 and 28 days after implantation. Each tube was immediately fixed in 10% formalin for 48hrs then transferred to 70% ethanol until being stained in the histology laboratory. The tube was then embedded in paraffin, cut in cross-section, and stained with H&E in order to observe the types of cells on the material surface under microscopy. We took pictures

of each tube and measured the thickness of the cell layers on the surface of the biomaterial.

5.2.6 Flow Cytometry

Flow cytometry was used to identify the population distribution of different types of cells contained in the PBS extracted from the peritoneal cavity of the mice. We wanted to study whether the implanted biomaterial caused any shifting of the population distribution. As mentioned earlier, we injected 2ml of PBS into the peritoneal cavity of the mouse to collect the cytokines and cells. The extract was centrifuged in order to separate the supernatant and cells. After removing the supernatant, we resuspended the cells in PBS. We used a hemacytometer to calculate the concentration of the cells, then centrifuged the cells again, and adjusted the volume of PBS in order to bring the concentration of the cells to approximately 1million cells /ml in PBS. After adjusting the cell concentration, we then used Flow Cytometry to determine the percentage of different cells in the sample. Using the dot plot with Forward-Scatter (measures the cell size) and Side-Scatter (measures the cell granularity) as the axes, we were able to observe four distinct populations separated from each other. They were assigned as debris/RBC (red blood cells), lymphocytes, monocytes and neutrophils according to the size and granularity. We then eliminated the population of debris/RBC from the cell count to obtain the total cell count of lymphocytes, monocytes and neutrophils. The population percentages of the three types of cells were then calculated.

5.2.7 Animals

We used female MRL purchased from The Jackson Laboratory and Female C57BL/6 mice were purchased from Charles River Breeding Laboratories (Wilmington, MA). All animal work was approved by the Animal Research Ethics Board at McMaster University. The surgeries and implantation were performed when the mice were 6-8 weeks old.

5.2.8 Statistical Analysis

Statistical tests were conducted using Microsoft Excel Data Analysis. Data is presented as mean ± standard error of the mean (sem).

5.3 Results

In our study, we investigated the mechanisms of fibrosis induced by biomaterials MRL and C57BL/6 mice by implanting a biomaterial (silicone) into the peritoneal cavity of the mice. We had four different treatments: i) 7 day implantation in MRL; ii) 7 day implantation in C57BL/6; iii) 28 day implantation in MRL; iv) 28 day implantation in C57BL/6 mice. The methods we used to observe and analyze the fibrotic response toward the implanted biomaterial were: i) we used ELISAs to measure the concentration of matrix metalloproteinase(MMP)-2 and MMP-9 from the lavage sample; ii) with the help of Flow Cytometry, we observed the shifting of cell population distribution in the peritoneal lavage with or without implant; iii) we stained the cross-sectionally cut biomaterial to observe the cellular behaviour on the surface of the implanted biomaterials. We wanted to investigate how MRL mice would respond differently than C57BL/6 mice

toward the fibrosis induced by implanted biomaterial.

MRL mice had higher MMP-2 and Pro-MMP-9 concentrations than C57BL/6 mice

MRL mice had shown different tissue regeneration and wound healing ability depending on the location of the tissue [11]. Within the same tissue, depending on the method of injury, this strain of mice showed different responses as well [12,13]. We were particularly interested in how MRL mice responded to a implanted biomaterial; whether it would be a scarless wonder or a typical fibrotic response. We focused our study on the activities and concentrations of MMP-2 and MMP-9.

From our results, MRL and C57BL/6 mice showed different MMP-2 concentrations as shown in Figure 5.2A. The difference was the largest at 7 days after the implantation. Under all three circumstances (naïve, 7 days and 28 days of implantation), MRL mice had higher concentrations of MMP-2 and C57BL/6. In MRL mice, MMP-2 level increased after 7 days of implantation and dropped back down to naïve level at the 28^{th} day of implantation. In C57BL/6 mice, MMP-2 peaked at 7 days of implantation, dropped slightly on the 28^{th} day, though still higher than naïve mice.

We observed a similar though not exact trend in Pro-MMP-9 concentration (Figure 5.2B). Under all three circumstances, MRL mice had higher concentrations of Pro-MMP-9 than C57BL/6 mice. In MRL mice, the concentration of Pro-MMP-9 peaked on the 7^{th} day of implantation, decreased on the 28^{th} day, though still higher than naïve mice. Similar trend was observed in C57BL/6 mice as well.

MRL mice had higher TGF-β1 concentration than C57BL/6

TGF-β1 is involved in many biological functions, particularly relevant to our study, it is a pro-fibrotic cytokine. In our results, we observed that TGF-β1 concentration (Figure 5.2C) showed similar trends to MMP-2 and Pro-MMP-9. As shown in Figure 5.2, in naïve, 7 days and 28 days implantation, MRL mice had higher concentration of this cytokine in the peritoneal lavage than C57BL/6 strain. The concentration for both strains of mice peaked on the 7th day of implantation. This could be an indication of possible positive feedback relationship between TGF-β1 and the MMPs.

The cellular behaviour on the surface of implanted materials showed indifference between MRL and C57BL/6 mice

We cut the sample in cross-section and treated it with H&E stain in order to observe the cell layer thickness and cellular behaviour on the surface of implanted biomaterials (Figure 5.3). The severity of acute inflammation and fibrosis was determined by the densities of different cell types attached to the surface of the biomaterial. In both strains of mice, there were severe inflammatory and fibrotic responses toward the implanted biomaterial. There were no significant differences observed from the histological images between the two mice strains on both the 7th and 28th day of implantation. We observed severe necrosis and the recruitment of neutrophils, monocytes, and macrophages on the surface debris of the biomaterial. Edematous of diffuse fibroplasias was also present. The debris on the 7th day of implantation was more cell-dense, and the thickness was more equally distributed around the circumference of the silicone tube. On the 28th day

of implantation, some area of the debris barely had any cellular activities and was left as collagen deposition (usually thinner in thickness), some area still displayed severe inflammation with high density of cells like neutrophils and macrophages. The only difference observed was that on the 28th day of implantation, there were occasional foreign giant body cells scattered within the cell layer on the surface of the biomaterial implanted to MRL mice.

The differences between the cells were observed by comparing the granularity and sizes of the cells under microscopy. The types of the cells were determined with the aid of Dr. Jacek M. Kwiecien.

The neutrophil population peaked on the 28th day of implantation in MRL mice

We used a flow cytometer to determine the distribution of cell types within the peritoneal cavity. Different cells play different roles in host response toward the implanted biomaterial. Neutrophils are the first line of cellular defense when a foreign material is detected in the body. We expected to see the populations of neutrophil peaked 7 days after implantation as inflammation was still in effect. As shown in Figure 5.3A, we did not observe a clear relationship between the population percentages of neutrophil and the concentrations of the two MMP's that we measured. In C57BL/6 mice, the populations of neutrophil were about the same in naïve mice, and 7 days after implantation; the population percentage was much lower on the 28th day of implantation. The opposite trend was observed in MRL mice, the concentrations of neutrophil peaked on the 28th day was much higher than on the 7th day and naïve mice. For lymphocyte

populations (Figure 5.3B), we observed the peak in MRL naïve mice. All other had approximately the same population percentages.

5.4 Discussion

In our study, we were particularly interested in the fibrotic response from the host toward the implanted biomaterials. Polymeric biomaterials are often used as scaffolds to support cells, and to deliver bioactive molecules in regenerative medicine. These biomaterials are typically designed to provide temporarily mechanical support during the replacement of the damaged tissue. Cells in the construct will interact with the surrounding environment, and repair the damaged tissues as the biomaterials degrade gradually without toxic effects to the body. Unfortunately, when implanted, biomaterials are treated as foreign objects by the body, and cause various host responses. Often after implantation, collagen is deposited on the surface of implanted biomaterials, known as encapsulation. The collagen layer would then block the communication between the delivered cells and the surrounding environment. The purpose of "regeneration" is defeated when severe fibrosis occurs. Fibrosis is not only relevant in regenerative medicine; it could also cause trouble in tissue/organ replacement, for example, heart valves. In addition, fibrotic capsule formation around medical devices, probes and drug delivery vehicles is likely to interfere with function. Other than fibrosis, acute and chronic inflammation could also occur when the body recognizes the implanted biomaterial as a foreign object. Inflammation could further damage the healthy tissues/organs in proximity to the implanted biomaterial [14].

In several studies, MRL mice showed the potential for scarless repair and regeneration of wounded tissue. The mice have shown scarless regeneration in ears [15,16]. MRL mice also regenerated myocardial tissue after a cryo-injury [17], and displayed accelerated healing in alkali-burned corneas with reduced inflammation [18]. There have also been cases in which MRL mice did not show the same scarless phenomena as the studies mentioned above, for example, heart injury induced by ischemia-reperfusion [19,20], and dorsal subcutaneous injury [21]. We were particularly interested in how MRL mice would respond to implanted biomaterials in the peritoneal cavity. We wanted to observe whether MRL mice would give a different perspective and insight on the mechanism of fibrosis induced by implanted biomaterials. We focused our study on finding the concentrations of MMP-2, Pro-MMP-9 and TGF-β in peritoneal lavage, the cellular behaviour on the surface of the implanted biomaterial, and the cell population distribution in the peritoneal lavage.

MMPs are involved in many biological pathways and pathological diseases, especially in remodeling responses involving collagen and other extracellular matrix molecules [22-24]. MMP-2 and MMP-9 are secreted by different types of cells in extracellular matrix remodeling at wounded tissue [25,26]. These two MMPs are up-regulated only in migratory, not stationary, fibroblasts [27]. Among other cells involved in wound healing that also produce MMPs are neutrophils and macrophages [28]. Studies have shown that MRL mice express higher levels of MMP-2 and MMP-9 [29,30], and tissue inhibitors of metalloproteinases (TIMP) levels are lower in MRL mice than in C57BL/6 mice [31]. On a cellular level, both neutrophils macrophages are positive for

MMP-2 and MMP-9, though at different time points, and MMPs were found in both pro and active form [32]. This gives us a possible explanation of the scarless healing: a higher expression MMP and less of its inhibitor in MRL mice. MMP-9 has also been shown to be involved in fetal scarless healing [33]. TGF-β1 is a well known pro-fibrotic cytokine which plays a key role in the process of fibrogenesis [34]; this has been demonstrated in many different organ systems [35]. TGF-β1 causes myofibroblasts to differentiate and induces the expression of connective tissue growth factor (CTGF), therefore increasing the production of collagen and fibronectin [36]. Studies have been done to show that transient adenoviral vector-mediated gene transfer of active TGF-β1 leads to progressive and severe fibrosis in different animal models [37-39].

Two separate studies have shown that MRL mice expressed higher levels of MMP-2, MMP-9 [40] and TGF-β1 [41,42] during wound healing process. In our study of "wound healing" toward an implanted biomaterial, we observed a similar trend. The concentrations of MMP-2, Pro-MMP-9 and TGF-β1 in the peritoneal lavage were measured using ELISA. MRL mice had higher concentrations than C57BL/6 mice of all three molecules whether implanted or not. For both strains of mice, the concentrations of all three molecules peaked on the 7^{th} day of implantation. On the 28^{th} day, the concentrations of MMP-2 and Pro-MMP-9 had gone back down close to the naïve animal levels; the concentration of TGF-β1 was still much higher than in naïve mice though significantly lower than the 7^{th} day. This could indicate a possible relationship between MMPs and TGF-β1 in the process of "wound healing" toward an implanted biomaterial. The longer lasting high concentration of TGF-β1 could just be another sign of this

cytokine's multi-functional interactions with cells and molecules in the process of host response toward the implanted biomaterial. A study on isolating the presence of either TGF-β1 or MMP-2, 9, by using the antibody, could give us a more direct indication of the relationship between the three molecules.

In our cell population distribution study, we observed a dramatic difference between the two strains. As shown in Figure 5.3a, C57BL/6 mice had much higher neutrophil population percentages in naïve model, and on the 7th day of implantation than MRL mice. The opposite relationship was observed on the 28th day of implantation. The population percentages of lymphocytes did not fluctuate as much as the neutrophils. Naïve MRL mice had the higher lymphocyte population percentages in all treatments. The trend that C57BL/6 mice had higher neutrophil population percentage than MRL mice agreed with the study done by Kench [43]. What was unexpected was the sudden rise of the neutrophil population in MRL mice on the 28th day of implantation. This could indicate a delayed inflammatory reaction toward the implanted biomaterial in the autoimmune MRL mice. A more detailed study of inflammatory markers (e.g. IL-1) could give us a more clear indication on what type of response was in process at different time points.

Though the concentrations of TGF-β1, MMP-2 and pro-MMP-9 and cellular distributions showed differences between the two mice, we did not observe a significant difference on the cellular behaviour on the surface of the implanted biomaterial. Both strains of mice displayed severe acute inflammation, necrosis, and diffuse fibroplasias. Cells like neutrophils, monocytes and macrophages were recruited to the biomaterial surface. On the 7th day of implantation, the tissue accumulation on the surface of the

biomaterial was more cellular dense. On the 28th day, some areas around the biomaterial surface barely had any cellular activity and was left as collagen deposition (usually thinner in thickness), some areas still displayed severe inflammation with high density of cells like neutrophils and macrophages. The measured differences between the two strains of mice at the molecular (MMP and TGF-β) and cellular (population distribution) levels were not reflected in histology. This could be an indication that there was possibly more than one mechanism involved in the fibrotic response toward the implanted biomaterial. The functions the MMP-2, MMP-9, and TGF-beta could possibly be replaced by other molecules. Alternatively, MMP-2, MMP-9 and TGF-β might not play an important role in biomaterial-induced fibrosis.

In conclusion, we found results that agreed with studies that were done on the wound healing in MRL mice: the concentrations of MMP-2, Pro-MMP-9 and TGF-β1 were all higher in MRL mice than C57BL/6 mice; MRL mice had lower populations of neutrophils in naïve mice and on the 7th day of implantation, though the population increased dramatically on the 28th day of implantation. We expected to see less severe fibrotic response in MRL mice, but it was not observed through histology. In both strains of mice, there was severe acute inflammation, recruitment of neutrophils, monocytes and macrophages with the presence of diffuse fibroplasias on the surface of the implanted biomaterial. Pathological fibrosis from wound healing and fibrosis induced by an implanted biomaterial might share the same pathway, but it is possible that there is more than one pathway/mechanism involved in the biomaterial-induced fibrosis, dependent on the mouse strain or type of material. There are many steps and feedback loops in the

process of fibrotic response. We have studied the mechanism of the "middle" part of this process, i.e. after at least one day of implantation when different types of cells were already attracted/migrated to the surface of the biomaterial. A future study on an even earlier stage of the process and its influence on subsequent steps of the fibrotic response could give us more insights in the biomaterial induced fibrotic response. We have observed the expected similarities between pathological fibrosis and biomaterial induced fibrosis, yet we did not observe a difference when it comes to histology.

List of Figures

Figure 5.1 Concentrations of Cytokines. **A)** MMP-2. **B)**Pro-MMP-9. **C)** TGF-β1. MRL mice had higher in all three cytokines at both time points (7 day and 28 day) than C57BL/6 mice. The concentrations of the three cytokines from the peritoneal lavage showed similar trend.

Figure 5.2 Cellular behaviour on the surface of the implanted biomaterial. **A)** C57BL/6 with 7 day implantation. **B)** MRL with 7 day implantation. In both strains we observed severe inflammation with the gathering of necrosis, neutrophils, monocytes and macrophages. We did not observe different cellular behaviour on the surface of the implanted biomaterial between the two mouse strains. **C)** C57BL/6 with 28 day implantation. **D)** MRL with 28 day implantation. On the surface, there was less cellular activity than the 7^{th} day, and was left with collagen deposition. We did not observe difference on the cellular behaviour on the surface of the implanted biomaterial between the two mouse strains, though there were occasional foreign body giant cells observed in MRL mice.

Figure 5.3 Population distribution percentages of cells. **A)** Neutrophils. The neutrophil populations in C57BL/6 mice were higher than MRL mice in naïve and 7 day implant treatment. It was interesting to observe the neutrophil population of MRL mice peaked on the 28^{th} day of implantation. **B)** Lymphocytes. We observed the highest population in MRL naïve mice. All three other treatments showed similar population distribution percentage.

Figure 5.1A)

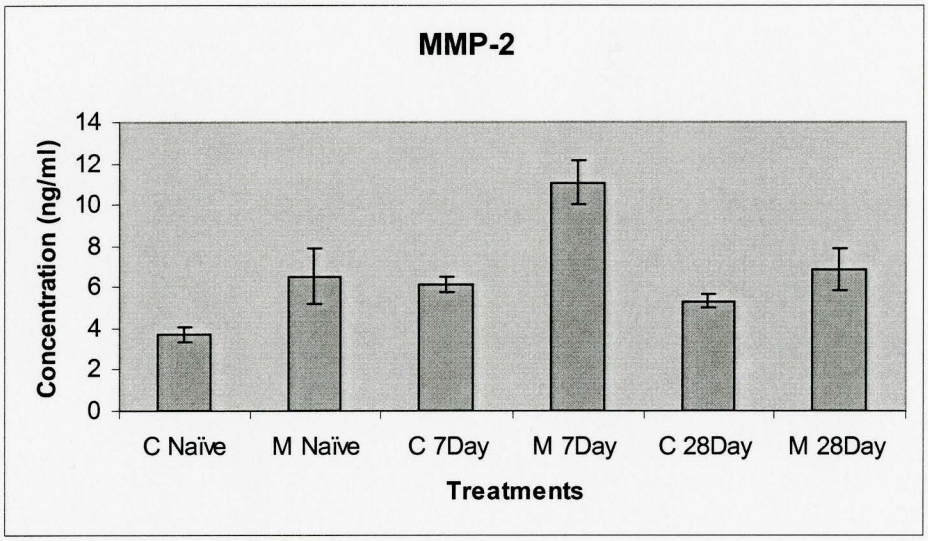

Figure 5.1B)

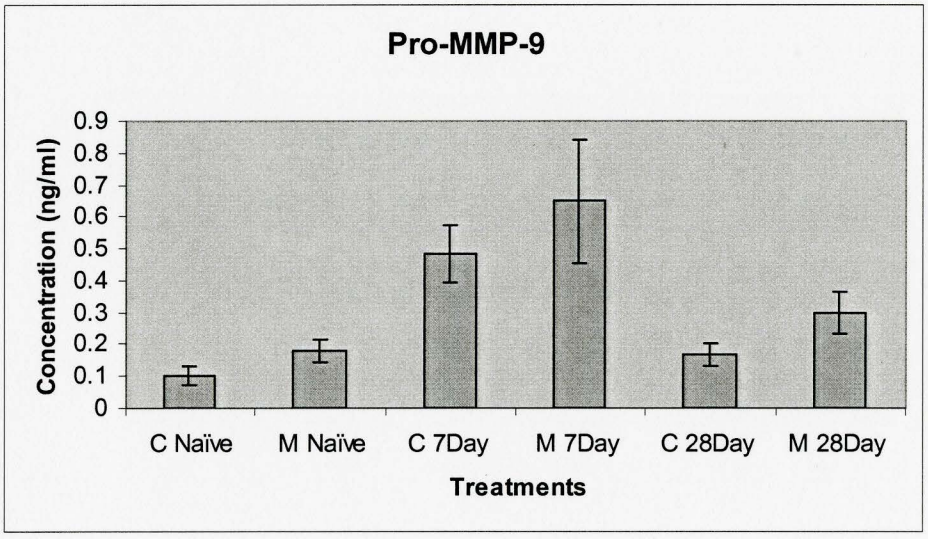

Figure 5.1C)

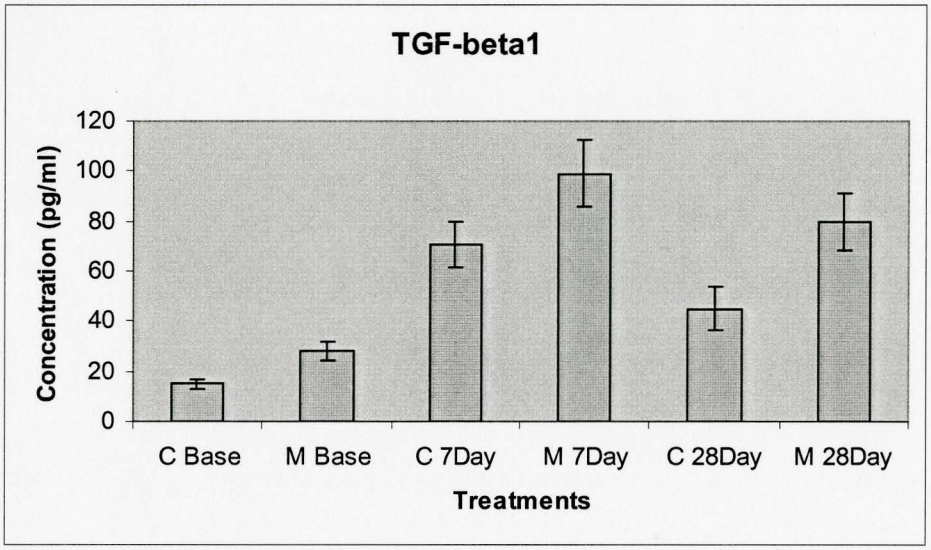
TGF-beta1
Concentration (pg/ml)
120
100
80
60
40
20
0
C Base
M Base
C 7Day
M 7Day
C 28Day
M 28Day
Treatments

Figure 5.2A)

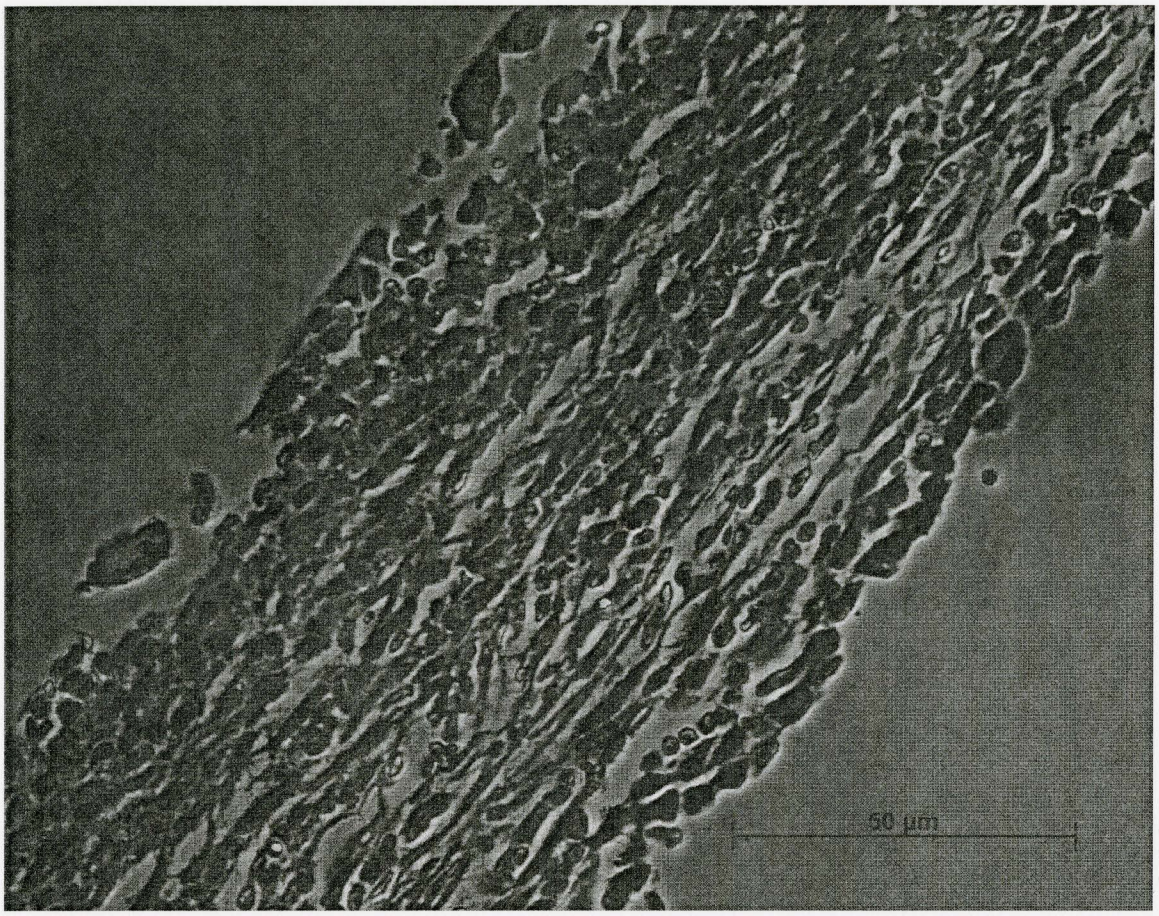

Figure 5.2B)

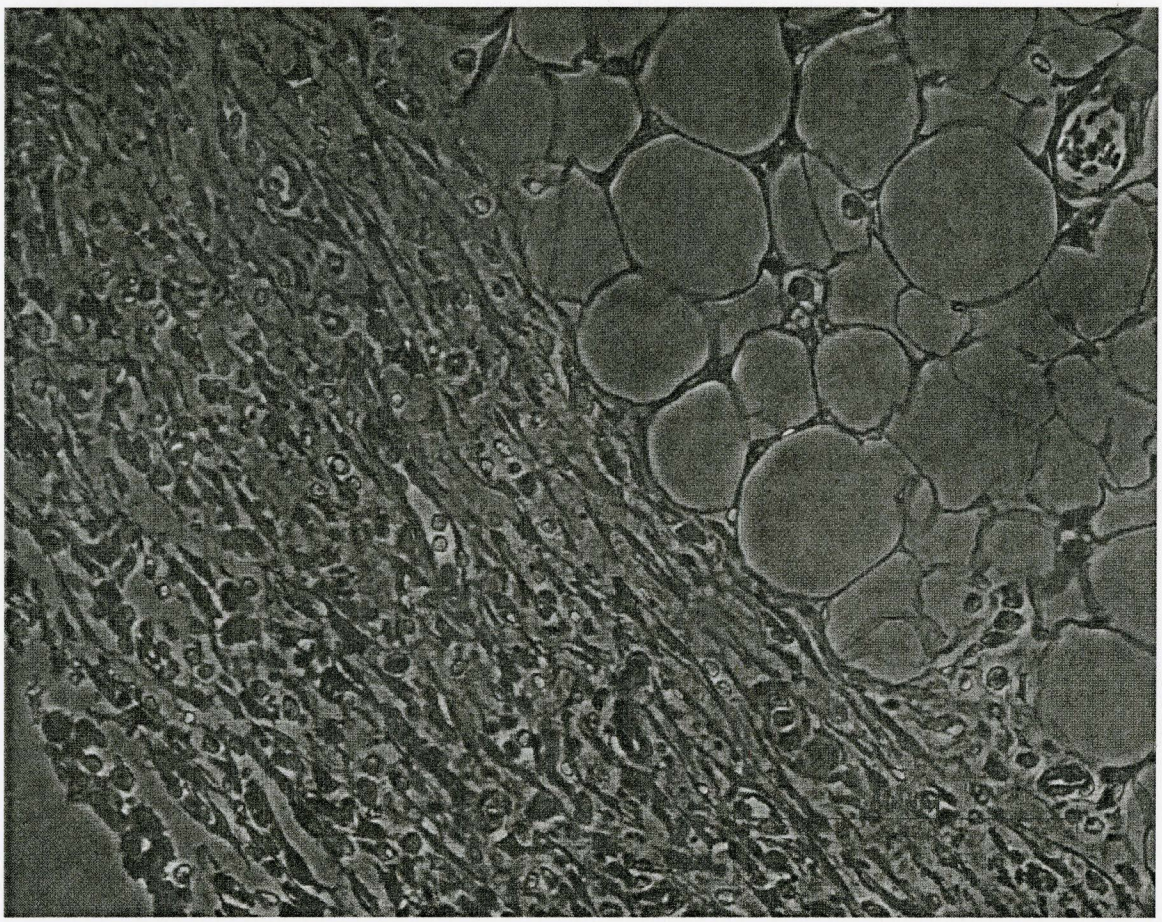

Figure 5.2C)

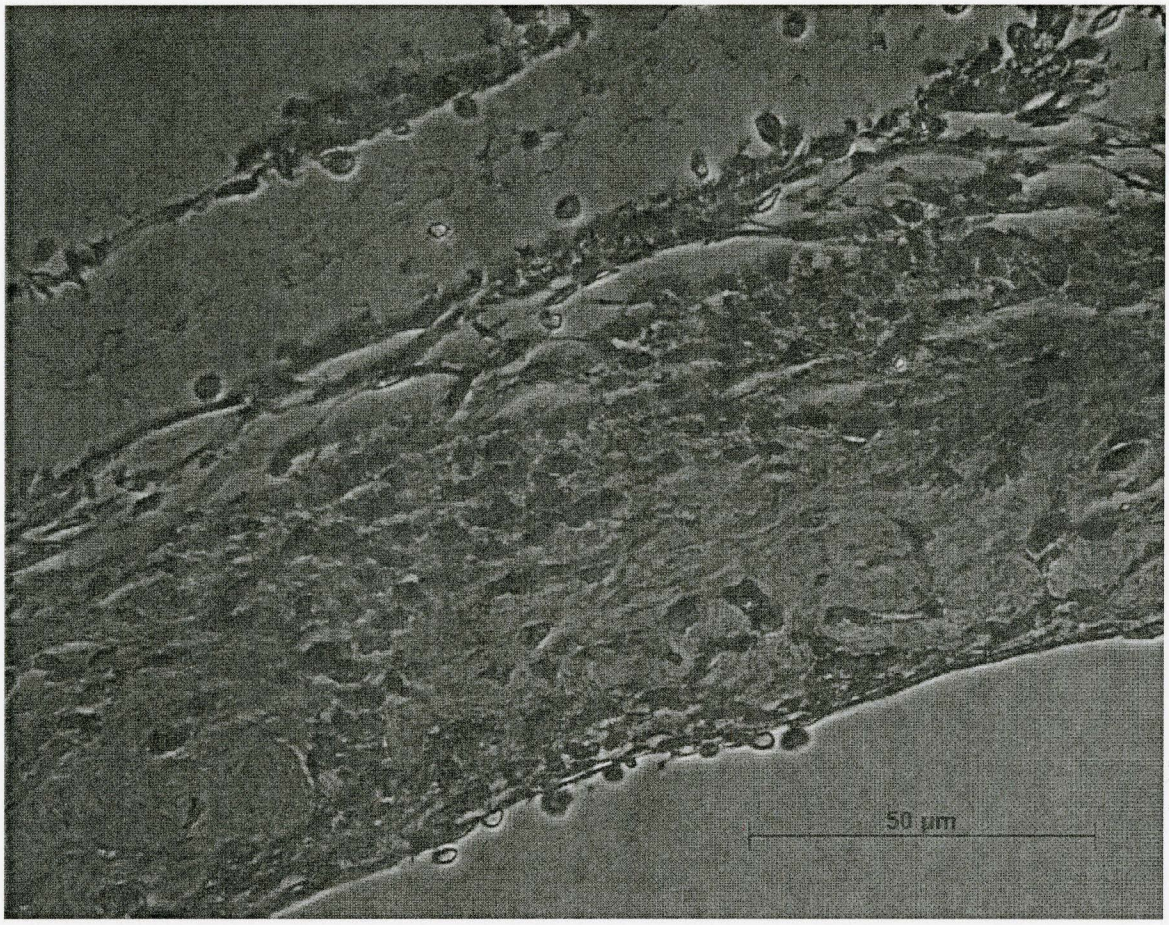

Figure 5.2D)

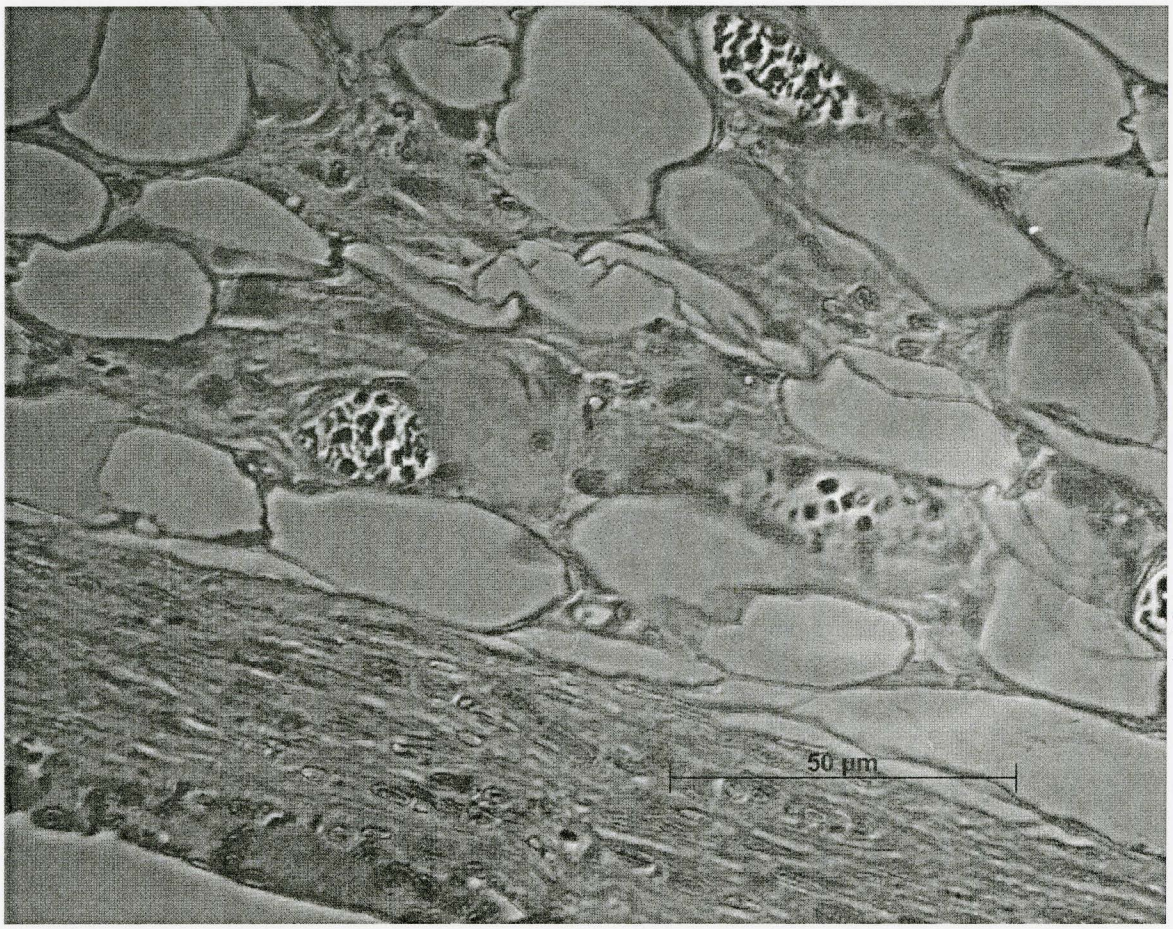

Figure 5.3A)

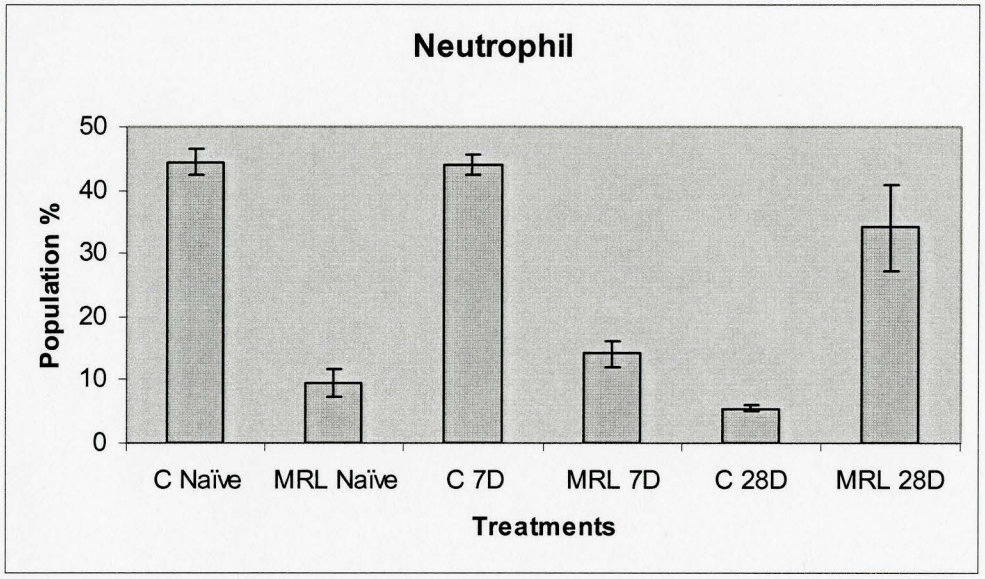

Figure 5.3B)

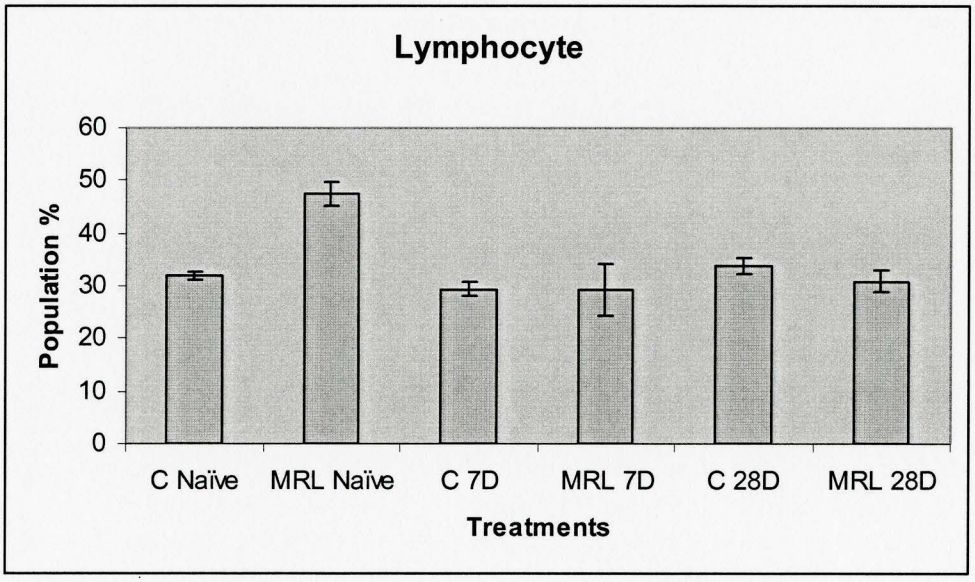

Reference List

[1] L. D. Clark, R. K. Clark, and E. Heber-Katz, A new murine model for mammalian wound repair and regeneration, Clin. Immunol. Immunopathol., 88 (1998) 35-45.

[2] J. M. Leferovich, K. Bedelbaeva, S. Samulewicz, X. M. Zhang, D. Zwas, E. B. Lankford, and E. Heber-Katz, Heart regeneration in adult MRL mice, Proc. Natl. Acad. Sci. U. S. A, 98 (2001) 9830-9835.

[3] J. M. Leferovich and E. Heber-Katz, The scarless heart, Semin. Cell Dev. Biol., 13 (2002) 327-333.

[4] E. Heber-Katz, J. Leferovich, K. Bedelbaeva, D. Gourevitch, and L. Clark, The scarless heart and the MRL mouse, Philos. Trans. R. Soc. Lond B Biol. Sci., 359 (2004) 785-793.

[5] M. Ueno, B. L. Lyons, L. M. Burzenski, B. Gott, D. J. Shaffer, D. C. Roopenian, and L. D. Shultz, Accelerated wound healing of alkali-burned corneas in MRL mice is associated with a reduced inflammatory signature, Invest Ophthalmol. Vis. Sci., 46 (2005) 4097-4106.

[6] D. W. Hampton, A. Seitz, P. Chen, E. Heber-Katz, and J. W. Fawcett, Altered CNS response to injury in the MRL/MpJ mouse, Neuroscience, 127 (2004) 821-832.

[7] A. S. Colwell, T. M. Krummel, W. Kong, M. T. Longaker, and H. P. Lorenz, Skin wounds in the MRL/MPJ mouse heal with scar, Wound. Repair Regen., 14 (2006) 81-90.

[8] I. Abdullah, J. J. Lepore, J. A. Epstein, M. S. Parmacek, and P. J. Gruber, MRL mice fail to heal the heart in response to ischemia-reperfusion injury, Wound. Repair Regen., 13 (2005) 205-208.

[9] D. Gourevitch, L. Clark, P. Chen, A. Seitz, S. J. Samulewicz, and E. Heber-Katz, Matrix metalloproteinase activity correlates with blastema formation in the regenerating MRL mouse ear hole model, Dev. Dyn., 226 (2003) 377-387.

[10] J. A. Kench, D. M. Russell, V. A. Fadok, S. K. Young, G. S. Worthen, J. Jones-Carson, J. E. Henson, P. M. Henson, and D. Nemazee, Aberrant wound healing and TGF-beta production in the autoimmune-prone MRL/+ mouse, Clin. Immunol., 92 (1999) 300-310.

[11] A. H. Beare, A. D. Metcalfe, and M. W. Ferguson, Location of injury influences the mechanisms of both regeneration and repair within the MRL/MpJ mouse, J. Anat., 209 (2006) 547-559.

[12] I. Abdullah, J. J. Lepore, J. A. Epstein, M. S. Parmacek, and P. J. Gruber, MRL mice fail to heal the heart in response to ischemia-reperfusion injury, Wound. Repair Regen., 13 (2005) 205-208.

[13] E. Heber-Katz, J. Leferovich, K. Bedelbaeva, D. Gourevitch, and L. Clark, The scarless heart and the MRL mouse, Philos. Trans. R. Soc. Lond B Biol. Sci., 359 (2004) 785-793.

[14] B. D. Ratner and S. J. Bryant, Biomaterials: where we have been and where we are going, Annu. Rev. Biomed. Eng, 6 (2004) 41-75.

[15] C. Rajnoch, S. Ferguson, A. D. Metcalfe, S. E. Herrick, H. S. Willis, and M. W. Ferguson, Regeneration of the ear after wounding in different mouse strains is dependent on the severity of wound trauma, Dev. Dyn., 226 (2003) 388-397.

[16] A. S. Colwell, T. M. Krummel, W. Kong, M. T. Longaker, and H. P. Lorenz, Skin wounds in the MRL/MPJ mouse heal with scar, Wound. Repair Regen., 14 (2006) 81-90.

[17] J. M. Leferovich, K. Bedelbaeva, S. Samulewicz, X. M. Zhang, D. Zwas, E. B. Lankford, and E. Heber-Katz, Heart regeneration in adult MRL mice, Proc. Natl. Acad. Sci. U. S. A, 98 (2001) 9830-9835.

[18] M. Ueno, B. L. Lyons, L. M. Burzenski, B. Gott, D. J. Shaffer, D. C. Roopenian, and L. D. Shultz, Accelerated wound healing of alkali-burned corneas in MRL mice is associated with a reduced inflammatory signature, Invest Ophthalmol. Vis. Sci., 46 (2005) 4097-4106.

[19] Y. S. Oh, L. E. J. Thomson, M. C. Fishbein, D. S. Berman, B. Sharifi, and P. S. Chen, Scar formation after ischemic myocardial injury in MRL mice, Cardiovascular Pathology, 13 (2004) 203-206.

[20] I. Abdullah, J. J. Lepore, J. A. Epstein, M. S. Parmacek, and P. J. Gruber, MRL mice fail to heal the heart in response to ischemia-reperfusion injury, Wound. Repair Regen., 13 (2005) 205-208.

[21] A. H. Beare, A. D. Metcalfe, and M. W. Ferguson, Location of injury influences the mechanisms of both regeneration and repair within the MRL/MpJ mouse, J. Anat., 209 (2006) 547-559.

[22] H. C. Grillo, C. M. Lapiere, M. H. Dresden, and J. Gross, Collagenolytic activity in regenerating forelimbs of the adult newt (Triturus viridescens), Dev. Biol., 17 (1968) 571-583.

[23] E. V. Yang and S. V. Bryant, Developmental regulation of a matrix

metalloproteinase during regeneration of axolotl appendages, Dev. Biol., 166 (1994) 696-703.

[24] E. A. Chernoff, C. M. O'Hara, D. Bauerle, and M. Bowling, Matrix metalloproteinase production in regenerating axolotl spinal cord, Wound. Repair Regen., 8 (2000) 282-291.

[25] W. C. Parks, Matrix metalloproteinases in repair, Wound. Repair Regen., 7 (1999) 423-432.

[26] B. Steffensen, L. Hakkinen, and H. Larjava, Proteolytic events of wound-healing--coordinated interactions among matrix metalloproteinases (MMPs), integrins, and extracellular matrix molecules, Crit Rev. Oral Biol. Med., 12 (2001) 373-398.

[27] L. Hakkinen, V. J. Uitto, and H. Larjava, Cell biology of gingival wound healing, Periodontol. 2000., 24 (2000) 127-152.

[28] V. W. Yong, C. A. Krekoski, P. A. Forsyth, R. Bell, and D. R. Edwards, Matrix metalloproteinases and diseases of the CNS, Trends Neurosci., 21 (1998) 75-80.

[29] E. Heber-Katz, J. Leferovich, K. Bedelbaeva, D. Gourevitch, and L. Clark, The scarless heart and the MRL mouse, Philos. Trans. R. Soc. Lond B Biol. Sci., 359 (2004) 785-793.

[30] D. Gourevitch, L. Clark, P. Chen, A. Seitz, S. J. Samulewicz, and E. Heber-Katz, Matrix metalloproteinase activity correlates with blastema formation in the regenerating MRL mouse ear hole model, Dev. Dyn., 226 (2003) 377-387.

[31] D. Gourevitch, L. Clark, P. Chen, A. Seitz, S. J. Samulewicz, and E. Heber-Katz, Matrix metalloproteinase activity correlates with blastema formation in the regenerating MRL mouse ear hole model, Dev. Dyn., 226 (2003) 377-387.

[32] E. Heber-Katz, J. Leferovich, K. Bedelbaeva, D. Gourevitch, and L. Clark, The scarless heart and the MRL mouse, Philos. Trans. R. Soc. Lond B Biol. Sci., 359 (2004) 785-793.

[33] Z. M. Peled, E. D. Phelps, D. L. Updike, J. Chang, T. M. Krummel, E. W. Howard, and M. T. Longaker, Matrix metalloproteinases and the ontogeny of scarless repair: the other side of the wound healing balance, Plast. Reconstr. Surg., 110 (2002) 801-811.

[34] J. Gauldie, M. Kolb, and P. J. Sime, A new direction in the pathogenesis of idiopathic pulmonary fibrosis?, Respir. Res., 3 (2002) 1.

[35] R. G. Wells, Fibrogenesis. V. TGF-beta signaling pathways, Am. J. Physiol

Gastrointest. Liver Physiol, 279 (2000) G845-G850.

[36] J. A. Lasky and A. R. Brody, Interstitial fibrosis and growth factors, Environ. Health Perspect., 108 Suppl 4 (2000) 751-762.

[37] P. J. Sime, Z. Xing, F. L. Graham, K. G. Csaky, and J. Gauldie, Adenovector-mediated gene transfer of active transforming growth factor-beta1 induces prolonged severe fibrosis in rat lung, J. Clin. Invest, 100 (1997) 768-776.

[38] P. J. Sime, Z. Xing, F. L. Graham, K. G. Csaky, and J. Gauldie, Adenovector-mediated gene transfer of active transforming growth factor-beta1 induces prolonged severe fibrosis in rat lung, J. Clin. Invest, 100 (1997) 768-776.

[39] M. Kolb, P. J. Margetts, P. J. Sime, and J. Gauldie, Proteoglycans decorin and biglycan differentially modulate TGF-beta-mediated fibrotic responses in the lung, Am. J. Physiol Lung Cell Mol. Physiol, 280 (2001) L1327-L1334.

[40] D. Gourevitch, L. Clark, P. Chen, A. Seitz, S. J. Samulewicz, and E. Heber-Katz, Matrix metalloproteinase activity correlates with blastema formation in the regenerating MRL mouse ear hole model, Dev. Dyn., 226 (2003) 377-387.

[41] J. A. Kench, D. M. Russell, V. A. Fadok, S. K. Young, G. S. Worthen, J. Jones-Carson, J. E. Henson, P. M. Henson, and D. Nemazee, Aberrant wound healing and TGF-beta production in the autoimmune-prone MRL/+ mouse, Clin. Immunol., 92 (1999) 300-310.

[42] D. Gourevitch, L. Clark, P. Chen, A. Seitz, S. J. Samulewicz, and E. Heber-Katz, Matrix metalloproteinase activity correlates with blastema formation in the regenerating MRL mouse ear hole model, Dev. Dyn., 226 (2003) 377-387.

[43] J. A. Kench, D. M. Russell, V. A. Fadok, S. K. Young, G. S. Worthen, J. Jones-Carson, J. E. Henson, P. M. Henson, and D. Nemazee, Aberrant wound healing and TGF-beta production in the autoimmune-prone MRL/+ mouse, Clin. Immunol., 92 (1999) 300-310.

Conclusions and Recommendations

In our work, we focused on the mechanism of biomaterial-induced fibrosis. We tackled three questions: i) how does the initial inflammatory response to the implanted biomaterial influence the fibrotic response, ii) how important is the SMAD3 gene in biomaterial-induced fibrosis and, iii) how do MRL mice respond to a implanted biomaterial. We analyzed our results from molecular, cellular and histological aspects.

To answer the first question, mice received one of four different treatments: i) silicone tube, ii) silicone tube with LPS, iii) PLGA coated silicone tube, and iv) PLGA coated silicone tube with LPS. The implant was placed in the peritoneal cavity for 3 days. The purpose of LPS is to induce acute inflammation. From our results, LPS induced a higher production of IL-1β when compared to the non-LPS-treated, but not significantly. The concentration of TGF-β1 did not increase with the application of LPS, but in fact, decreased slightly. For the concentrations of IL-1β and TGF-β1 in the peritoneal lavage, we did not find a direct relationship between the two cytokines, but we observed that the silicone implant induced higher productions of both cytokines than the PLGA coated silicone tube did. The cell layer on the implanted silicone tube was much thicker than the cell layer on the PLGA surface. Finally, the silicone tube with LPS treatment induced the highest neutrophil population in the peritoneal lavage. We concluded that the fibrotic response was affected by the type of implanted biomaterial rather than severity of acute inflammation.

To answer our second question, we had four different treatments: i) 1 day implantation of a silicone tube in SMAD3 KO mice, ii) 7 day implantation of a silicone

tube in SMAD3 KO mice, iii) 1 day implantation of a silicone tube in WT mice, and iv) 7 day implantation of a silicone tube in WT mice. In Smad3 KO mice, the concentration of TGF-β1 did not differ between the two time points, and on the 7th day, the cell layer on the surface of the implanted silicone tube was much thicker as expected. We did not observe a significant difference on the cellular behaviour at the surface of the implanted biomaterials at either time point between the two mice. We found an increased neutrophil population in the peritoneal lavage with the implantation, though again, no difference between SMAD3 null and WT mice. Finally, the population of the monocytes increased with the implantation and the duration of implantation for both mice. We did not observe a significant difference in biomaterial induced fibrotic response between the two mouse strains.

With our MRL project, we wanted to investigate whether this strain of mouse produces a non-typical fibrotic response to the implanted biomaterial. We had four different treatments: i) 7 day silicone tube implantation in MRL mice, ii) 28 day silicone tube implantation in MRL mice, iii) 7 day silicone tube implantation in C57BL/6 mice, and iv) 28 day silicone tube implantation in C57BL/6 mice. We did not observe a difference in cellular behaviour and cell layer thickness on the surface of the implanted biomaterial between the two strains of mice. We did observe higher concentrations on MMP-2, Pro-MMP-9 and TGF-β1 in MRL mice at both time points. A result that was unexpected was that MRL mice had peak neutrophil population on the 28th day of implantation when the response was expected to be mostly encapsulation and fibrosis instead of severe inflammatory response.

For future studies, we would suggest investigating the importance of the presence of TGF-β1. We found a fibrotic response in all our treatments and also the presence of TGF-β1. Though its concentration did not always correlate to the severity of the fibrotic response, it could mean that the response only needs a certain concentration to trigger the pathway, though there is also a potential of negative feedback when the concentration of this cytokine reaches a limit. Another possibility is that there is another mechanism/pathway that guides the biomaterial-induced fibrosis. A complete elimination of the cytokine could help us determine the existence of a pathway which does not involve TGF-β1.

The cellular behaviour on the surface of the implanted biomaterial did not change between the mice strains in all three of our projects. The only time it was different was when there were two types of biomaterials which gives us a possibility that the surface structure and chemistry, and the initial contact is the key to the following fibrotic response.

Another issue that would need to be considered is the attachment of intestines to the implanted biomaterials. When implanted, often the tube was tangled with the intestines and the detaching caused bleeding of the intestine. A fixture of the implant at desired location would be desired.

In conclusion, we found that: i) the fibrotic response to the implant is heavily dependent on the type of biomaterial, ii) TGF-β1 is involved in fibrotic pathway toward the implanted biomaterial but there is potentially another pathway existing, iii) MRL mice had a higher production of TGF-β1, MMP-2 and Pro-MMP9 but the response to

biomaterials was as severe as in a pro-fibrotic mouse strain.

Appendix A

ELISA (IL-1β) BD (Cat. No. 559603)

For a 96 well-plate

Capture Antibody: 1:250 dilution (with Coating Buffer)
48ul Capture Ab + 12 ml Coating Buffer

Coating Buffer
0.1M Sodium Carbonate, pH 9.5

Detection Antibody: 1:250 dilution (with Assay Diluent)
48ul Detection Antibody + 12ml Assay Diluent

Enzyme Reagent: 1:250 dilution (with Assay Diluent)
48ul Enzyme Reagent + 12ml Assay Diluent

Standards:

Std	Original	Std.2000	Std.1000	Std.500	Std.250	Std.125	Std.62.5	Std.31.3
Conc	**130ng/ml**	2000pg/ml	1000pg/ml	500pg/ml	250pg/ml	125pg/ml	62.5pg/ml	31.3pg/ml
	12ul	12ul of Original	350ul of Std.2000	350ul of Std.1000	350ul of Std.500	350ul of Std.250	350ul of Std.125	350ul of Std.62.5
Assay Diluent		768ul	350ul	350ul	350ul	350ul	350ul	350ul

Assay Diluent
PBS + 10% FBS = 19.2 + 10 + 10 + 3 = 42.2 ml → 50ml(FBS: 5ml)

Wash Buffer
PBS + 0.05%Tween-20 = 300ul/well × 96 × (3+3+5+5+7) = 662.4ml → 900ml (Tween-20: 0.45ml)

Substrate Solution (TMB)
100ul/well ×96 = 9.6ml → 12ml (6ml A + 6ml B)

Stop Solution (1M H_3PO_4)
50ul/well ×96 = 4.8ml → 6ml

Procedure

1. Add 100ul diluted **Capture Ab** to each well. Incubate **overnight** at **4°C**.
2. Aspirate and wash 3 times.
3. Block plates: 200 ul **Assay Diluent** to each well. Incubate **1hr** at RT.

4. Aspirate and wash 3 times.
5. Add 100ul **standard or sample** to each well. Incubate **2hr** at RT.
6. Aspirate and wash 5 times.
7. Add 100ul diluted **Detection Ab** to each well. Incubate **1hr** at RT.
8. Aspirate and wash 5 times.
9. Add 100ul diluted **Avidin-HRP** (Enzyme Reagent) to each well. Incubate **30min** at RT.
10. Aspirate and wash 7 times.
11. Add 100ul **Substrate Solution** to each well. Incubate **30min** at RT **in dark**.
12. Add 50ul **Stop Solution** to each well. Read at 450nm within 30min with λ correction 570nm.

Note: Prepare these solution 15min ahead before use.

Appendix B

TGF – β1 ELISA

Materials Requrired:

Coating Buffer: 0.1M Na_2HPO_4, adjust to pH 9 using NaH_2PO_4

Washing Buffer: 0.5mL Tween-20 in 1L PBS

Blocking Buffer: 10% FBS in PBS

Stop Solution: 1M Phosphoric Acid (Mix 115mL 85% Phosphoric Acid with deionized water to make 1L solution)

Capture Antibody: 48µL Stock Antibody + 11.952mL Coating buffer

Detection Antibody: 12µL Stock Antibody + 11.988mL Blocking buffer

Enzyme Solution: 10µL HRP + 9.990mL Blocking buffer

Substrate Solution: 6mL Reagent A + 6mL Reagent B (Make immediately before use)

TGF- β1 Standards:

Standard	Stock	Std. 125	Std. 62.5	Std. 31.25	Std. 15.625	Std. 7.81	Std. 3.9	Std. 0
Conc.	250 ng/mL	125 pg/mL	62.5 pg/mL	31.25 pg/mL	15.625 pg/mL	7.8125 pg/mL	3.90625 pg/mL	0pg/mL
		10µL of Original	2mL of Std. 125	2mL of Std. 62.5	2mL of Std. 31.25	2mL of Std. 15.625	2 mL of St. 7.81	
Blocking		19.990 ml	2mL	2mL	2mL	2mL	2mL	2mL

g B u f f e r								

Method:

1) Capture Antibody
    a. Add 100µL of capture antibody solution to each well
    b. Seal plate and incubate overnight at 4°C

2) Blocking
    a. Aspirate capture antibody and wash plate 3 times
    b. Add 200µL blocking buffer to each well
    c. Seal plate and incubate 1 hour at room temperature

3) Standards and Samples
    a. Aspirate blocking buffer and wash plate 3 times
    b. Add 100µL standard solution or sample solution to the wells
    c. Seal plate and incubate for 2 hours at room temperature

4) Detection Antibody
    a. Aspirate standards and samples and wash 4 times
    b. Add 100µL of detection antibody to each well
    c. Seal plate and incubate for 1 hour at room temperature

5) Enzyme Solution
    a. Aspirate detection antibody and wash 5 times
    b. Add 100µL of enzyme reagent to each well
    c. Seal plate and incubate 30 minutes at room temperature

6) Substrate
    a. Aspirate enzyme solution and wash 5 times
    b. Add 100µL Substrate solution to each well
    c. Seal plate and incubate 30 minutes at room temperature in **DARK**
    d. Add 50µL stop solution
    e. Read optical density at 470nm